PROTEOMIC ANALYSIS OF CORE HISTONES AND THEIR VARIANTS IN *TETRAHYMENA THERMOPHILA*

Kanwal Ashraf

A THESIS PRESENTED TO FACULTY OF GRADUATE STUDIES
IN PARTIAL FULFILLMENT OF THE REQUIREMENTS
FOR THE DEGREE OF

MASTER OF SCIENCE

Graduate Program in
Biology
York University
Toronto, Ontario
June 2015

Abstract

The fundamental repeating unit of eukaryotic chromatin is the nucleosome which is formed when 146bp of DNA is wrapped around a core histone octamer consisting of two histone H2A-H2B heterodimers and one H3/H4 tetramer. Histones are synthesized in the cytoplasm and are transported into the nucleus via function of many protein factors including histone chaperones. For example, NASP and Asf1 histone chaperones function in the transport of newly synthesized H3/H4 whereas Nap1 plays a role in shuttling of H2A/H2B. Inside the nucleus H3/H4 are deposited onto the DNA either in a replication dependent (RD) or independent (RI) manner by CAF1 and HIRA histone chaperones, respectively. To characterize histone transport machinery and chromatin assembly proteins in *T. thermophila*, I used affinity purification combined with mass spectrometry to identify protein-protein interactions of core histone H2A, variants Hv1 and H3.3 as well as linker histone MLH1. I found that H2A co-purifies with putative $Spt16^{Tt}$ and $Pob3^{Tt}$ subunits of the *T. thermophila* FACT complex. $Spt16^{Tt}$ reciprocally co-purified with several subunits of RNA polymerase II/III, consistent with a role of the FACT complex in transcription regulation. Proteomic analysis of Hv1 indicated that it co-purifies with an Importinβ3, suggesting a possible mechanism of targeting Hv1 specifically to the MAC and not to the MIC. My data also indicated that H2A, Hv1 and H3.3 co-purify with putative PARP1 and PARP2 proteins suggesting that ribosylation of histones might have a critical role in regulating chromatin dynamics in this model organism.

Acknowledgement

First and foremost, I must thank Allah who granted me courage and passion to complete this work. His blessing has always remained with me.

I would like to extend my sincere gratitude towards many people who have helped me throughout this project. Firstly, sincere thanks to my supervisor Dr. Ronald E Pearlman whose guidance, patience and kindness has remained invaluable throughout my stay in his laboratory. His passion for science has inspired many including myself. He taught me lessons that would certainly remain an asset during my further academic endeavours. Secondly, I would like to thank my co-supervisor Dr. Jeffrey Fillingham who initially introduced me to the world of *Tetrahymena* and research in molecular biology. He is not only an excellent mentor but also a great friend who helped me succeed in my master's research.

Thirdly, I would like to thank Dr. Jyoti Garg who taught me many practical skills and guided me on several aspects of the project. I would also like to extend my sincere thanks to Dr. Takahiko Akematsu for his initial help with microscopy. Fourthly, special thanks to Dr. Jean Philippe Lambert from Gingras laboratory at the Lunenfeld-Tanenbaum Research Institute for his continuous assistance with mass spectrometry. Fifthly, I would like to thank Syed Nabeel Haider Shah (Fillingham lab), a great colleague whose help and collaboration was essential to come this far in my research project. Sixthly, I thank all of the Pearlman and Fillingham lab members, particularly Mathew Cadorin, Renu Jeyapala and Nora Dannah for being such wonderful friends.

I also sincerely thank Dr. Peter Cheung for being on my supervisory committee and providing invaluable timely feedback. My gratitude also extends to the staff of the department of biology, York University. Finally, I sincerely thank my family for always

being very supportive. It would certainly have not been possible to come this far in my studies without their help and support.

Table of Contents

List of Tables

List of Figures

List of appendices

List of abbreviations

Å	angstrom (1.0 x 10-10 meters)
AP	affinity purification
APS	ammonium persulfate
Asf1	Anti-silencing factor 1
BES	breakage eliminated site
BLAST	Basic Local Alignment Search Tool
bp	base pair
Caf1	Chromatin assembly factor 1
C-	Carboxy
CBS	chromosome breakage site
CNPL1	Conserved nucleoplasmin like 1
ddH2O	double distilled water
DMSO	Dimethyl sulfoxide
DNA	Deoxyribonucleic acid
EDTA	Ethylenediaminetetraacetic acid
FACT	Facilitator of transcription
FZZ	3x FLAG-ZZ epitope tag
GFP	Green fluorescent protein
Hira	Histone regulator A
IgG	Immunoglobin G
Kb	Kilo base pair
kDa	kilodalton
KO	Knockout

M	molar
MAC	macronucleus
MIC	micronucleus
MS/MS	tandem mass spectrometry
μ	micro
MW	molecular weight
N-	amino
NASP	Nuclear autoantigenic sperm protein
NP-40	nonidet P-40
NPM	Nucleoplasmin
Nrp1	NASP related protein 1
ORF	Open reading frame
PAGE	Polyacrylamide gel electrophoresis
PARP	Poly ADP ribose polymerase
PBS	Phosphate buffered saline
PCR	Polymerase chain reaction
PMSF	Phenylmethanesulfonylfluoride
PSF	Penicillin streptomycin fungizone
PTM	Post-translational modifications
RD	Replication dependent
RI	Replication independent
rpm	rotations per minute
SAINT	Significance analysis of interactome
scnRNA	scan RNA

SDS	Sodium dodecyl sulfate
snRNA	small nuclear RNA
SPP	Sequestrin proteose peptone
SPT16	Suppressor of Tys 16
TAP	Tandem affinity purification
TBE	tris/borate/EDTA
TEMED	tetramethylethylenediamine
TEV	Tobacco etch virus
UTR	Untranslated region
UV	Ultraviolet
v/v	volume/volume
WCE	Whole-cell extract
WT	Wildtype
w/v	weight/volume
YT	yeast extract tryptone

1- Introduction

Eukaryotes package their genomic DNA in the form of a nucleoprotein complex called chromatin. The primary repeating unit of chromatin is the nucleosome which is formed when 146bp of DNA is wrapped around a core histone octamer consisting of two histone H2A-H2B heterodimers and one H3/H4 tetramer (Luger et al. 1997) (Figure 1). The core histones interact with each other through a common structural motif called the histone fold (Alva et al. 2007). Structural studies have revealed that two H3/H4 dimers interact with each other to form a tetramer through a four-helix bundle mediated by the H3 histone folds (Luger et al. 1997). Subsequently, each half of the H3/H4 tetramer is joined by one H2A/H2B dimer through a four-helix bundle between H2B and H4 histone folds (Figure 1).

In addition to the nucleosomal core particle (NCP), eukaryotic chromatin also contains linker histone H1. The linker H1 functions primarily in the formation of higher order chromatin structure. H1 binds with the nucleosomal dyad and the linker DNA region at its entry and exit points to the NCP (Simpson 1978; Kepper et al. 2008; Harshman et al. 2013). The binding of H1 is thought to facilitate nucleosomal stabilization and functions in the overall compaction of the chromatin structure (reviewed in Harshman et al. 2013).

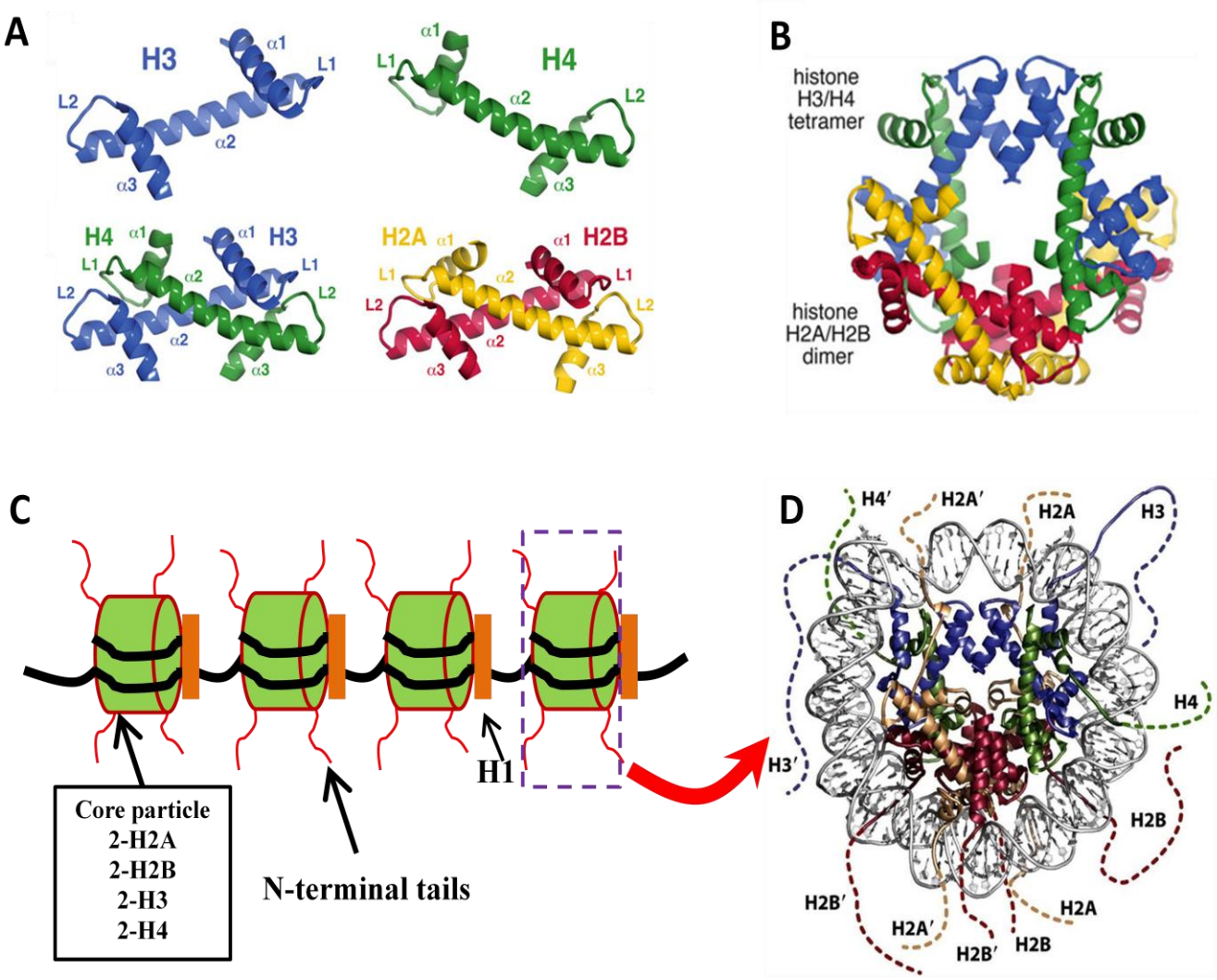

Figure 1: Depiction of histone fold hetero dimers and nucleosomal particles consisting of DNA wrapped around a histone core particle octamer. **A**- Histone fold of core histones as well as dimers formed via histone folds are depicted. **B**- Structural conformation of histone octamer. **C**- Repeating units of nucleosomes wrapped by DNA. The histone N-terminal tails that protrude outside of the nucleosme are also shown. Individual linker histones are shown in orange. **D**- Structure of nucleosome wrapped by DNA is shown (Images adopted: A and B from Fundamentals of Chromatin (ISBN: 978-1-4614-8623-7); 'C' designed after various reviews e.g. (Jiang and Pugh 2009; Czaja et al. 2012); 'D' from *Molecular Cell Biology 6th edition* (Lodish 2008).

Chromatin structure not only provides a way to package the genome but it also influences all DNA-mediated cellular processes including gene transcription, replication, recombination as well as repair (reviewed in Mariño-Ramírez et al. 2005; Aalfs and Kingston 2000). Chromatin remodeling is a general term used to describe direct changes in chromatin structure. Previous studies have shown that chromatin structure can be remodeled via three

basic mechanisms including 1) post-translational modifications (PTMs) such as acetylation and phosphorylation at specific amino acid residues found within N- or C-terminal tails as well as in the globular regions of the histones, 2) physical disruption of the nucleosomes via ATP-dependent chromatin remodeling complexes such as the SWI/SNF complex (Vignali et al. 2000); and 3) replacement of canonical/major histones with their variants (detailed below) in a DNA replication independent manner (Fischle et al. 2003; reviewed in Biterge and Schneider 2014)

1.1- Histones and their Variants

The histones have remained highly conserved throughout eukaryotic evolution indicating their essential role in the organization of chromatin structure (Talbert et al. 2012). For example, histone H4 shares greater than 90% sequence identity between budding yeast and humans. Such high degree of conservation underscores the presence of strong functional constraints that might have been operating on these proteins throughout the course of evolution (Piontkivska et al. 2002). The core histones are expressed from multiple copies of genes often found in clusters throughout the eukaryotic organisms. For instance, two copies of each of the core histone genes are present in the budding yeast genome (Osley 1991), whereas in higher organisms this complexity rises to 10-20 copies of each gene; e.g. human H4 is encoded by at least 12 genes (Piontkivska et al. 2002). Similarly linker histones, which exhibit relatively less sequence conservation (Eirín-López et al. 2004), are also found in increasing complexity along the evolutionary ladder. For example, budding yeast has only one H1 encoding gene whereas in humans 11 distinct isoforms are present (Eirín-López et al. 2004).

Despite the high degree of conservation, variants for all core histones except H4 and linker histone H1 have been described on the basis of differences in their primary amino acid sequences (Talbert et al. 2012; Weber and Henikoff 2014). The variants can be categorized as either replicative or replacement histones. The replicative histones (also called canonical histones) are expressed strictly during S-phase of the cell cycle and are deposited onto chromatin in a DNA replication dependent (RD) fashion (Kamakaka and Biggins 2005). The canonical histones which are encoded by multiple genes arranged in clusters are devoid of introns. Their mRNA transcripts are not polyadenylated but instead a 'stem loop binding protein (SLBP)', whose expression also peaks during S phase, stabilizes them (Marzluff and Duronio 2002). These features allow for a coordinated transcription of canonical histones during the S phase of cell cycle (Marzluff et al. 2008).

The replacement variants, or non-canonical histones, are expressed throughout the cell cycle and are primarily deposited in a DNA replication independent (RI) manner (Kamakaka and Biggins 2005). They are present as a single gene copy, contain introns and their mRNAs are polyadenylated (Kamakaka and Biggins 2005). These features have been implicated to function in the post-transcriptional regulation of these genes (Old and Woodland 1984). The selective insertion of histone variants into chromatin can alter nucleosomal properties (reviewed in Weber and Henikoff 2014). For example, replacement histone variants contain distinct amino acids, not present in their canonical counterparts, that might be subject to various unique PTMs which can alter the nucleosomal properties (see below for PTMs) (McKittrick et al. 2004; Kamakaka and Biggins 2005). In addition, the presence of histone variants can affect the nucleosomal stability resulting in an altered chromatin conformation (Biterge and Schneider 2014). For example, nucleosomes containing H3.3, a replacement variant of histone H3, are inherently less stable and have been associated

with an active chromatin state (Jin et al. 2009). These features can serve as an example for the functional significance of these quantitatively minor histone variants.

1.1.1-Histone H3 variants

In humans, eight histone H3 variants have been described including H3.1, H3.2, H3.3 H3t, CENP-A, H3.X, H3.Y and H3.5. Among these variants, H3.1 and H3.2 are the canonical histones whose expression is restricted to S phase and are deposited via a RD chromatin assembly pathway (Hake and Allis 2006; Biterge and Schneider 2014). The remaining variants including H3.3, H3t, CENP-A, H3.X, H3.Y and H3.5 are deposited via a RI pathway and can further be categorized based on their tissue specificities, i.e. H3.3, CENP-A, H3.X, and H3.Y are somatic histone variants whereas H3t and H3.5 are only expressed in testis (Hamiche and Shuaib 2013). Mammals have evolved two canonical H3s in the form of H3.1 and H3.2 which differ from each other only at one amino acid residue (residue 96 in humans) (see Figure 2). However lower organisms such as fruit flies contain only one canonical histone H3 which resembles mammalian H3.2 (Hake and Allis 2006). Budding and fission yeasts possess only one histone H3 which is similar to the metazoan H3.3 and can be deposited via both the RD and RI pathways (Choi et al. 2005; Dion et al. 2007; Jamai et al. 2007).

One of the most extensively studied quantitatively minor H3 variant is H3.3. H3.3 has been shown to be evolutionarily conserved and is found throughout the major eukaryotic lineages (Talbert et al. 2012). Mammalian H3.3 differs from the major H3.1/H3.2 at only five/four amino acid positions respectively (see Figure 2). The small 'AAIG' motif found within the histone fold of H3.3 has been shown to be sufficient for its RI deposition (Ahmad and Henikoff 2002; Goldberg et al. 2010). In humans, epitope tagged H3.1 and H3.3 were found to co-purify with distinct histone chaperones suggesting that RD and RI chromatin

assembly of H3 is mediated by unique protein complexes (Tagami et al. 2004). The canonical H3.1 exclusively co-purified with a three subunit histone chaperone complex called "chromatin assembly factor 1" (CAF1) whereas H3.3 was found to interact with "histone regulator A" (HIRA), (Tagami et al. 2004). HIRA is an evolutionarily conserved H3/H4 chaperone that has been shown to function primarily in the RI chromatin assembly pathway (Green et al. 2005; Balaji et al. 2009). Genome wide studies have shown that HIRA is necessary for the RI deposition of H3.3 in mammalian embryonic stem cell (ESC) lines, neuronal precursor as well as in HeLa cells (Goldberg et al. 2010; Ray-Gallet et al. 2011). Recently, HIRA has been found to be required for the de novo assembly of H3.3 in the male pro-nucleus of fruit flies suggesting the functional conservation of this histone chaperone (Orsi et al. 2013).

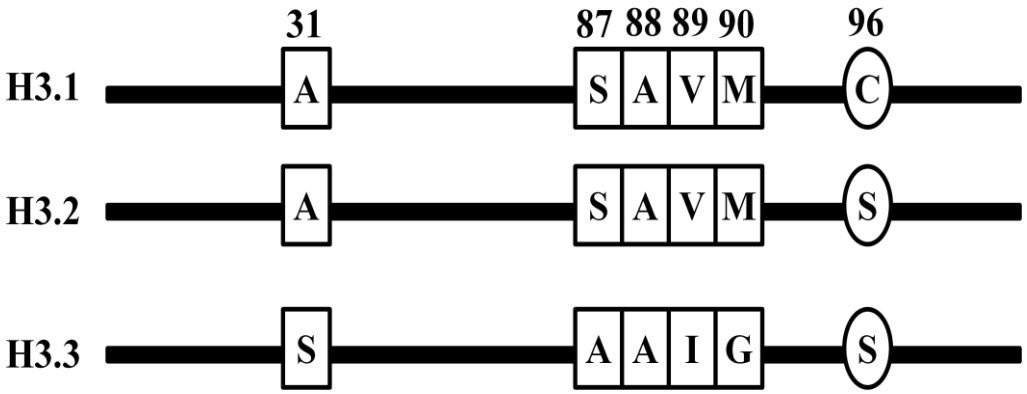

Figure 2: Comparison of H3 RD and RI variants. The critical residues required for RI deposition of H3.3 are indicated. Image adopted from (Elsaesser and Allis 2010).

In differentiated, non-dividing cells, H3.3 constitutes over 25% of the total H3 in the chromatin (McKittrick et al. 2004). Several recent studies have shown that H3.3 is enriched in the euchromatic regions and is associated with transcriptionally active genes (Goldberg et al. 2010; Ray-Gallet et al. 2011; Kraushaar et al. 2013; Ha et al. 2014). For example, in ESC lines, H3.3 is enriched at transcription start sites (TSS), gene bodies as well as transcription end sites (TES) of actively transcribed genes (Goldberg et al. 2010). Genome wide studies

have also demonstrated high turnover rates for H3.3-containing nucleosomes at enhancers and promoters which are associated with active transcription marks such as H3 lysine 4 methylation (H3K4me1), H3K4me3, H3K9 acetylation (ac) and H3K27ac (Kraushaar et al. 2013). In *Drosophila melanogaster*, replacement of H3 with H3.3 has been observed to occur predominantly at the sites of RNA polymerase II and H3K4me PTM mark (Mito et al. 2005). Consistent with these findings, a recent report using chromatin immunoprecipitation followed by sequencing (ChIP-seq) analyses revealed that in HeLa cells, H3.3 is enriched at the sites of elongating RNA PolII in a HIRA dependent manner (Ray-Gallet et al. 2011). Taken together these studies strongly suggest the association of H3.3 with active gene transcription. Furthermore, consistent with an accumulation in the euchromatic regions, H3.3 is rich in PTMs generally associated with gene transcription (McKittrick et al. 2004; Hake et al. 2006). For example, H3.3 is enriched with H3K9ac, H3K14ac, and H3K4me3 PTMs, all of which have been associated with transcriptional activation (Loyola et al. 2006). Furthermore, in ESCs H3.3 deposition rates have been detected to be highest at sites associated with active histone marks including H3K4me3, H3K9ac and H3K27ac (Ha et al. 2014). In contrast to H3.3, the canonical histones H3.1/H3.2 are typically enriched with marks associated with gene silencing such as H3K27me3 and H3K9me3 (Hake et al. 2006).

A recent study has implicated H3.3 in epigenetic inheritance (Ng and Gurdon 2008). It was shown that in non-muscle cell lineages of nuclear transplant embryos, incorporation of H3.3 at the *MyoD* promoter correlates with the epigenetic memory of gene expression (Ng and Gurdon 2008). Strikingly, authors found that K4 of H3.3 is essential for the observed epigenetic inheritance of the gene expression pattern. Substituting H3.3 K4 to E4 which cannot be methylated results in the loss of epigenetic memory (Ng and Gurdon 2008). This finding suggests that specific PTM marks on H3.3 have essential functions in the context of

gene expression regulation. Consistent with the essential functions of H3.3, its loss results in semi-lethality in mice (Bush et al. 2013). Loss of H3.3 in *D. melanogaster* results in widespread transcriptional defects. In fact null flies have severe phenotypes of male meiotic defects including chromosomal segregation impairment (Sakai et al. 2009).

Recent evidence indicates that H3.3 is not strictly associated with euchromatic regions and can also be found within repressed and poised genes (Delbarre et al. 2010; Goldberg et al. 2010). Consistently, H3.3 has also been found to be associated with pericentric and telomeric chromatin regions (Wong et al. 2009; Drané et al. 2010; Lewis et al. 2010). Distinct histone chaperones including a complex comprised of the death-associated protein (DAXX) and the alpha-thalassemia/mental retardation X-linked syndrome protein (ATRX) is associated with H3.3 at these heterochromatic loci (Wong et al. 2009; Drané et al. 2010; Goldberg et al. 2010; Lewis et al. 2010). In addition, a phosphorylated form of chromatin-bound protein DEK, which is another H3.3 chaperone, has been proposed to interact with *D. melanogaster* nuclear ecdysone receptor and potentially functions in directing H3.3 to regulatory elements to enhance transcription (reviewed in Campos and Reinberg 2010; Sawatsubashi et al. 2010). In fact recent evidence indicates that DEK is essential for proper loading of ATRX and H3.3 on telomeres (Ivanauskiene et al. 2014).

Although H3.3 is primarily incorporated into chromatin via a RI pathway, it can also be deposited during DNA replication. For example in *D. melanogaster,* H3.3 utilizes both the RD and RI pathways to get deposited onto DNA (Ahmad and Henikoff 2002). Consistent with these findings, it was recently shown that in HeLa cells H3.3 is also deposited during S-phase of the cell cycle in a HIRA dependent manner (Ray-Gallet et al. 2011). CENP-A is a centromere-specific H3 variant and is deposited during early G1 phase in a RI manner (Stellfox et al. 2013). Recent evidence indicates that H3.3 is deposited during S at

centromeres where it functions as a place-holder for CENP-A to be incorporated during G_1 phase (Dunleavy et al. 2011). Consistent with these observations, in *Tetrahymena thermophila*, a unicellular eukaryotic ciliate protozoan, H3.3 has been shown to be deposited via both RD and RI pathways, with the latter being the predominant mode of incorporation (Cui et al. 2006). In *T. thermophila*, canonical H3 has been found be non- essential for survival if cells are over-expressing H3.3. It was also found that vegetative *T. thermophila* cells lacking H3.3 are viable and do not exhibit any phenotype (Cui et al. 2006). Nevertheless, H3.3 is required to produce viable sexual progeny and plays a critical role in the germline micronuclei late in conjugation (Cui et al. 2006). Furthermore, consistent with the described association of metazoan H3.3 with gene expression, *T. thermophila* H3.3 was also found to predominantly localize in the transcriptionally active macronucleus (Cui et al. 2006). Taken together these studies highlight the diverse and biologically significant functions of H3.3 including roles during embryo development, chromatin organization, gene expression regulation and epigenetic inheritance (Szenker et al. 2011).

1.1.2- H2A and its variants

A unique feature of the histone H2A family is the presence of an extended C-terminal tail that is the target of some of the most bulky PTMs such as SUMOylation and ubiquitination (Vissers et al. 2008; Thambirajah et al. 2009; Wratting et al. 2012). In humans it has been shown that truncating the C-terminal tails of H2A results in an altered gene expression pattern suggesting their functional significance in maintaining the proper chromatin structure (Karaczyn et al. 2009). In addition to the canonical H2As, five major variants including H2A.Z, MacroH2A, H2A-Bbd, H2AvD, and H2A.X have thus far been detected (Kamakaka and Biggins 2005). Some of the H2A variants are present in a lineage specific manner (Kamakaka and Biggins 2005). For example, H2A.Bbd (Barr Body

Deficient) is a mammalian-specific H2A variant which is not present in invertebrates (Eirín-López et al. 2008). H2A.Bbd is thought to facilitate both the transcription activation by destabilizing the nucleosomes and processing of initial mRNAs (Tolstorukov et al. 2012). Similarly, MacroH2A is restricted to vertebrates and primarily localizes to the inactive X-chromosome where it is believed to function in the maintenance of transcriptionally silent chromatin (Costanzi and Pehrson 1998). Remarkably, Bdelloid rotifers lack canonical H2As and instead contain unusually massive variants (Van Doninck et al. 2009). The presence of these unusual H2A variants in Bdelloid rotifers is thought to be an adaptation to survive in the environmental conditions in which these organisms reside (Van Doninck et al. 2009).

The variant H2A.X is typically characterized by the presence of a C-terminal SQ motif. Upon DNA damage the highly conserved serine residue present within the SQ motif is phosphorylated and the phosphorylated form is denoted as γH2A.X. γH2A.X has been shown to have a central role in the accumulation of DNA damage repair factors (Downs et al. 2000; Thambirajah et al. 2009). In budding and fission yeasts the major H2A proteins are more similar to the mammalian H2A.X variant rather than the canonical H2A subtypes (Downs et al. 2000; Kamakaka and Biggins 2005). In contrast to yeasts where H2A.X is the only major H2A, in *T. thermophila* one of the two canonical H2As contains an SQ motif and functions similarly to the metazoan H2A.X upon DNA damage (discussed later) (Song et al. 2007). These observations highlight the fact that evolutionary pressures have ensured the presence of H2A.X possibly due to its essential roles in the DNA damage repair pathway.

Among H2A variants, H2A.Z is the most conserved and is found throughout the eukaryotic lineage (Talbert et al. 2012). At the amino acid level, H2A.Z shares ~ 60% similarity with the core histone H2A within the same species (Thatcher and Gorovsky 1994; Talbert et al. 2012). Remarkably however, H2A.Z is more conserved to its counterparts

across various lineages (~80% similarity for most species) (Bönisch and Hake 2012) suggesting that H2A.Z is functionally distinct from the major H2As. H2A.Z variants are known as the yeast Htz1, *T. thermophila* hv1, *D. melanogester* H2Av and mammalian H2A.Z. H2A.Z was identified in the 1980s and studies have shown that it contributes to an estimated 5-10% of all nucleosomal H2A variants (Redon et al. 2002). The structural studies have indicated that H2A.Z containing NCP is similar in overall topology to that of H2A-containing nucleosomes (Suto et al. 2000). However, it was found that the presence of H2A.Z might confer unique structural properties distinct from those of canonical H2A (Suto et al. 2000). For example, the L1 loop which functions to mediate interaction between two H2A/H2B dimers is altered in H2A.Z NCPs in such a way that it favors the presence of a second H2A.Z/H2B dimer within the same nucleosome (Suto et al. 2000). Due to these differences it was hypothesized that presence of the canonical H2A and H2A.Z within the same NCP would have destabilizing effects (Suto et al. 2000). Subsequent studies, however, have reported contrasting observations. For example, some studies indicated that H2A.Z containing nucleosomes are more stable than the canonical H2A NCPs (Thambirajah et al. 2006). Park et al. (2004) have shown that H2A.Z containing mono-nucleosomes are more resistant to salt dissociation than the canonical H2A containing NCPs suggesting that H2A.Z results in nucleosomal stability (Park et al. 2004). In contrast, several other studies have concluded that H2A.Z confers instability when present within the NCPs (Zhang et al. 2005; Bönisch et al. 2012). Recent studies have demonstrated that H2A.Z/H3.3 double variant containing NCPs are highly unstable indicating a role of variants in gene transcription activation (Jin and Felsenfeld 2007). Consistent with these results, it was later found that in humans H2A.Z/H3.3 containing NCP are enriched within nucleosome-free regions of active promoters, enhancers and insulator regions (Jin et al. 2009). Taken together these studies

highlight the fact that the presence of histone variants has the potential to alter nucleosomal properties and chromatin structure.

Whether or not expression of H2A.Z is essential is species specific. For example, H2A.Z is essential in mouse (Faast et al. 2001), fly (van Daal and Elgin 1992) and frog (Iouzalen et al. 1996). Similar to the higher eukaryotes, in *T. thermophila* Hv1 is an essential gene and its loss causes lethality (Liu et al. 1996). Hv1 is found primarily in the transcriptionally active macronucleus throughout the life cycle of *T. thermophila*. However, Hv1 does localize to the transcriptionally silent micronucleus only during early stages of conjugation, the only time when it is transcriptionally active (Allis et al. 1986; Stargell et al. 1993). These observations indicate that this variant might be involved in the activation of gene expression. This notion was further supported by studies in yeast which indicated that Htz1 is required for the proper expression of ~200 genes (Kobor et al. 2004; Mizuguchi et al. 2004). Htz1 is enriched at the promoter of several genes and is necessary for the recruitment of the transcriptional machinery (Guillemette et al. 2005; Bernstein et al. 2007; Zilberman et al. 2008). It has been suggested that H2A.Z might be involved in defining the boundaries of heterochromatin and euchromatin (Meneghini et al. 2003). It was demonstrated that Htz1 localizes within the actively transcribed regions of the yeast genome, in particular those flanking heterochromatin that is associated with the Sir silencing complex (Meneghini et al. 2003). Recent studies also suggest that H2A.Z mutant cells show a defect in DNA repair which in turn results in genomic instability (Xu et al. 2012).

H2A.Z has been found to play vital roles in both transcription activation as well as repression (Raisner et al. 2005; Marques et al. 2010; reviewed in Bönisch and Hake 2012). Recent evidence suggests that the presence of H2A.Z can affect the positioning and mobility of NCPs which in turn could differentially increase or decrease the availability of DNA for

the binding of activating and repressive regulatory factors (Guillemette et al. 2005; Marques et al. 2010). In addition, the presence of specific PTMs might have a role in the observed contrasting functions of H2A.Z. For example, acetylated H2A.Z is enriched within active regions and is thought to function as a positive regulator of gene transcription (Zlatanova and Thakar 2008). In contrast, ubiquitinated H2A.Z is thought to be a marker of transcription repression (Zlatanova and Thakar 2008). Consistent with the role of PTMs on H2A.Z, *T. thermophila* Hv1 is acetylated at GGK motif found within the N-terminal tail (Ren and Gorovsky 2001). The acetylation of Hv1 is believed to be critical for the proper functioning of Hv1 in gene transcription (Ren and Gorovsky 2001; Ren and Gorovsky 2003). Similarly, the N-terminal tail of budding yeast Htz1 is acetylated at K3, K8, K10 and K14 residues and mutants lacking the acetylable K14 exhibit defects in chromosome transmission, telomeric silencing and DNA repair (Keogh et al. 2006; Millar et al. 2006).

Several independent studies have revealed the involvement of a novel protein complex called the Swr1-complex in the recruitment of H2A.Z (Krogan et al. 2003; Kobor et al. 2004; Mizuguchi et al. 2004). Swr1 functions as an ~1 MDa complex containing 14 different polypeptides (reviewed in Nguyen et al. 2013) including catalytic 'Swr1' (a member of the ATP-dependent SWI/SNF family of chromatin-remodeling factors). It replaces canonical H2A with H2A.Z in an ATP-dependent manner (Luk et al. 2010). In budding yeast, histone chaperones including Nucleosome assembly protein 1(Nap1) and chaperone for H2A.Z-H2B (Chz1) have been shown to provide Htz1/H2B to the Swr1 complex for deposition (Straube et al. 2010). While Nap1 can function both as H2A/H2B and Htz1/H2B chaperones, Chz1 is a highly specific chaperone for Htz1/H2B (Luk et al. 2007; Straube et al. 2010). Taken together these studies have highlighted the essential roles of H2A

variants, particularly H2A.Z, in the regulation of gene expression, chromatin integrity and DNA repair.

1.2- Histone Chaperones and their roles in chromatin dynamics

The assembly of genomic DNA and histones into chromatin is a fundamental process that may affect a broad range of gene regulatory processes such as DNA repair, DNA replication and progression through the cell cycle (reviewed in Fischle et al. 2003). To regulate the process of chromatin assembly/disassembly, cells have evolved several protein factors known as histone chaperones (Keck and Pemberton 2012). Histone chaperones act as donors and acceptors during assembly and disassembly of nucleosomes and deposit histones onto DNA in an orderly manner without themselves being a part of the chromatin (De Koning et al. 2007). Histone chaperones have a variety of different functions including shielding of positive charges on histones to prevent any nonspecific interactions with DNA (Keck and Pemberton 2012). There are several histone chaperones identified to date and they appear to have specific preferences for binding to either H3-H4 or to H2A-H2B (De Koning et al. 2007; Hondele and Ladurner 2011; Keck and Pemberton 2012). Examples of histone chaperones include Nucleoplasmin (NPM) and Nucleosome assembly protein 1 (Nap1) both of which are H2A-H2B chaperones, as well as Histone regulator A (HIRA), Chromatin assembly factor -1 (CAF-1) complex, Anti silencing factor 1 (Asf1) and Nuclear auto antigenic sperm protein (NASP) all of which are H3-H4 chaperones. There are also chaperones that can function for both the H2A-H2B and H3-H4 histones, e.g. Facilitator of chromatin transcription (FACT) complex.

Initiation of chromatin assembly begins in the cytoplasm where histones are synthesized during S phase and are then transported into the nucleus (reviewed in Roth and

Allis 1996). Several studies have shown that newly synthesized histones contain specific PTM marks. For example, newly synthesized histone H4 carries an evolutionarily conserved diacetylation mark at K5 and K12 residues (Jackson et al. 1976; Sobel et al. 1995; Li et al. 2012). These PTMs are thought to be important for the proper transport and deposition of histones (De Koning et al. 2007; Hondele and Ladurner 2011; Keck and Pemberton 2012). The processes of transporting newly synthesized histones, assembling them onto DNA and disassembly of old histones during DNA replication and transcription are all mediated by several histone chaperones as well as karyopherin (importins/exportins-Kaps) proteins (De Koning et al. 2007).

The current view is that newly synthesized histones are transported to the nucleus in a stepwise manner in which distinct chaperones and Kaps have been shown to be involved (Li et al. 2012). The transport pathway of H2A/H2B is still largely unclear, however histone chaperone Nap1 along with a Kap114 have been shown to mediate this process in yeast (Mosammaparast et al. 2001; Mosammaparast et al. 2002). In contrast to the H2A/H2B, newly synthesized histones H3/H4 are transported via a pathway that has been well elucidated. For example, in humans, newly synthesized histones H3.1/H4 are transported to the nucleus by shuttling through at least four different cytosolic complexes (Campos et al. 2010; Alvarez et al. 2011). The process is initiated by heat shock proteins HSP90 that bind with newly synthesized histones to possibly aid in their proper folding. Subsequently, NASP binds with these newly synthesized histones and facilitates in Hat1/Hat2 mediated deposition related H4 acetylation. Finally these histones are passed onto a chaperone Anti-silencing factor 1 (Asf1) which along with Importin4 transports these histones to the nucleus (Campos et al. 2010; Alvarez et al. 2011; for review Keck and Pemberton 2012). Inside the nucleus, yet another set of histone chaperones have been shown to play crucial roles in chromatin

assembly. As noted earlier, canonical histones are deposited via RD chromatin assembly (Campos et al. 2010; Alvarez et al. 2011) whereas histone variants are deposited via the RI chromatin assembly pathway (Ahmad and Henikoff 2002; Green et al. 2005). The three subunit protein complex CAF1 that physically interacts with Asf1, functions to deposit histones H3.1/H4 onto replicating DNA whereas RI assembly of H3.3 is mediated by HIRA (Tagami et al. 2004). Both CAF1 and HIRA interact with Asf1 in a mutually exclusive manner via conserved B-domain regions (Sherwood et al. 1993; Tang et al. 2006) (Figure 3). These studies underscore the importance of histone chaperones and their role in histone metabolism. Below, a brief overview of histone chaperones including NPM and NASP, as well as the FACT complex, is provided.

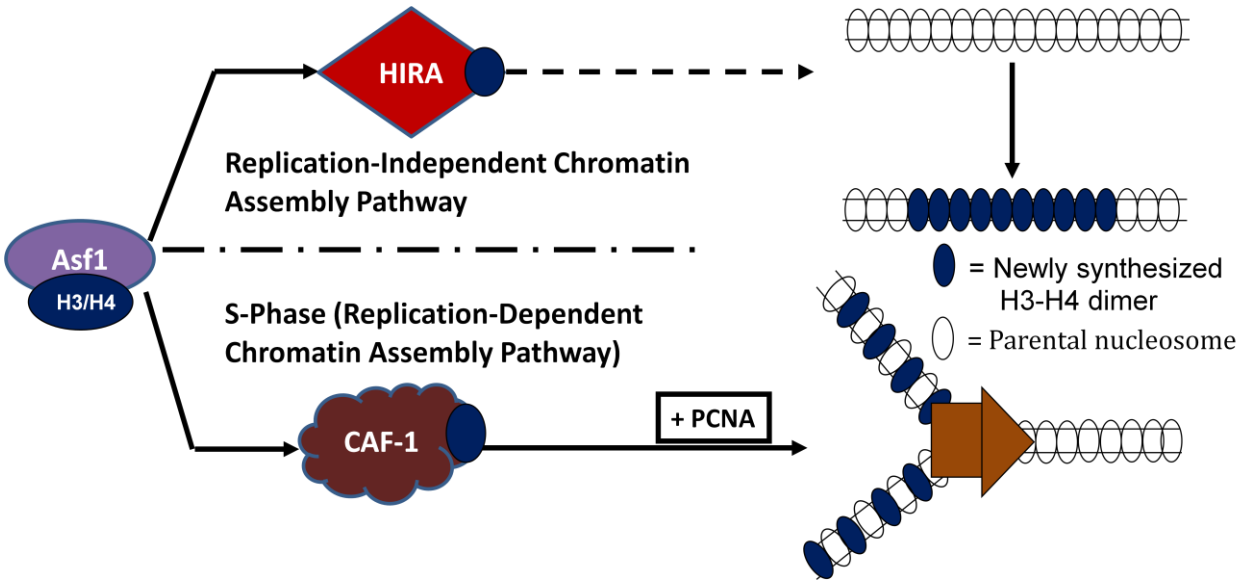

Figure 3: Chromatin assembly pathway: A general view. Inside the nucleus Asf1 functions to pass newly synthesized histones H3/H4 either to the HIRA complex (RI pathway) or to CAF-1 (RD pathway). The thick arrow denotes the replication fork (Image adopted from Fillingham and Greenblatt 2008)

1.2.1- Nucleoplasmin- the chaperone of H2A-H2B

Originally isolated from African clawed frog (*Xenopus laevis*) egg extracts, Npm (also referred to in the literature as NP or Npm2) was described as an acidic chaperone protein capable of assembling nucleosomes binding specifically with H2A/H2B (Dingwall et al. 1987; Dingwall and Laskey 1990). *X. laevis* oocytes store a large amount of soluble histones that are required for DNA replication post-fertilization, and Npm2 have been suggested to function as a buffer for these soluble histones (Dingwall et al. 1987; Dingwall and Laskey 1990). In vertebrates three paralogous forms of Npm are found which have been categorized as Npm1, Npm2 and Npm3, whereas invertebrates contain only one Npm-like protein (Eirín-López et al. 2006). Vertebrate Npm1-3 proteins are transcribed from three different genes encoding three similar proteins that differ in their length and domain structure as depicted in Figure 4 (reviewed in Frehlick et al. 2007). The Npm1-3 proteins differ from each other in their expression and localization patterns, but one hallmark of nucleoplasmins is a well-conserved N terminus (core region) which usually contains a small acidic domain and a C-terminus which contains one acidic domain in the case of Npm3 and two or more acidic domains in the case of Npm1/2 as shown in Figure 4 (reviewed in Frehlick et al. 2007). Furthermore, Npms can localize in the nucleus and hence contain a nuclear localization signal (NLS). For Npm1 (also known as B23, numatrin, and NO38), it additionally contains a nucleolar localization signal (NoLS) as well as a nuclear export signal (NES) and an RNA-binding domain (RBD). Both the NoLS and RBD are thought to be required for Npm1 functions during ribosome biogenesis (Borer et al. 1989).

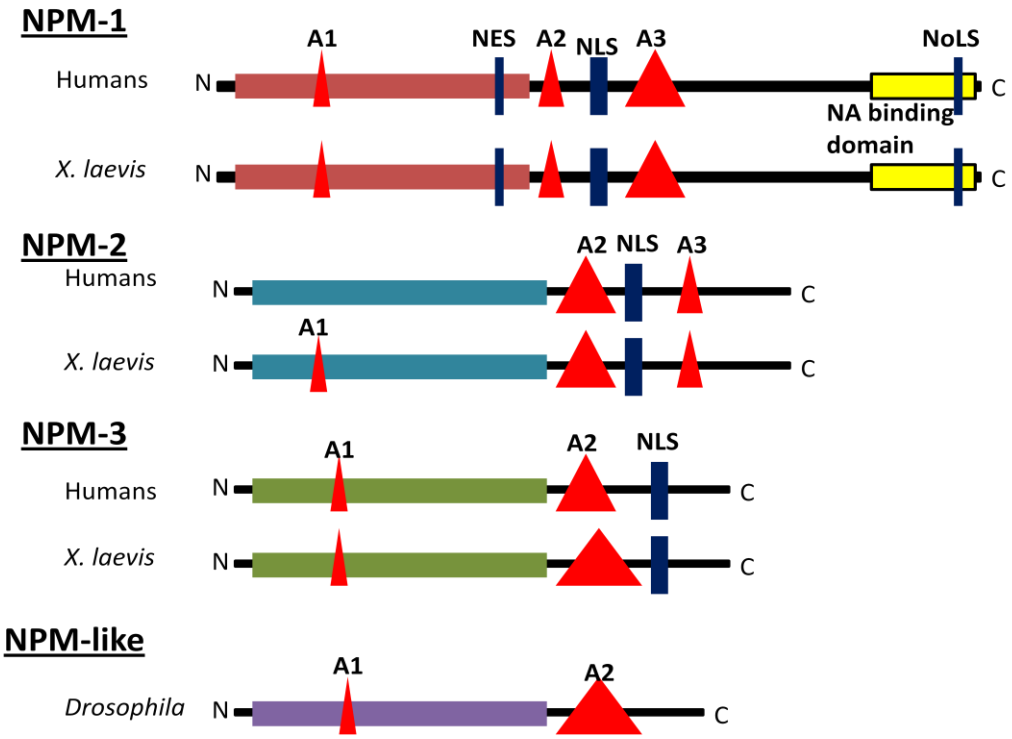

Figure 4: Comparison of different Npm family members. Acidic patches are shown in red whereas localization signals are shown in dark blue. The nucleic acid binding domain is shown in yellow for Npm1. The core N-terminal domains are shown in pink, blue green and purple for Npm1, 2, 3 and Npm-like proteins, respectively. Image adopted from (Frehlick et al. 2006).

Npm1-3 family members may have some functional redundancy. For example, disruption of the Npm2 gene in mice, which is specifically expressed in growing oocytes, leads to noticeable defects in female fertility and loss of heterochromatin and deacetylated histone H3 in early embryonic cells (Burns et al. 2003). In Npm2-KO mice, Npm1 and Npm3 were found to have some compensatory roles (Burns et al. 2003) suggesting functional redundancy among Npm family members. As noted above Npm2 proteins have been shown to function in soluble H2A/H2B storage (Dingwall et al. 1987; Dingwall and Laskey 1990). In *X. laevis*, Npm2 functions both in the removal of protamines (Prieto et al. 2002) and the subsequent deposition of H2A/H2B dimers, signifying its important role in chromatin decondensation and proper nucleosome formation (Dingwall et al. 1987; Dingwall and Laskey 1990). Similar to Npm2, Npm1 has also been demonstrated to be important for

several chromatin related processes. For example, inactivation of Npm1 in mice results in defects in centrosome duplication (Grisendi et al. 2005), DNA replication (Takemura et al. 1999), transcriptional regulation (Swaminathan et al. 2005), histone chaperone activity, and nucleic acid binding (Wang et al. 1994). In contrast to Npm1/2, the Npm3 is the least characterized family member (Finn et al. 2012). Npm3 is ubiquitously expressed across various tissues (Shackleford et al. 2001) and within mammalian oocytes it has been found to be crucial for chromatin de-condensation (McLay and Clarke 2003).

1.2.2- Nuclear autoantigenic sperm protein (NASP)

NASP originally discovered in *X. laevis* oocytes and named as N1/N2 was found to be highly specific for H3/H4 binding. Similar to Npm2, NASP was thought to provide a buffering mechanism for soluble H3/H4 required for DNA replication in the early embryo (Kleinschmidt et al. 1985; Dilworth et al. 1987). The mammalian homolog of N1/N2 was subsequently identified in rabbit testes and was found to be a highly autoantigenic protein and hence was named accordingly, i.e. NASP (Welch et al. 1990). Later studies showed that among mammals, NASP exists in alternatively spliced isoforms that are differently expressed either in testes or somatic cells (Richardson et al. 2000). The full length NASP (tNASP) is primarily expressed in embryonic tissues and testes whereas the smaller version is found in all dividing cells (Richardson et al. 2000).

Studies in mice revealed that knocking out its gene results in early embryonic lethality indicating NASP expression is essential (Richardson et al. 2006). It has also been shown that NASP is a cell cycle regulated proteins and its over expression results in cell cycle delay from the G1/S border (Richardson et al. 2000; Alekseev et al. 2003). In humans, NASP functions in an array of cellular processes. For example, it participates in di-acetylation of newly synthesized H3/H4 in a Hat1-complex dependent manner, functions as an H1

chaperone and fine tunes a soluble reservoir of histones H3/H4 in humans (Finn et al. 2008; Campos et al. 2010; Cook et al. 2011).

NASP has recently been shown to be conserved throughout the eukaryotes with a motif architecture of four tetratricopeptide repeats (TPR) (Nabeel-Shah et al. 2014). Interestingly, it has been shown that different TPR motifs in NASP bind with differential affinity for H1 and H3/H4 (Wang et al. 2008). For example, TPR2 which has acidic residues interacts with H1 whereas TPRs3/4 are responsible for H3/H4 binding (Wang et al. 2012). Recently, it was also shown that the NASP ortholog in *Saccharomyces cerevisiae*, Hif1 functions in nucleosome formation via an interaction with specific species of RNA (Knapp et al. 2014). In addition, deletion of Hif1 results in defects in telomeric silencing and DNA double strand break repair (Ai and Parthun 2004). Taken together these studies suggest that NASP has diverse functions within cells ranging from histone transport to nucleosome assembly.

1.2.3- The FACT (facilitates chromatin transcription) Complex:

In budding yeast, FACT consists of two proteins: Spt16 (suppressor of Ty 16) (also called Cdc68) and Pob3 (Pol1 binding protein3) (Rowley et al. 1991; Evans et al. 1998). Yeast Spt16 protein was identified based on its roles in transcription and cell cycle controls (Rowley et al. 1991) whereas Pob3 was co-purified with DNA polymerase II (Wittmeyer and Formosa 1997). In budding yeast FACT is required for transcribing genes with highly positioned nucleosomes at the 5' end of the transcribed region suggesting a role in transcription initiation (Jimeno-González et al. 2006). In addition to its role in transcription initiation, FACT has also been found to have important functions in transcription elongation in several organisms (Saunders et al. 2003). FACT's role in transcription elongation was established *in vivo* through genetic interactions with known elongation factors TFIIS and

Spt4 (Orphanides et al. 1998). ChIP experiments showed that FACT associates with active genes *in vivo* and co-localizes with RNAPII (Mason and Struhl 2003).

In humans, Spt16 (SUPT16H) is a 140 kDa subunit which is 36% identical to the *S. cerevisiae* Spt16 whereas the Pob3 is an 80 kDa subunit (SSRP1 in human) (Orphanides et al. 1998). FACT interacts with nucleosomes and acts as a H2A-H2B dimer chaperone (Orphanides et al. 1999). The chaperoning activity of FACT is required for two different processes, first, to facilitate the removal of histones in front of elongating Pol II and secondly, in the reassembly of the nucleosome (Winkler and Luger 2011). It has been shown that the absence of yeast FACT results in the improper deposition of histones during transcription elongation which results in the high levels of free histone, leading to a delay in cell cycle progression at G1 phase (Morillo-Huesca et al. 2010). It was shown that covalently cross linked histones within nucleosomes abrogate FACT dependent transcription indicating that histone octamers must be disassembled during transcription (Orphanides et al. 1999). Thus it was concluded that FACT is involved in nucleosome disassembly, a notion strongly supported by the physical interaction of Spt16 with H2A/H2B and Pob3 association with H3/H4 (Belotserkovskaya et al. 2003). Moreover, FACT was also found to possess histone chaperone activity suggesting that FACT functions in the nucleosomal re-assembly during transcription (Belotserkovskaya et al. 2003).

Besides its critical role in transcription, FACT complex has also been shown to be important for DNA replication and DNA repair (reviewed in Reinberg and Sims 2006). For example, FACT is important for replication in *X. laevis* egg extracts (Okuhara et al. 1999). In humans, FACT co-purifies with MCM helicase components where it has been shown to enhance the MCM helicase activity *in vitro* (Tan et al. 2006). Similarly, in budding yeast DNA polymerase-α, DNA replication factor RPA as well as the MCM helicase, all of which

are required for initiation of replication from origins and for lagging strand synthesis, have been demonstrated to co-purify with FACT (Wittmeyer and Formosa 1997; Gambus et al. 2006; VanDemark et al. 2006). Consistent with these observations, Pob3 mutants exhibit replication defects (Schlesinger and Formosa 2000). Furthermore, Spt16 has been demonstrated to localize to replication origins in G1 and early S phases (Han et al. 2010). Taken together, FACT has demonstrable functions in transcription initiation, elongation, as well as DNA replication.

1.3- Histone post-translation modifications

Histones can be post-translationally modified, particularly at their amino (N) terminal tails and these modifications have been shown to influence various aspects of chromatin dynamics including chromatin assembly, gene expression regulation, and formation of various chromatin states such as heterochromatin and euchromatin (reviewed in Keck and Pemberton 2012). Some of the histone PTMs include acetylation, phosphorylation, methylation (mono, di and trimethyl), SUMOylation, ubiquitylation and ribosylation marks (Fischle et al. 2003). These reversible covalent modifications have been linked with specific biological outcomes. For example, an enrichment of H3K9 me3, H3K27me3 and H3K20me3 have been associated with transcriptionally inert heterochromatic regions whereas H3K4me3 and H3K36me3 PTMs have been linked with transcriptionally active regions (reviewed in Rivera et al. 2014). In addition, H3K56ac, a PTM found within the histone globular region, has an important role in chromatin assembly during DNA replication and repair. H3K56ac has been implicated to function to loosen the interaction of histones with DNA, suggesting a role in chromatin assembly (Masumoto et al. 2005). In budding yeast, H3K56ac is mediated by a fungal specific histone acetyltransferase Rtt109 (Driscoll et al. 2007; Han et al. 2007),

in conjunction with Asf1 (Recht et al. 2006). In humans, several HATs including CBP/p300 (Das et al. 2009) and Gcn5 (Tjeertes et al. 2009) have been implicated in mediating H3K56ac. H3K56ac is also highly abundant in the distantly related ciliate *T. thermophila* (Garcia et al. 2007) suggesting that this PTM is evolutionarily conserved, however the enzyme responsible for H3K56ac in *T. thermophila* has not yet been identified (Garcia et al. 2007). Furthermore, an abundant histone PTM, di-acetylation of H4 at K5 and K12, mediated by histone acetyl transferase1 (Hat1) enzyme, has been shown to be important for chromatin assembly (Allis et al. 1985; Parthun 2007). This diacetylation of H4K5/12 is highly conserved across the eukaryotic lineage ranging from ciliates to humans (reviewed in Parthun 2012). These observations underscore the evolutionary conservation and biological relevance of histone PTMs in various chromatin related process.

Another histone PTM is the addition of ADP-ribose subunits mediated by a large family of evolutionarily conserved enzymes called Poly (ADP-ribose) polymerases (PARPs) (Citarelli et al. 2010). This modification has been shown to be important for various chromatin related processes, particularly DNA double strand break repair, chromatin compaction as well as transcription regulation (De Vos et al. 2012). Interestingly, recent evidence indicated that in humans, newly synthesized H3/H4 are ribosylated in the cytoplasm, although the functional significance and enzymology behind this PTM remains unknown (Alvarez et al. 2011). A brief overview of some well characterized PARP family enzymes and the biological significance of ADP-ribosylation is provided below.

1.3.1- Poly (ADP-ribose) polymerases (PARPs)

ADP-ribosylation mediated by PARPs is a PTM in which one ADP-ribose moiety from NAD^+ is transferred to specific amino acid residues of the substrate proteins (reviewed in Hottiger 2011) (Figure 5-A). This protein-linked ADP-ribose in turn can act as an acceptor

of additional ADP-ribosylation and an elongation of this chain then results in poly ADP ribosylated proteins. Subsequently, branching in ADP-ribose chains can be introduced with (1'–2') ribose–ribose linkages (Ko and Ren 2012) (Figure 5-A). In contrast to oligomeric or polymeric ADP-ribose (PAR) modifications, mono-ADP-ribosylation is found more commonly within cells (Wielckens et al. 1981). Also most of the poly-ADP-ribosylated proteins studied thus far have been found to be nuclear whereas mono-ADP-ribosylated proteins are predominantly cytoplasmic (reviewed in Messner and Hottiger 2011). In eukaryotic cells, known ADP-ribose acceptor residues include lysine, arginine, glutamate, aspartate, cysteine, phospho-serine and asparagine (reviewed in Messner and Hottiger 2011).

In humans the PARP family includes 17 members with PARP1 being the first to be identified (for review Schreiber et al. 2006). PARP-1 contains two N-terminal zinc fingers (Zn1 and Zn2) (Figure 5-B), which mediate binding to DNA double strand breaks during repair processes and can enhance PARP1 activity up to 500 fold (Eustermann et al. 2011; Langelier et al. 2011). An additional Zn3 domain functions in binding to DNA as well as transmits the DNA binding signal to the PARP catalytic (CAT) domain. PARP1 also has an automodification domain (AD) which mediates self-PARylation. The AD contains a BRCT fold, which functions to mediate protein-protein interactions during DNA repair (Loeffler et al. 2011), and several residues that are targeted for PARP1 automodification. PARP1 also has a C-terminal Trp-Gly-Arg (WGR) domain which binds with DNA near the 5' terminus and mediates domain–domain contacts essential for DNA-dependent activity (Langelier et al. 2012). The catalytic activity is carried out by a CAT domain composed of two sub-domains (helical sub domain–HD, and ART) (Figure 5-B).

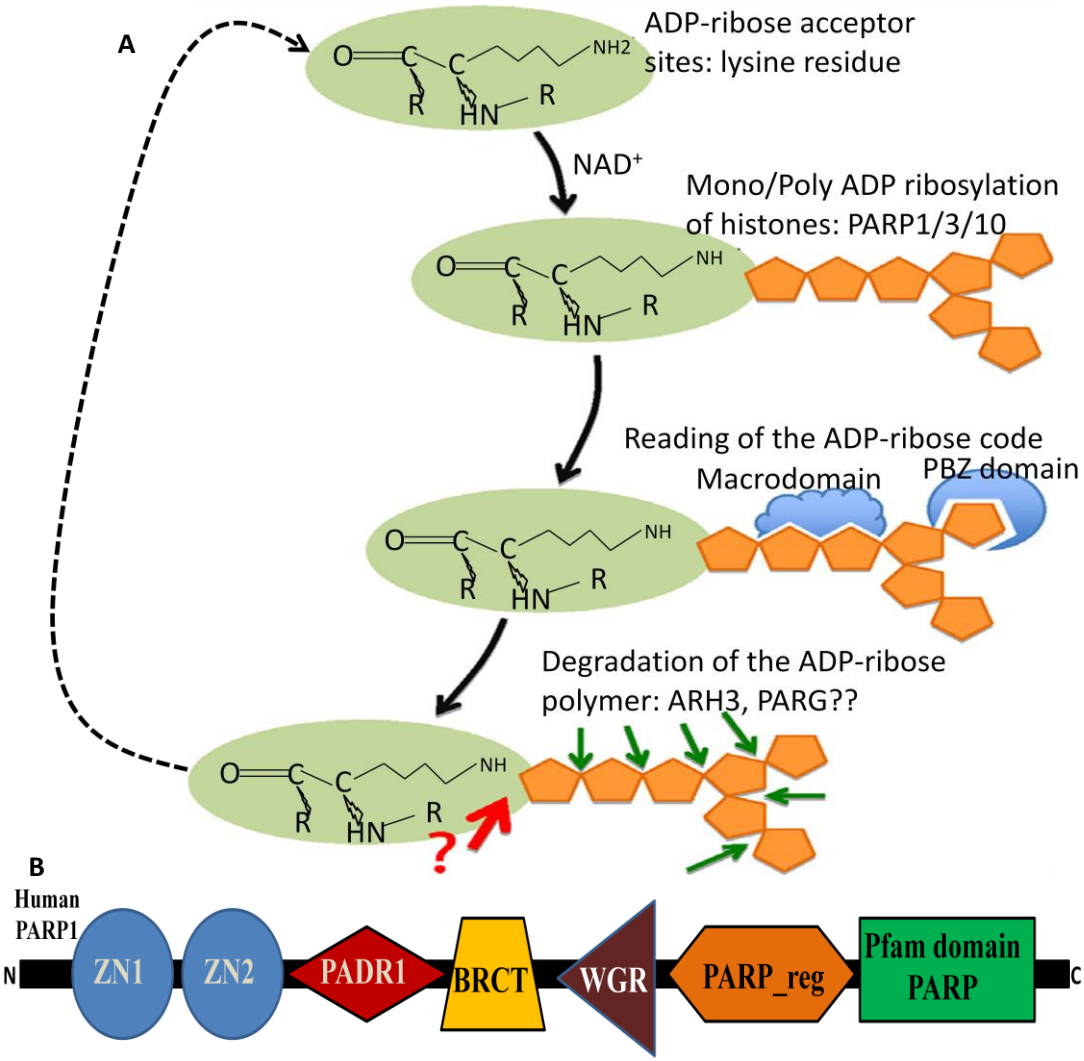

Figure 5: Process of ADP-ribosylation of histone and domain architecture of human PARP1. **A**: The ADP-ribosylation cycle is depicted starting from synthesis on a lysine acceptor residue, recognition by specific factors such PBZ domain proteins, and finally degradation by ARH3 or PARG has been depicted. Note '?' denotes that the specific enzyme responsible for lysine-ADP-ribosylation bond breakage is as yet unknown. The image was adopted from (Hottiger 2011). **B**: Domain architecture of human PARP1 is represented based on SMART domain analysis.

Based on structural organization and the presence or absence of intact CAT domains, PARPs have been sub-divided into two classes; (i) bona fide PARPs (PARP1–6) which contain conserved glutamate residues in the CAT domain that are essential for the formation of PAR chains; (ii) PARP 7–17 which lack the conserved glutamate residues (reviewed in Messner and Hottiger 2011) . It should be noted that among PARPs only a sub-set have been predicted to be able to produce PARs (PARP-1 to PARP-5a and PARP-5b), while two are

inactive enzymes (PARP-9 and PARP-13) and the remaining PARPs are predicted to only produce a mono-ADP-ribose modification (Kleine et al. 2008).

Histone have been demonstrated to be a substrate of PARPs, however, thus far only PARP1/3/10 have been shown to ADP-ribosylate histones (Yu et al. 2005; Messner et al. 2010; Rulten et al. 2011). In contrast to PARP1/3/10, PARP2 was not found to be able to ADP-ribosylate histone tails *in vitro* (Messner et al. 2010). Experimentally ribosylation modification has proven to be difficult to detect on histones *in vivo*. This is because under physiological conditions only a small fraction of all histone proteins (less than 1%) are ADP-ribosylated (Stone et al. 1977; Boulikas 1989). Earlier work has shown that purified core as well as linker histones from rat liver nuclei and from HeLa cells are ribosylated, although the specific PARP enzyme responsible for these modifications was not detected (Burzio et al. 1979). Potentially, histones can be ADP ribosylated immediately after their synthesis in the cytoplasm and during transport to the nucleus, as well as after their incorporation into chromatin (reviewed in Messner and Hottiger 2011). A recent study has provided evidence that in humans, histones H3/H4 are poly-ADP-ribosylated in the cytoplasm (Alvarez et al. 2011). It was reported that newly synthesized histones H3 and H4 are poly-ADP-ribosylated prior to their dimerization in the cytoplasm (Alvarez et al. 2011). Because poly-ADP-ribosylation was one of the earliest PTM marks detected, it was suggested that it might have a function in the proper folding of the newly synthesized histones (Alvarez et al. 2011). Nevertheless the specific PARP responsible for this PTM mark was not reported. Another study isolated the H3.1 and H3.3 pre nucleosomal assembly complexes in humans and reported the co-purification of PARP1 and PARP2 (Drané et al. 2010). These results raise the possibility that PARP1/2 might be the enzymes responsible for the poly-ADP-ribosylation of newly synthesized H3/H4, although experimental verification awaits further

analyses. A recent study has shown that auto-ribosylation of PARP1 switches its role from a chromatin architectural protein to a histone chaperone capable of nucleosome formation activity (Muthurajan et al. 2014).

In humans three members of the PARP family including PARP-1, PARP-2 and PARP-3 have been shown to be catalytically activated upon binding to DNA damage and function in repair of double strand breaks (Amé et al. 1999; D'Amours et al. 1999; De Vos et al. 2012). PARP1 has also been shown to be a transcriptional regulator where it can bind with the promoter elements and regulate gene expression (Kraus and Lis 2003). For example, several studies have provided evidence that ribosylation of chromatin by PARP1 loosens chromatin and makes it accessible for the transcription machinery (Kraus 2008). The functional significance of PARP1 can be estimated by the fact that it is up-regulated in several cancers (Jagtap and Szabó 2005). As well PARP1 null animals exhibit hypersensitivity to DNA damaging agents (Shall and de Murcia 2000). These studies highlight the role of PARP family proteins in a wide range of chromatin related processes. Nevertheless, the full extent of diverse functions carried out by PARPs has only begun to be elucidated and a complete understanding is still far from complete.

1.4- The model organism: *Tetrahymena thermophila*

Tetrahymena thermophila is a unicellular eukaryotic model organism in the phylum Ciliophora and is commonly found in freshwater ponds and lakes (Orias et al. 2011). *T. thermophila* carries four (tetra) membrane-like (hymen) oral structures (Lynn and Doerder 2012) and has been named accordingly. Furthermore, as evident from its name, *T. thermophila* is able to survive under high temperature conditions ranging from 12˚C to 42˚C. However, the optimal growth temperature is 30˚C. Ciliates are distantly related to mammals

and carry ~ 2,280 human orthologs as per the 2006 genome annotation (Eisen et al. 2006). In addition, several core processes including chromatin regulation as well as DNA replication have been found to be highly conserved, thus making *T. thermophila* an excellent model organism to understand several key biological processes (reviewed in Orias et al. 2011).

1.4.1- *T. thermophila* exhibits nuclear dimorphism

Similar to other ciliates, *T. thermophila* exhibits nuclear dualism with two spatially and structurally distinct nuclei present within the same cell. The bigger nucleus called the macronucleus (MAC) is polyploid and contains ~45 copies of most genes as well as ~9000 copies of rDNA (reviewed in Orias et al. 2011). The MAC genome has been sequenced (Eisen et al.,2006) and it contains ~104Mb of DNA with roughly 24,725 known or predicted protein coding genes (Xiong et al. 2012). During vegetative growth of *T. thermophila*, all gene expression occurs from the MAC which is not sexually inherited and is the somatic nucleus (reviewed in Orias et al. 2011).

In contrast to the MAC, the smaller nucleus called the micronucleus (MIC) is diploid and it remains mostly silent during vegetative growth and ensures faithful transmission of the genetic material to the progeny. The MIC genome is ~120Mb in size indicating that it has ~15% greater DNA complexity than the MAC (reviewed in Orias et al. 2011). This discrepancy between two genomes is due to "internally eliminated sequences" (IESs) that are present in the MIC but are deleted from the MAC (Yao et al. 1984).

1.4.2- Two life cycles of *T. thermophila*

The *T. thermophila* life cycle has two phases, vegetative growth and the sexual phase called conjugation. A brief description of each is provided below.

1.4.3- Vegetative growth

Vegetative growth of *T. thermophila* features asexual reproduction through binary fission (reviewed in Orias et al. 2011). During vegetative growth the MIC divides by mitosis and is responsible for the equal distribution of the MIC DNA between two daughter cells. During vegetative growth, the MIC remains transcriptionally silent and hence is not subject to any selective pressures against loss of MIC chromosomes. In fact, frequently in nature, cells without a MIC are found. Thus cells can keep growing vegetatively without the presence of a MIC.

In contrast to the MIC, the MAC divides by amitosis and does not have any mechanism of equal segregation of alleles. Consequently, the MAC genetic contents are randomly distributed to the daughter nuclei. This feature of *T. thermophila* biology allows for phenotypic assortment. In phenotypic assortments a heterozygote can eventually become homozygous for a particular gene (reviewed in Orias et al. 2011). The process of phenotypic assortment can be accelerated in laboratory settings by selecting for a particular gene locus of interest (Figure 6).

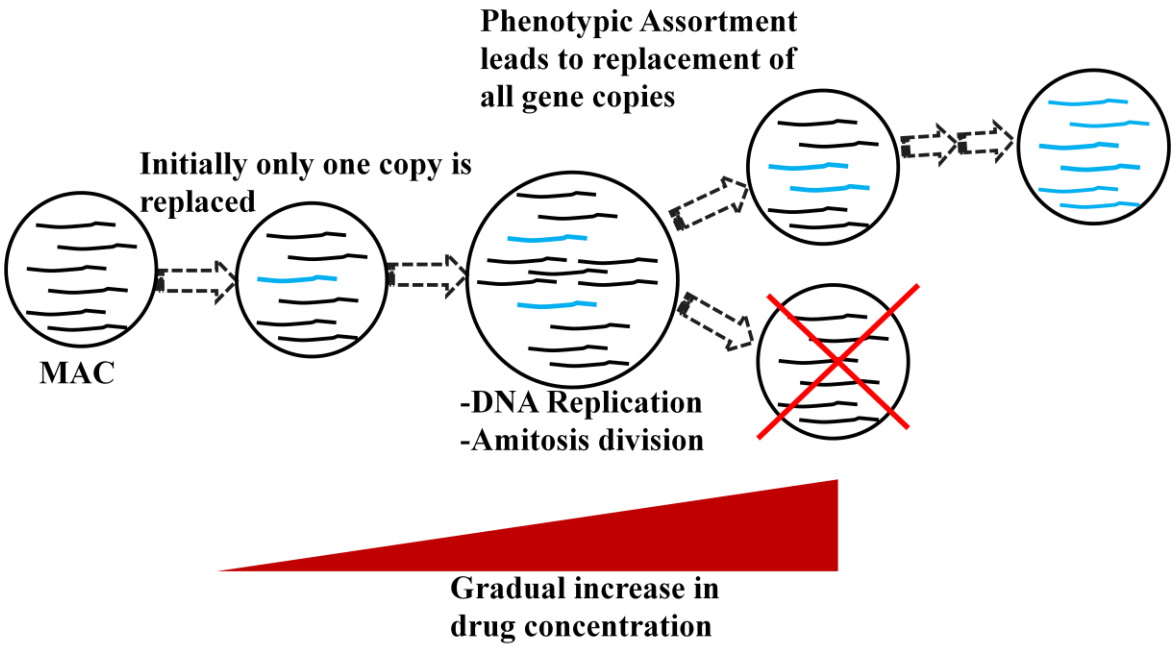

Figure 6: Cartoon of accelerated phenotypic assortment in the MAC. In the beginning only one copy of a MAC chromosome or allele is replaced as a result of biolistic transformation of a gene targeting vector. The MAC divides by amitosis lacking any mechanism of equal allelic segregation. As the cell divides, selective drug concentration is increased gradually. This selects for only those cells that receive more and more replaced gene copies until MAC homozygosity is achieved. Note: Image has been designed as a part of collaborative effort with Nabeel-Shah S and Fillingham JS.

1.4.4- Conjugation

Another feature of *T. thermophila* is that it has seven different mating types (I to VII). Cells from one type are capable of mating with any other mating type but not with the cells of same mating type (Martindale et al. 1982). Within laboratory settings mating or conjugation can be induced when cells of different mating types are starved and mixed in approximately equal numbers.

During conjugation, cells of two different mating types fuse at their oral apparatuses and each embark on a journey of intricate events as outlined below (Figure 7). To begin with, the MIC starts elongating and adopts a typical shape termed "crescent" which marks the initiation of prophase. Following meiosis I and meiosis II reductional divisions four haploid nuclei are produced. One of these nuclei is then selected and remains in the anterior of the cell whereas the remaining three nuclei are degraded. The selected nucleus then divides once by mitosis and produces two identical nuclei referred to as pro-nuclei. One of the pro-nuclei is called the migratory nucleus whereas the other one is called the stationary nucleus. The paired cells exchange their migratory nuclei which are then fused to the stationary nuclei present within each mating partner. This results in the generation of a zygotic nucleus with restored diploid genetic content within each mating partner. The zygotic nucleus undergoes two rounds of mitosis which results in 4 genetically identical diploid nuclei. Two of these resulting nuclei found in the anterior of the cells differentiate into macronuclei whereas the remaining two posterior nuclei remain as diploid micronuclei. Within these differentiating MACs, site-specific DNA rearrangements and mating type determination occurs. The developing MACs termed anlagen start swelling whereas the parental old MAC moves toward the posterior end of the cell and initiates degradation in a processes that resembles lysosomal autophagy (Akematsu and Endoh 2010). At this stage, the gene expression

switches to the developing MACs. The parental MAC continues getting degraded until after the mating pairs are separated (ex-conjugants). In addition, one of the two new MICs is also destroyed in the ex-conjugants. Upon introducing the food source, in each ex-conjugant the MIC divides by mitosis and cells undergo their first post-zygotic cell division resulting in 4 karyonide cells (Martindale et al. 1982) (Figure 7 A-K).

During conjugation, the emergence of the new MAC requires extensive programmed DNA rearrangements, resulting in the removal of ~15% of DNA from the anlagen. The remainder of the anlagen genome is then endo-replicated ~ 50 times (Yao et al. 1984). Two types of genome rearrangements have been reported. The first one involves the removal of MIC specific sequences from the anlagen. These sequences are called internally eliminated sequences (IES) and are ~6000 in number with varying length (0.5 to 20 Kb) (Yao et al. 1984). The elimination of IES has been demonstrated to occur through an RNAi-like pathway and a scan RNA model has been suggested (Mochizuki et al. 2002). The second type of DNA rearrangement is chromosome breakage which occurs at conserved sites of a 15bp sequence (BES for breakage eliminated sequence) (Fan and Yao 2000). The breakage of five germline-derived chromosomes results in generation of nearly 250 unique somatic chromosomes (Yao et al. 1990). The enzymology behind BES is currently unclear.

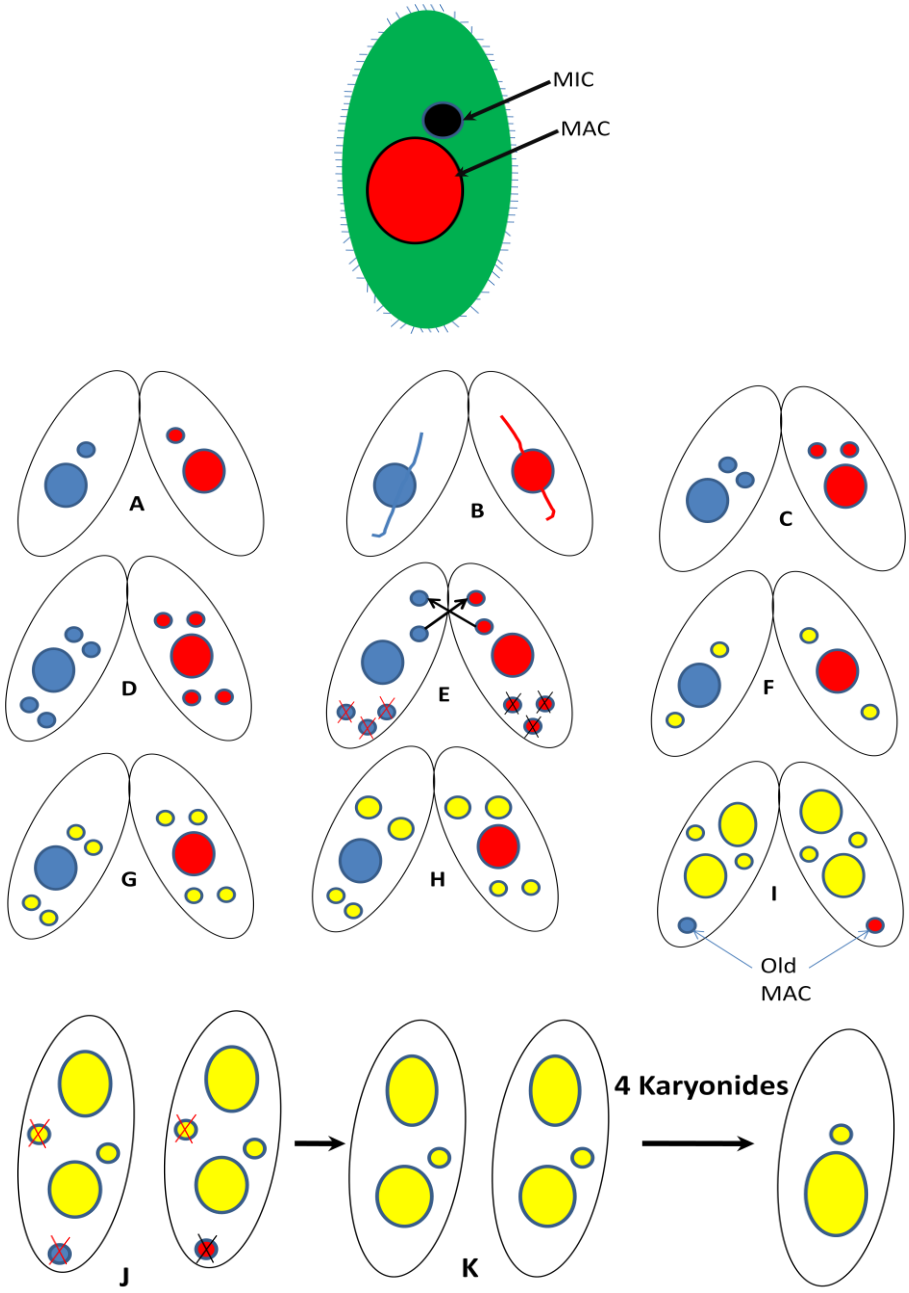

Figure 7: *T. thermophila* conjugation events. **Top**: Vegetative cell with distinct MIC and MAC is shown. Cilia are also depicted. **Bottom: A-J**: Different stages of conjugation are depicted (see text for details). Image designed an adaptation of (Martindale et al. 1982).

1.4.5- Utility of *T. thermophila* as a model system

T. thermophila has been long used as an experimental tool and its unique biology offers an excellent opportunity to study various cellular as well as developmental processes. It has a short generation time (~2 ½ hours) and cells can be grown to large volumes in axenic medium. To facilitate molecular genetic analyses, the fully sequenced MAC genome (Eisen et al. 2006) is freely available through *Tetrahymena* genome database (TGD*:* http://ciliate.org/index.php/home/welcome). Furthermore, micro-array based gene expression profiles for all of the predicted as well as experimentally verified open reading frames are available throughout growth, starvation and conjugation phases of the *T. thermophila* life cycle (Miao et al. 2009) (http://tfgd.ihb.ac.cn/). A gene network analysis based on the available expression profiles has also been constructed providing useful insights into gene function (Xiong et al., 2011). Recently, expression profiles based on RNA-seq analysis have also been reported which significantly enhanced existing genome annotation and provided a comprehensive view of global transcriptome of *T. thermophila* (Xiong et al. 2012). ~5.2% of *T. thermophila* genes undergo alternative splicing, a number that has not been observed in any other unicellular eukaryote (Xiong et al. 2012). These features make *T. thermophila* a suitable unicellular eukaryote to study alternative splicing.

In addition, several molecular and biochemical tools have been developed to investigate *in vivo* gene function. For example, exact gene replacement via homologous recombination (HR) is possible facilitating the creation of epitope tagged cell lines as well as knock out (KO) strains (Hai et al. 2000). Cells can be transformed by a variety of methods including electroporation, microinjection, as well as biolistic transformation (Bruns and Cassidy-Hanley 2000; Turkewitz et al. 2002).

The polyploid MAC provides a rich source of chromatin. This feature makes *T. thermophila* particularly suitable for studying chromatin dynamics. Furthermore, the spatial distinction of transcriptionally active and silent chromatin states in the form of MAC and MIC, respectively, offers a compelling opportunity to study the assembly pathways as well as functional aspects of different chromatin states. *T. thermophila* utility as a model organism can be appreciated by the fact that it has led to several key discoveries in basic science including those of catalytic RNA and telomerase, both of which led to Nobel prizes (Kruger et al. 1982; Greider and Blackburn 1985).

1.5- Thesis rationale

Chromatin exists in a variety of forms that regulate most aspects of DNA mediated transactions such as gene expression as well as formation of distinct functional domains of chromatin (reviewed in Mariño-Ramírez et al. 2005; Aalfs and Kingston 2000). PTMs of the canonical core histones are used as marks to define distinct chromatin regions. For example, an enrichment of H3K27me3 marks signify tightly condensed heterochromatin (reviewed in Rivera et al. 2014) whereas acetylation of H3K4me2 relaxes the chromatin and facilitates transcription (Bernstein et al. 2005). How these histone PTMs are targeted to certain chromatin regions and how these epigenetic marks are maintained during DNA replication is not fully understood.

Histone variants are expressed throughout the cell cycle and their incorporation onto chromatin can alter its biophysical properties. To deposit histone onto chromatin, cells can adopt two pathways, DNA replication dependent (RD) and replication independent (RI) chromatin assembly (Smith and Stillman 1991; Green et al. 2005). During RD chromatin assembly, newly synthesized canonical histones are deposited onto replicating DNA whereas

histone variants are assembled via the RI pathway. RD and RI chromatin assembly pathways are mediated by distinct protein complexes. For example, H3.1/H4 RD assembly is mediated by the CAF1 complex whereas HIRA has been shown to be responsible for H3.3 deposition in the RI pathway (Smith and Stillman 1991; Tagami et al. 2004; Green et al. 2005) . Similarly, the H2A variant H2A.z is deposited in the RI pathway via the SWRI complex (Kobor et al. 2004). The discovery of these protein complexes and their roles in mediating distinct assembly pathways has elucidated several aspects of chromatin dynamics. However how histone variants are targeted to certain genomic regions remains poorly understood.

An accumulating body of evidence has correlated defects in chromatin assembly pathways with disease formation in humans (Burgess and Zhang 2013; Ronan et al. 2013). For example, in humans RI chromatin assembly chaperone HIRA is located in a small region on chromosome 22 which often is deleted in DiGeorge syndrome (Lorain et al. 1996). Numerous studies have shown that defective histone PTMs such as acetylation can lead to the formation of several disorders including leukemia, epithelial cancers, fragile X syndrome, and Rubinstein-Taybi syndrome (Timmermann et al. 2001; Ronan et al. 2013). In addition, histone acetylation has been found to be significantly reduced in Alzheimer's disease (Zhang et al. 2012). Studying how histone dynamics are regulated within cells and what chaperones or protein factors might function in their deposition as well as modification should help provide a better understanding of chromatin mediated processes.

The spatial distinction of two structurally and functionally distinct nuclei in *T. thermophila*, i.e., transcriptionally active MAC and transcriptionally silent MIC, offers a unique opportunity to study chromatin-related processes. The *T. thermophila* genome encodes four H3 genes including *HHT2* (major H3), *HHT3* (H3.3), *HHT4* (H3.4) and a centromeric histone *CNA1* whereas *HTA1*, *HTA2* and *HTA3* respectively encode two H2A

proteins and their variant Hv1. Furthermore, *T. thermophila* also contains specialized linker histones for each nucleus, i.e. MAC specific H1 and MIC specific MLH1 (Micro-linker histone 1). Previous studies have shown that similar to higher eukaryotes *T. thermophila* major H3s are deposited via RD chromatin assembly whereas H3.3 is predominantly deposited through the RI pathway (Cui et al. 2006). Cui et al. (2006) found that while H3.3 mainly localizes to the MAC consistent with its role in gene transcription, small amounts of H3.3 were also found in the MIC. The observed MIC localization was suggested to be a consequence of inefficient entry of H3.3 into the RD pathway (Cui et al. 2006). However, which histone chaperones might be involved in these processes is not known. In contrast to H3.3—a non- essential gene in *T. thermophila*, H2A variant Hv1 was found to be essential for cell viability (Liu et al. 1996). In addition, consistent with its functions in gene transcription, Hv1 was found to be exclusively in the MAC during vegetative growth (Stargell et al. 1993). However, how Hv1 is specifically targeted to the MAC is currently unknown.

To gain functional insights into histone dynamics I initiated a proteomic analysis of major histones H3 and H2A as well as replacement histones H3.3 and Hv1 in *T. thermophila.* Specifically, I was interested to identify and investigate the role of interacting proteins that might be involved in chromatin assembly, histone PTMs as well as targeting the histone variants to specific nuclei. Using affinity purification combined with mass spectrometry (AP-MS), I expected to identify and gain insights into functions of histone interacting proteins and their role in chromatin-related processes.

1.6- Summary

To study the protein-protein interactions of histones, I engineered *T. thermophila* cell lines expressing C-terminal FZZ (3×FLAG-Tev-ZZ) epitope tagged *HHT3* (H3.3), *HTA1* (H2A), *HTA3* (Hv1) and *MLH1* from their native chromosomal loci. Specifically, my objective was to provide a comprehensive view of the histone interactome in *T. thermophila* and derive functional insights. The FZZ epitope tag permitted me to carry out affinity purification for each protein of interest. The co-purifying proteins were analyzed by mass spectrometry (MS) to identify binding partners. My results indicated that the major histone H2A-FZZ co-purified with H2B, putative Spt16 (Spt16^{Tt}) and Pob3 (Pob3^{Tt}) subunits of the *T. thermophila* FACT complex, as well as a putative Npm1-like^{Tt} histone chaperone. These results suggest that Npm is an ancient chaperone of H2A/H2B that was present well before the emergence of modern metazoans. Interestingly, H2A also co-purified with putative PARP2^{Tt} and PARP6^{Tt} proteins suggesting that soluble histones in *T. thermophila* might be subject to ADP-ribosylation activity. To confirm these interactions, I engineered Spt16^{Tt} and PARP6^{Tt} *T. thermophila* cell lines expressing C-terminal FZZ epitope tags from native chromosomal loci and performed AP-MS. My data indicated that Spt16^{Tt} co-purified with Pob3^{Tt} further reinforcing the idea that the composition of the two subunit FACT complex is evolutionarily conserved.

MS data also indicated that Hv1 interacts with Importinβ3 protein which has previously been shown to predominantly localize in the MAC (Malone et al. 2008). The Hv1-Importinβ3 interaction suggests a possible mechanism of targeting Hv1 specifically to the MAC and not to the MIC. In addition, my data also established that H3.3-FZZ co-purifies with a histone chaperone NASP-related protein 1 (Nrp1) as well as PARP6. Nrp1 has previously been identified as an Asf1^{Tt} interacting protein (Garg et al. 2013) and belongs to

an evolutionarily conserved family of H3/H4 chaperones (Finn et al. 2008). These results have revealed a complex interplay among histones, histone chaperones and several other protein factors including putative histone modifying enzymes that might function in regulating histone dynamics such as their flow to distinct nuclei in *T. thermophila*.

Chapter 2: Materials and Methods

2.1- Equipment

An Eppendorf 5424 centrifuge was used to carry out all room temperature centrifugations in 1.5ml Eppendorf tubes. For all 4°C centrifugations, a Sorvall Legend Micro 21R refrigerated microcentrifuge (Thermo Scientific) was employed. Similarly, for 5/50ml Falcon tubes, centrifugations at room temperature and at 4°C, Centra CL32 (IEC) and Sorvall Legend RT centrifuges were used, respectively. To centrifuge large cultures (500ml) of *T. thermophila*, an Avanti J-30I (Beckman Coulter) was employed. GeneAmp PCR System 9700 (Applied Biosystems) was used for polymerase chain reactions (PCR). All bacterial cultures were grown using Innova 2300 platform shaker (New Bruswick scientific). *T. thermophila* cells were grown using G10 Gyrotory shaker (New Bruswick scientific).

2.2- Cell Strains

T. thermophila cell strains of inbreeding line B, CU428 [*Mpr*/*Mpr* (VII, mp-s)] and B2086 [*Mpr*$_+$/*Mpr*$_+$ (II, mp-s)], were obtained from the *Tetrahymena* stock center Cornell University, Ithaca N.Y (https://tetrahymena.vet.cornell.edu/). 1×SPP axenic media (see Appendix 1) was used to grow *T. thermophila*.

2.3- Sequence Data Retrieval

In order to acquire gene sequences of *HHT2*, *HHT3*, *HTA1*, *HTA3*, and *MLH1* which respectively encode histones H3, H3.3, H2A, Hv1 and MLH1, the *T. thermophila* genome database (http://ciliate.org) was used. These genes were identified in the database based on available annotations emerging from previous work. In addition, multiple sequence alignments were built using Clustal Omega (http://www.ebi.ac.uk/Tools/msa/clustalo/) and ClustalX color coding (Appendix 2) was used to represent the resulting alignments.

Furthermore, the network diagram of physically interacting proteins was constructed using cytoscape version 3.02 (Shannon et al. 2003).

2.4- Media, buffers, solutions

Recipes for all media, buffers, and solutions used in this study are provided in Appendix 1.

2.5- Growth conditions

2.5.1- *E.coli* cell growth:

Genetically engineered vector pBKS-FZZ was transformed into *E. coli* cells, which were grown on LB+ ampicillin (100μg/ml; LB+amp) plates overnight at 37°C. Subsequently plates were stored at 4°C. To isolate plasmid DNA, 1.5 mL *E.coli* culture was grown overnight in LB+amp liquid medium with continuous shaking at 250 rpm at 37°C.

For long term storage of *E. coli* cells, glycerol stocks were prepared such that 0.8mL of overnight liquid *E. coli* culture was mixed with 0.8ml of sterile 50% glycerol in a 1.8ml CryoPure cryovial (Sarstedt), mixed well and stored at -80°C.

2.5.2 *T. thermophila* growth:

T. thermophila were grown vegetatively in sterile flasks in sequestrin proteose peptone (SPP) medium supplemented with penicillin-streptomycin-fungizone (PSF) at 30°C with shaking at 90 rpm. No more than 1/10 volume of culture to the volume capacity of the flask was used to allow for efficient aeration of the cells.

Phenotypic assortment and cell selection was carried out by growing the vegetative cells in 96-well microtiter plates (Sarstedt) in SPP medium. The medium was inoculated with the appropriate concentration of the drug paromomycin. To starve the *T. thermophila* cells, they

were harvested by centrifuging at 3000rpm for 5min and re-suspended in 10mM Tris-HCl, pH 7.4. Starvation was carried out without shaking the cells for 18 hours.

To freeze the *T. thermophila* cells, they were grown overnight as described above and were harvested by centrifuging at 3000rpm for 5min. Cells were re-suspended in 10mM Tris-HCl, pH 7.4 and again were harvested by centrifuging at 3000rpm for 5min. Finally cells were re-suspended in 10mM Tris-HCl, pH 7.4 for starvation which continued for two days at 30°C without shaking in a 500ml Erlenmeyer flask. After two days, cells were aspirated to 250µl and 10% DMSO (Sigma) in 10mM Tris pH 7.4 was immediately added (final DMSO concentration=8%) to re-suspend the cells. CryoPure cryovials (Sarstedt) were used to store 0.5ml of DMSO treated cells which were then stored in liquid nitrogen.

2.6- *T. thermophila* genomic DNA extraction

Genomic DNA extraction of *T. thermophila* wild type strains B2086 or CU428 was performed following the method of (Gaertig et al. 1994). 1ml cells growing in log phase were collected in 1.5ml Eppendorf tubes and were harvested at room temperature by centrifugation at 3,000 rpm for 2 minutes. The supernatant was discarded and the pellet was re-suspended in 500µl of *T. thermophila* lysis solution. Lipids and protein were removed from the cell lysate using phenol:chloroform (1:1) extraction. This step was performed twice as follows: To the 500µL cell suspension (100µl cell lysate + 400µl lysis solution) 250µl phenol and 250µl chloroform was added. The solution was mixed to homogeneity until it turned opaque. The solution was centrifuged at 11,000rpm-13,000rpm for 1min at room temperature. The top layer (~500µl) was transferred to a new 1.5ml Eppendorf tube. Subsequently, an equal volume of chloroform was added and homogeneity was achieved by mixing the solution. Once again the sample was centrifuged at the same speed for 1min at room temperature and the top layer (~500µl) was transferred to a new 1.5ml Eppendorf tube. Then 200µl of 5M

NaCl and 800µl of isopropanol were added to the sample to precipitate the DNA. The sample was centrifuged at 13,000 rpm for 2 minutes at room temperature and the supernatant was discarded. The DNA pellet was washed with 200µl of 70% ethanol, and this step was repeated to ensure the removal of residual isopropanol. The pellet was dessicated in a vacuum dessicator for 30 minutes to remove any ethanol residue from the sample. Finally the pellet was resuspended in 100µl ddH_2O and 1µl of RNase (10mg/ml) was added. The sample was incubated at 37°C for 1 hour and stored overnight at 4°C and subsequently at -20°C.

2.7- *E. coli* plasmid DNA isolation

Extraction of plasmid DNA from *E. coli* was done as follows: 1.5mL of culture was grown overnight and then according to the method outlined in High-Speed Plasmid Mini Kit from GeneAid, plasmids were extracted. The sample (plasmid) was analyzed by electrophoresis through an 0.8% agarose gel (made with 1X TBE and stained with 0.1% v/v of 10mg/ml ethidium bromide for UV visualization.

2.8- Polymerase chain reaction (PCR)

In order to perform PCR, a 20µl reaction was set up in a 0.2mL thin-walled PCR tube as follows: 1µl Forward Primer (30pmol/µl), 1µl Reverse Primer (30pmol/µl), 7µl ddH_2O, 1µl genomic *T. thermophila* DNA and 10µl 2x Prime STAR Max DNA Polymerase (TaKaRa). Reactions were carried out using the following conditions (Table 1) and recovery of the PCR product was assessed via agarose gel electrophoresis (see Appendix 3 for primers):

Table 1: Table summarizes the PCR conditions used to amplify T. thermophila gene loci

PCR step	Temperature	Time
Initial denaturation	98°C	5 min
The following cycle was repeated 35 times		
Denaturation	98°C	10 seconds
Annealing	55°C	15 seconds
Elongation	72°C	1 min
Final elongation	72°C	10 min

2.9- DNA restriction digestions and gel extraction

Using appropriate enzymes (see below) with manufacturer (New England BioLabs) specifications for digestion conditions, both the plasmid and the PCR products were digested. PCR and enzymatic cleanup of the products were carried out using an EZ-10 Spin Column PCR Products Purification Kit (Bio Basic). Gel extractions were carried out with an EZ-10 Spin Column DNA Gel Extraction Kit (Bio Basic). All procedures were carried out using manufacturers' specifications.

2.10- DNA ligation and transformation into competent *E. coli*

Ligation reactions were setup using the following conditions: linear plasmid DNA digested with appropriate restriction enzymes 20-100 ng (~1 µl) was used, PCR insert 5µl (depending on PCR to plasmid concentration), 2 µl of 10×T4 DNA ligase buffer, T4DNA ligase enzyme 1U and if needed ddH2O (final volume 20 µl). The mixture was left at room temperature for 1hour. After this, 25µl high-efficiency competent *E. coli* cells (NEB DH5-alpha, New England BioLabs) were added and transformation was carried out using the "High Efficiency Transformation Protocol" for "C2987" provided by New England BioLabs. Briefly, DNA 1-10ng was mixed with cells and left on ice for 30 minutes. Subsequently, cells were heat shocked at 42˚C for 20 seconds and were placed on ice for 5 min, after which 950µl SOC media was added. Cells were grown at 37˚C for 1hour with shaking at 250 rpm. Finally, cells were spread on LB+Amp agar plates and were grown overnight at 37˚C.

2.11- DNA sequencing

To conform that genes of interest and DNA was successfully ligated into the desired gene targeting vector, DNA sequencing was carried out at The Centre for Applied Genomics (The Hospital for Sick Children), or at the Core DNA Sequencing Facility, York University). The sequencing primers are listed in Appendix 3.

2.12- Construction of 3xFLAG-TEV-ZZ (FZZ) gene targeting vectors

Genetically engineered plasmid pBKS-FZZ was provided by Dr. Kathleen Collins, (University of California, Berkely, CA) and was used to target *T. thermophila* gene loci of interest. The plasmid was designed to target the genes to the correct endogenous locus for creating C-terminal epitope tagged proteins. The plasmid contained a triple FLAG tag fused to a tobacco etch virus cleavage site followed by two repeats of the Z domain of the *Staphylococcus aureus* protein A (3xFLAG-TEV-ZZ, or FZZ). For selective drug marker, a NEO2 cassette which confers paromomycin antibiotic resistance has also been integrated in the plasmid. Notably, NEO2 does not have homology to any *T. thermophila* endogenous locus and thus risk of false integration via homologous recombination has been eliminated.

To engineer FZZ epitope tagging vectors, the following method was employed: The PCR primers were designed 1 kb upstream and downstream of the predicted stop codons for each of the selected genes. The PCR reaction was set up to amplify DNA using primers with built-in restriction sites. Upstream forward and reverse primers had *KpnI* and *Xho1* sites, respectively, whereas downstream forward and reverse primers carried *NotI* and SacI sites, respectively (See Appendix3 for primer sequences). The PCR products were further digested with appropriate restriction enzymes, i.e. *KpnI, Xho1* (upstream) and *NotI, SacI,* (downstream) respectively to create sticky ends. Cloning (ligation) of the PCR product into

the FZZ epitope tagging vector was set up as described above. The molecular cloning was a 2-step sequential ligation process in which the upstream region was cloned as the first step and once confirmed with sequencing, then the downstream region was cloned and sequenced. Once both regions were cloned, the plasmid was digested with *KpnI* and *SacI* restriction enzymes to make the vector linear before transforming into *T. thermophila*.

2.13- Transformation of *T. thermophila*

Biolistic transformation (Bruns and Cassidy-Hanley 2000) with a PDS-1000/He Biolistic particle delivery system (Bio-Rad) was used to transform *T.thermophila* for macronuclear gene replacement.

50ml of B2086 or CU428 wild type *T. thermophila* cells were grown to log phase (2×10^5 cells/ml) in SPP+PSF medium with gentle shaking overnight. The next day, cells were pelleted followed by washing (twice) with 10mM Tris-HCl pH 7.4. Subsequently, cells were re-suspended in 50ml 10mM Tris-HCl pH 7.4 in a flask and were starved (~18 hours) at 30ºC without shaking.

Linearized DNA (1µg/µl) was coated on 1.0µm gold particles (Bio-Rad) for each transformation. Briefly, 3-4µl of DNA to 25µl of gold beads (per transformation), 25µl of ice cold 2.5M calcium chloride , and 10µl of cold 0.1M spermidine (Sigma) were vortexed at 4°C for 15mins. The DNA coated gold was washed with 200µl of 70% ice cold ethanol followed by another wash with 200µl of 100% ice cold ethanol. Finally, 20µl of 100% ice cold ethanol was used to re-suspend the DNA coated gold pellets.

In order to wash and sterilize the apparatus, the gene gun parts were washed with ddH_2O and 70% ethanol. Flying disks washed with 70% ethanol and dried were used to coat the gold coated DNA. Starved *T. thermophila* cells were centrifuged at 3000 rpm at room temperature

and re-suspended in 1ml of 10mM Tris-HCl pH 7.4. The 'gene gun' was assembled, and 1mL of starved cells was concentrated on a pre-wet (10mM Tris-HCl pH 7.4) 9cm filter paper. A 900psi rupture disc (Bio-Rad) was dipped into isopropanol and fitted into the holder and tightened. The concentrated cells were placed in the second slot from the bottom in the gene gun. Cells were bombarded with DNA coated gold particles at ~900psi at a pressure of 25-26psi. The cells along with the filter paper were transferred to pre-warmed 50mL SPP medium and incubated at 30°C for 4 hours with gentle shaking to recover.

Cells were transferred to a 96-well microtiter plate, 200µl per well, after adding 100mg/ml of paromomycin to a final concentration of 100µg/ml. Cells were incubated at 30°C for 4 days. Following the incubation period, cells were observed under the microscope for robust growth which was followed by the transfer of growing cells to higher drug concentration. By increasing the drug concentration in a stepwise fashion, phenotypic assortment was achieved such that all endogenous copies of the gene were replaced with the FZZ-tagged versions. This is generally achieved when cells are able to grow at 1mg/ml of paromomycin.

2.14- Western blot analysis

Western blot analysis was performed to examine the expression of the tagged proteins. A trichloroacetic acid (TCA) approach, as previously described (Bright et al. 2010), was used to prepare *T. thermophila* cell extracts. Briefly, cells growing in log phase were harvested in Eppendorf tubes by centrifugation at 13,000rpm at room temperature for 2 minutes. After washing the resulting pellets with 10mM Tris-HCl pH 7.4, cells were re-suspended in 100µl of 10mM Tris-HCl pH 7.4. 10% TCA was added and cells were left on ice for 20 min. Cells were centrifuged at room temperature and the supernatant was discarded. The resulting pellet was resuspended in 100µl of 2× SDS buffer and 1µl of 1N NaOH was added to neutralize the

solution. After boiling the samples for 5min, extracts were either frozen at -80°C for later use or were immediately loaded onto gels.

Sodium dodecyl sulfate polyacrylamide gel electrophoresis (SDS-PAGE) was used to separate the proteins based on size. To prepare the gels, a 5% stacking gel was layered on top of a 10% running gel. Then 2×10^5 cell equivalents per sample were resolved alongside 5µl of PiNK Plus Prestained Protein Ladder (Appendix4). In 1× SDS-running buffer the gel was electrophoresed at a constant voltage of 100V for 1-2 hours. The separated proteins were transferred on PVDF membrane (Bio-Rad) activated in 100% methanol using 1x Western transfer buffer at 10V overnight or 75V for 2 hours. Subsequently, the membrane was blocked in 5% Blotto for 1 hour at room temperature followed by three 5 minutes washes in 1x PBS to get rid of excessive milk proteins.

Western blots were incubated with monoclonal mouse α-FLAG (Sigma-Aldrich) primary antibody diluted 1:3000 in 5% BLOTTO. To control for equal loadings, monoclonal mouse α-actin (GenScript) primary antibody diluted 1:1000 in 5% BLOTTO was used. Both incubations were carried out for 1 hour at room temperature. Blots were washed three times (5 minute each) using 1x PBS and incubated with horseradish peroxidase-conjugated polyclonal goat α –mouse (Cedarlane) secondary antibody diluted 1:3000 in 1% BLOTTO for one hour at room temperature. Finally, to remove any excessive antibody, blots were washed three times as above and were visualized using Denville Scientific's HyGLO Chemiluminescent HRP AntiBody detection Kit (E2500) according to manufacturer specifications

2.15- Tandem affinity purification (TAP)

To isolate the native protein complexes of epitope tagged proteins, Tandem Affinity Purification (TAP) was performed. TAP is a two step purification procedure (see details below) which ensures the stringent removal of any contaminating non-specific proteins. However, such harsh conditions can also potentially result in loosing real but transient interactions. Therefore, to improve the probability of capturing any transient interactions, I also performed a one step affinity purification procedure for each protein of interest (details on TAP modifications are provided below).

T. thermophila were grown in 500ml of 1×SPP to a final concentration of 3×10^5 cells/ml and were pelleted. The resulting pellets were used as a starting material for the TAP. 25ml of 2×Lysis buffer as well as 50ml of 1×Lysis buffer was prepared and 500µl of protease inhibitor (sigma) + 200µl 100mM PMSF prepared in isopropanol was added to each of these buffers prior to lysing the cells. Cells were resuspended in an equal volume of ice-cold 2x lysis buffer (protease inhibitors added) and the total volume of the solution was adjusted to 15ml with 1x lysis buffer+protease inhibitors. 300µl of 10% NP-40 (final 0.2% v/v) and 5µl of benzonase nuclease (Sigma) was added. Tubes were incubated for 1 hour at 4°C with end-to-end rotation in order for benzonase to digest released genomic DNA.

In order to clarify the whole cell extracts (WCE), cells were divided into 1.5ml Eppendorf tubes and centrifuged at 14,000rpm for 30 minutes at 4°C. The clarified supernatants were pooled in a 50ml falcon tube (Note: 100µl of WCE was saved as input material for WB analysis) and IgG-Sepharose (chromatography resin for the first step of affinity purification) was prepared (see below) and added to the pooled supernatants.

The IgG-Sepharose was washed and equilibrated in the lysis buffer prior to use. Each affinity purification requires 250µl (200µl will also work) of packed bead volume (PBV) of the IgG-sepharose. Beads were washed and equilibrated into 1x lysis buffer i.e. 1:1 of beads: buffer. The resulting slurry was added to each sample which was then set on end-to end rotations for 4 hours.

Upon completion of the IgG incubation period, samples were centrifuged at 4,000rpm for 5 minutes at 4°C. 20ml of 300mM NaCl wash buffer (IPP300) was used to wash the beads once, followed by two washes with 15ml of 1×Tev buffer. The beads were then transferred to separate 1.5ml Eppendorf tubes along with 750µl of 1x TEV buffer. To this 8µl of TEV Protease enzyme (2mg/ml) (kind gift from Dr. Jack Greenblatt, University of Toronto) was added for an overnight end to end rotation at 4°C. This releases IgG bound proteins by cleaving at the TEV site. On the following day, the samples were centrifuged at 2,000rpm for 2 minutes at 4°C, and the supernatant (TEV eluate) was collected into individual ice-cold 1.5ml Eppendorf tubes. To ensure that all of the eluted proteins have been collected, the remaining beads were re-suspended in 600µl of IPP100 buffer and were again centrifuged at 2,000rpm for 2 minutes at 4°C. The supernatant was transferred to the previous supernatants in the ice-cold 1.5ml Eppendorf tubes.

In the second step of TAP, agarose beads conjugated with anti-FLAG antibody (M2 agarose beads- Sigma) were used. 30µl of M2-agarose was used for each sample. The beads were first washed with IPP100 buffer by rotating them for 3 minutes at 4°C and centrifuging at 3,000rpm for 2 minutes at 4°C. Beads were re-suspended in an equal volume of IPP100 buffer. The resulting slurry was divided into pre-chilled Eppendorf tubes and the TEV eluate from each sample was added. The tubes were rotated end-to-end for three hours at 4°C.

After three hours of incubation, beads were washed once with IPP100 buffer followed by two washes with IPP100 made without NP40. The pellet was re-suspended in 750µl of 2mM $CaCl_2$/20mM Tris and centrifuged at 5,000 rpm for 1 minute at room temperature. After removing the supernatant, 500µl of freshly prepared 0.5M NH4OH was added and the tubes were rotated for 20minutes at room temperature. The eluted proteins were collected by centrifugation at 5,000 rpm for 2 minutes at room temperature. The resulting samples containing proteins were transferred to pre-chilled Eppendorf tubes and stored at -80°C for MS and Western blot analyses.

The one step affinity purification procedure does not involve IgG-Sepharose binding and TEV cleavage steps. In this case, the clarified WCEs were directly transferred to 50µl of M2-agarose beads. The remaining steps are the same as outlined above.

In order to visualize the affinity purified proteins silver staining was carried out. The affinity purified material was electrophoresed on a 4-10% gradient SDS-gel. The staining was performed using 'ProteoSilver' silver stain kit (Sigma), and manufacturer guidelines were followed. Image was taken using chemi-doc system (Bio-rad).

2.16-Mass spectrometry and SAINT analysis

The MS analysis was carried out by Dr. J.P. Lambert at the collaborating laboratory of Dr. Ann-Claude Gingras in the Lunenfield-Tanenbaum Research Institute at Mount Sinai Hospital, Toronto. TAP purified proteins eluted in 0.5M NH_4OH were dried using a speed-vac at 4°C and were re-suspended in concentrated HCl . To cleave the peptides in solution, trypsin digestion was carried out. A capillary column (75µm id) packed in-house with 10cm Reprosil-Pur 120 C18-AQ, 3uM (Dr-Maisch GmbH; Germany), pre-equilibrated with 2% acetonitrile (ACN) and 0.1% formic acid was used to manually bomb load the trypsin

digested peptides. This reversed-phase high-performance liquid chromatography column and a linear trap quadrupole (LTQ) mass spectrometer were placed in line via an electrospray ionization delivery system. The ionized species were analysed by tandem mass spectrometry (MS/MS). Data dependent acquisition parameters on the mass spectrometer were: 1 centroid MS (mass range 400-2000) followed by MS/MS on the 5 most abundant ions. The resulting data files were analysed by a statistical evaluation program Mascot version 2.3 against the *T. thermophila* RefSeq protein database (NCBI). The fragment mass tolerance was 0.6Da (monoisotopic mass) and the mass window for the precursor was +/- 3Da average mass. The ion score cut off was 35 and a protein hit must have two "bold red peptides" to be considered, where red indicated that peptide was the top scoring match, and bold indicated that the protein was the highest scoring match in which the peptide was found (Lambert, personal communication).

In order to provide statistical significance to individual protein-protein interactions data were subjected to SAINT*express* (Significance Analysis of INTeractome) analysis (Teo et al. 2014). Briefly, for assigning a value to individual protein-protein interactions SAINT takes quantitative spectral counts into consideration. Based on quantitative data, the SAINT algorithm assumes that a prey protein captured with bait is either its true interactor or a non-specific binder. The prey must be present in significantly higher abundance relative to its abundance in the negative controls for qualifying as a true interactor (Choi et al. 2012; Teo et al. 2014). Thus a probability value to an interaction is assigned by comparing data from negative control and experimental AP-MS. A rigorous discrimination between true and false interactions is achieved by taking data from biological replicas into consideration. In many experiments, some prey proteins are expected to co-purify with a given bait (for example, subunits of a protein complex). However, often the quantitative evidence is not sufficient for

these preys and are therefore assigned low scores by the SAINT. To overcome such limitation, SAINT*express* incorporates prior information regarding prey-to-prey relationship into the scoring by the Markov Random Field (MRF), which can adjust the posterior probabilities for the prey pairs that are known to be related (Teo et al. 2014). SAINT*express* reports the Bayesian false discovery rate (BFDR) estimated at all probability thresholds (Teo et al. 2014). Throughout the present study a BFDR≤ 1% was employed as a threshold to qualify as a true interactor.

2.17- Indirect Immunofluorescence

Cells were grown to mid log phase, washed in 10mM Tris-HCl, pH 7.7 and fixed in 4% paraformaldehyde. Fixed cells were membrane-permeabilized with cold acetone for 20 min. Incubation with primary mouse anti-FLAG antibody (Sigma) was at a 1:500 dilution at 4°C overnight in 1×PBST. Cells were washed three times in 1×PBS. Incubation in secondary antibody fluorescein isothiocyanate-conjugated goat anti-mouse (Pierce) was for 1 h at room temperature. For nuclear counterstaining 4,6-diamidino-2-phenylindole dihydrochloride (DAPI) was employed. For immunofluorescence analysis a rReichert-Jung polyvar microscope was used. Images were acquired in JPEG format. Final image preparation was carried out using ImageJ software.

Chapter 3: Results

The goal of my thesis work is to identify protein-protein interactions of histones, a first step to the longer term analysis of their functional significance using the *Tetrahymena thermophile* model. I began by engineering *T. thermophila* cell lines to stably express C-terminal FZZ epitope tagged core histone *HTA1*, histone variants *HTA3 and HTT3* and MIC linker histone *MLH1* from their native chromosomal loci. To achieve this, I first constructed targeting vectors for each gene by PCR amplifying two separate 1kb DNA fragments from upstream (UP) and downstream (DOWN) of the respective predicted start and stop codons (Figure 8A) (also appendix5 for the restriction maps of the loci and PCR products). The primers I designed to amplify UP and DOWN DNA sequences contained at their 5' ends restriction enzyme recognition sites appropriate to clone them in the gene targeting vectors in-frame with DNA sequence encoding an FZZ (3xFLAG-TEV-ZZ) epitope tag (See Figure 8B). When completed, each engineered gene targeting vector was then introduced into growing *T. thermophila* using the biolistic method (Gaertig and Gorovsky 1992). Because the gene targeting vectors bear homology to the 3` region of the MAC locus of interest, the FZZ tag is inserted via homologous recombination so that when the corresponding mRNA is translated the C-terminus of the target protein is in-frame with the FZZ epitope tag (Figure 8C). The position of the insert was verified using a PCR based strategy (see Appendix5 for the PCR products and primer positions used).

As previously described, the polyploid MAC divides by amitosis and does not possess a mechanism for equal allelic segregation. Thus eventual homozygosity in the MAC is achieved for the targeted locus via phenotypic assortment. This process can be accelerated by a gradual increase of the drug used to select for presence of the tagging cassette resulting in those cells receiving an increasing number of the mutant allele after each round of cell

division (see Introduction; Figure 6). Thus MAC homozygous strains for the targeted gene can be achieved as long as the epitope tag itself does not have any functional consequence.

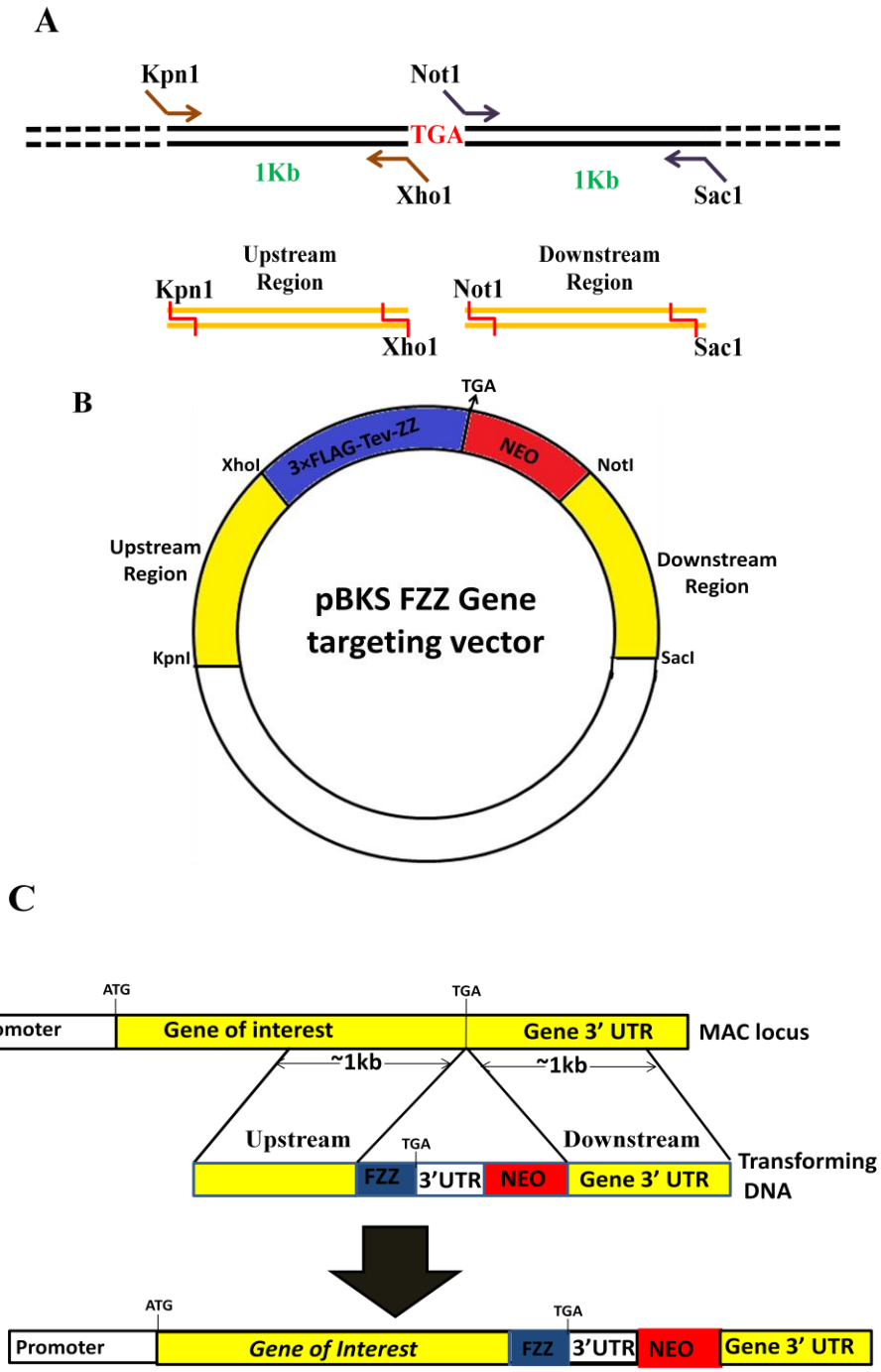

Figure 8: Schematic representation of gene tagging vector construction strategy. A- The relative position of the primers along with built-in restriction sites is shown . **B**- The map of the gene targeting vector is shown where different regions are shown in various colors. The stop codon TGA is also indicated. **C**- The process of homologous recombination used to insert the FZZ tag into the MAC gene locus is presented.

3.1- Characterization of Histone H2A

The *T. thermophila* genome encodes two major histone H2A proteins (gene names *HTA1* and *HTA2*) which at the protein level are nearly identical to each other with only three amino acid differences in the central core region (Liu et al. 1996). Nevertheless, the C-terminus of the two proteins differ significantly from each other where H2A.1 (encoded by *HTA1*) has an additional five residues (Liu et al. 1996). These additional five residues include an SQ motif which is conserved across species and provides a target site for phosphorylation by a specific protein kinase family (Song et al. 2007). The SQ motif phosphorylation has been shown to function in double strand break (DSB) repair during mitosis, meiosis, and amitosis in *T. thermophila* (Song et al. 2007). Thus *T. thermophila* H2A.1 can be considered H2A.X albeit it differs from mammals where H2A.X is a quantitatively minor component (Rogakou et al. 1998) (see Figure 9A).

It was also found that neither *HTA1* nor *HTA2* alone are essential for *T. thermophila* vegetative growth suggesting that the function of the encoded proteins is redundant (Liu et al. 1996). In order to learn about the protein apparatus involved in deposition of H2A, I generated stable *T. thermophila* cell lines expressing *HTA1* with a C-terminal FZZ epitope tag from their MAC locus. The FZZ epitope tag carries one 3xFLAG (F) and 2 protein A moieties (Z) separated by a TEV cleavage site, permitting a two step tandem affinity purification procedure of the fusion proteins (Puig et al. 2001). The purified fusion protein are analyzed by mass spectrometry to identify any co-purifying and thus potentially interacting proteins. In order to assess the successful expression of the fusion protein H2A.1-FZZ (H2A-FZZ hereafter), I performed a Western blot analysis on whole cell- extracts prepared from both H2A-FZZ as well as wild type lines. As apparent from figure 9B, a strong signal of ~33kD was detected in the H2A-FZZ lanes when blots were probed with

anti-FLAG antibody. In contrast, no signal was present in the wild type lanes. These results indicate that FZZ tagged H2A proteins are successfully expressed in *T. thermophila.*

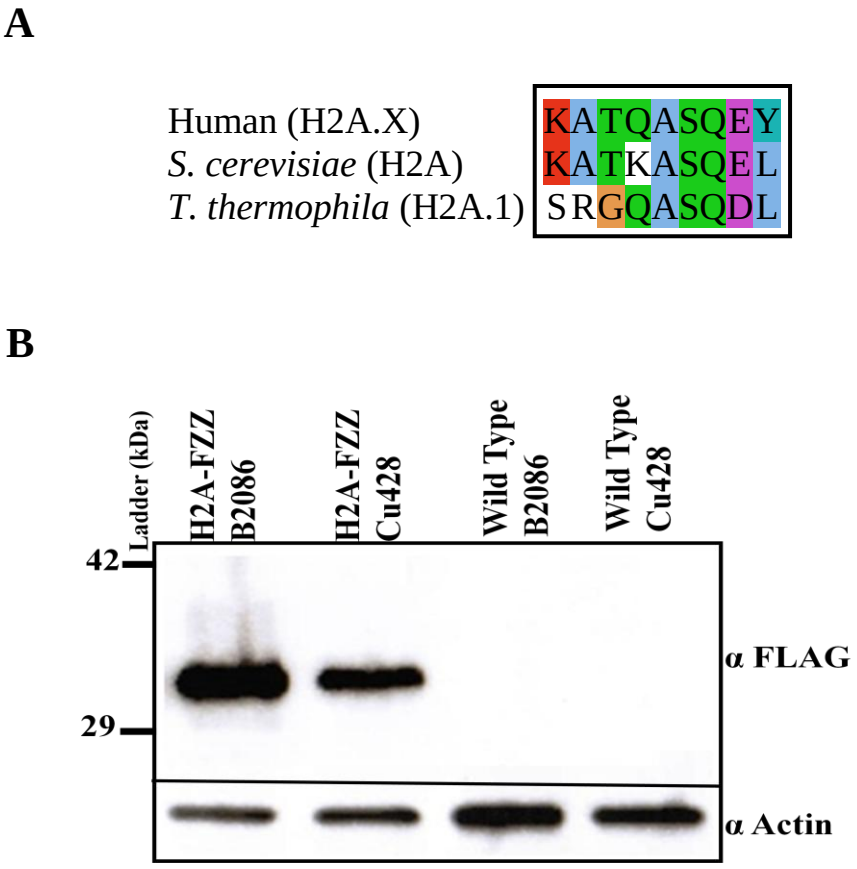

Figure 9: Sequence alignment and Western blot analysis indicating the successful expression of H2A-FZZ. **A-** Multiple sequence alignment of H2AX C-terminal SQ motif. **B-** The top panel shows the expression of H2A-FZZ when probed with anti-FLAG antibody whereas the bottom panel is a loading control probed with anti-actin antibody. Note the H2A-FZZ signal was observed at ~33kDa which is the expected size of the fusion protein (H2A size 14.77kDa+FZZ size 18kDa). Cu428 and B2086 are strains of Mating Type II and VII, respectively**.**

Previous studies have shown that *T. thermophila* histone H2A localizes to both the MIC and MAC during vegetative growth (Song et al. 2007), as expected for a core histone. To examine the localization pattern of H2A-FZZ an indirect immunofluorescence (IF) analysis was carried out. In accordance with previous observations (Song et al. 2007), H2A-FZZ localized in both the MIC and MAC during vegetative growth (see Figure 10). These observations indicate that the presence of the FZZ tag on H2A does not interfere with its

correct localization and is consistent with the fusion protein being functional at least for its transport. Further experiments are required to fully establish whether the tagged H2A also gets incorporated onto chromatin as efficiently as the wild type (see discussion). Subsequently, I performed tandem affinity purification (TAP) using whole cell extracts prepared from vegetative H2A-FZZ and wild type strains. The recovery of the purified H2A-FZZ was assessed by Western blot analysis. As shown in figure 11, a signal corresponding to the expected size was detected in the H2A-FZZ input as well as TAP lanes whereas no signal was present in the wild type lanes. The size difference between H2A-FZZ input and TAP lanes (see figure 11) is due to the TEV cleavage which indicates successful removal of the protein A component of the FZZ tag (~8kD).

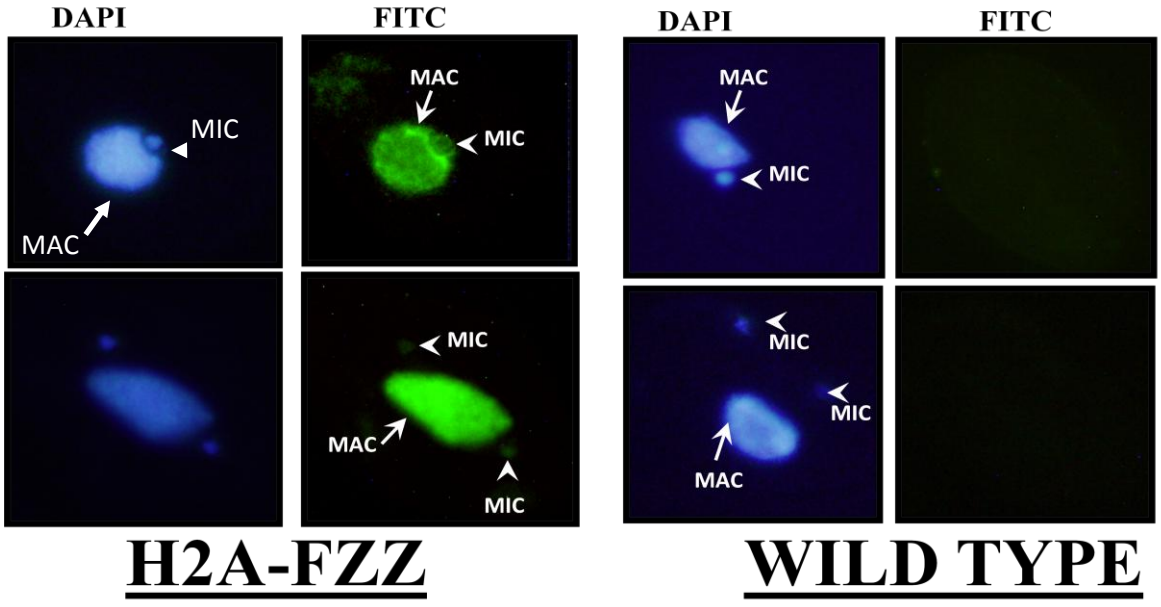

Figure 10: Indirect immunofluorescence of H2A-FZZ and untagged wild type cells using anti-FLAG antibody. Cells were stained with DNA-specific dye DAPI to observe the positions of the nuclei. H2A localizes to both the MAC and MIC whereas no signal was detected in the wild type cells. Arrows represent MAC whereas arrow heads denote MICs. Note: Bottom panels indicate dividing cells during vegetative growth where MIC has already divided whereas MAC is about to undergo amitosis.

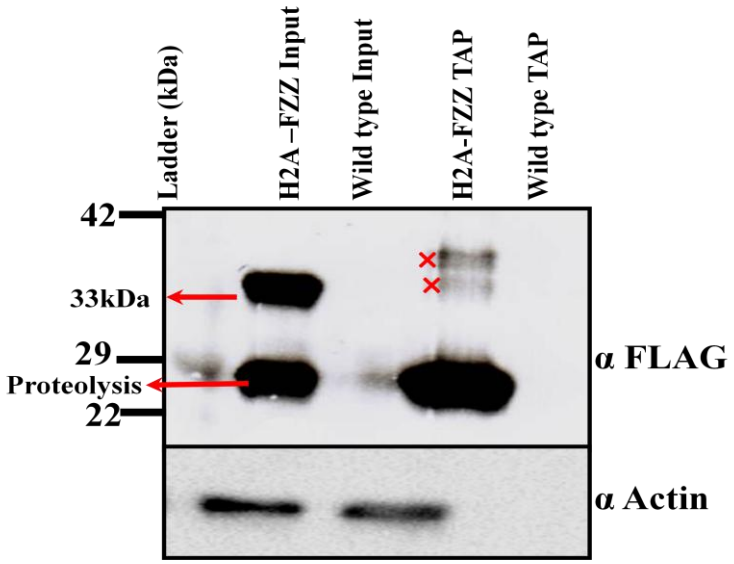

Figure 11: Western blot indicating the recovery of purified H2A-FZZ. The top panel which was probed with anti-FLAG antibody shows the recovery of H2A-FZZ. No signal was detected in the wild type lanes. The bottom panel was probed with anti-actin antibody used as loading control. The red crosses indicate possible mono or ploy ubiquinated H2A isoforms which were enriched during the TAP purification protocol. The size of the major H2A-FZZ band after TAP is lower than the 33kDa band which was detected in the input lane. This is due to the TEV cleavage of the ZZ peptide.

In order to identify the set of H2A-FZZ co-purifying proteins, MS analysis was performed on the TAP material. It is important to note that the AP-MS procedure was repeated at least twice in order to provide experimental replicas for the SAINT analysis (see methods). SAINT analysis of the AP-MS data established 16 interacting partners of H2A-FZZ with a Bayesian false discovery rate (BFDR) $\leq$ 1%. In order to provide for the visual representation of the MS identified co-purifying proteins, H2A affinity purified material was SDS gel electrophoresed and was silver stained (Figure 12-A). The recovery of H2B suggests that H2A-FZZ is functional to form hetero dimmer with H2B and the presence of the FZZ tag does not abolish this interaction. The MS data from the two independent rounds of H2A-FZZ affinity purifications are summarized in Table 2 . The "Gene ID" denotes the *T. thermophila* accession numbers and spectral counts indicate the total number of spectra summed from at

least two independent biological replicas. SAINT analysis revealed that H2A-FZZ co-purifies with *T. thermophila* putative FACT complex subunits including homologs of yeast Spt16 (TTHERM_00283330) and POB3 (TTHERM_00049080) ($Spt16^{Tt}$ and $POB3^{Tt}$ hereafter). These results suggest that the FACT complex has a conserved interaction with histone H2A/H2B. Furthermore, the identification of both $Spt16^{Tt}$ and $POB3^{Tt}$ points out that the composition of the FACT complex itself is evolutionarily conserved, in turn suggesting functional conservation (see below). In addition to the FACT complex, SAINT analysis also identified TTHERM_00429890 as an H2A interacting partner. BLAST searches against the NCBI non-redundant database using the predicted protein sequence of TTHERM_00429890 showed that it shares similarity with the NPM-family of proteins (cut off score for inclusion e^{-5}). This observation was further supported by SMART domain analysis which indicated that the identified putative NPM-like protein contains a conserved N-terminal "Nucleoplasmin (PF03066)" domain. Interestingly, the C-terminus of the putative NPM-like protein contains a nucleolar localization signal as predicted by the 'NOD' web server (http://www.compbio.dundee.ac.uk/www-nod/index.jsp) (see Figure 12-B). This suggests that similar to what has been found in other organisms such as mammals, the putative NPM-like protein might have a role in ribosome biogenesis (Finn et al. 2012). In addition MSA analysis indicated that similar to the other NPM-family members (see introduction), the putative NPM-like protein contains at least three acidic stretches giving it an overall negative charge (theoretical Pi 4.62). Based on homology and domain architecture (also see Figure 12), and in accordance with *T. thermophila* nomenclature guidelines, I have named this protein as Cnpl1 (**C**onserved **NP**M-**l**ike 1).

SAINT analysis also revealed three putative PARP proteins as H2A interacting partners. The identified PARPs include TTHERM_00726470, TTHERM_00823980 and

TTHERM_00502600 which are annotated as *T. thermophila* PARP2, PARP4 and PARP6, respectively. While the exact role of H2A co-purifying PARPs in *T. thermophila* is unknown, a plausible hypothesis would be that ribosylation of histones H2A after their synthesis might be required for their assembly onto chromatin (see discussion). Another notable co-purifying protein identified by the SAINT is TTHERM_00150000 which has been annotated as MutS domain III family protein involved in DNA mismatch repair (see ciliate.org). BLAST analysis indicated that TTHERM_00150000 shares homology (e^{-64}) to the budding yeast MSH6 which has been shown to be required for mismatch repair during mitosis and meiosis (Drotschmann et al. 2002). The functional significance of this interaction in *T. thermophila* requires further investigation.

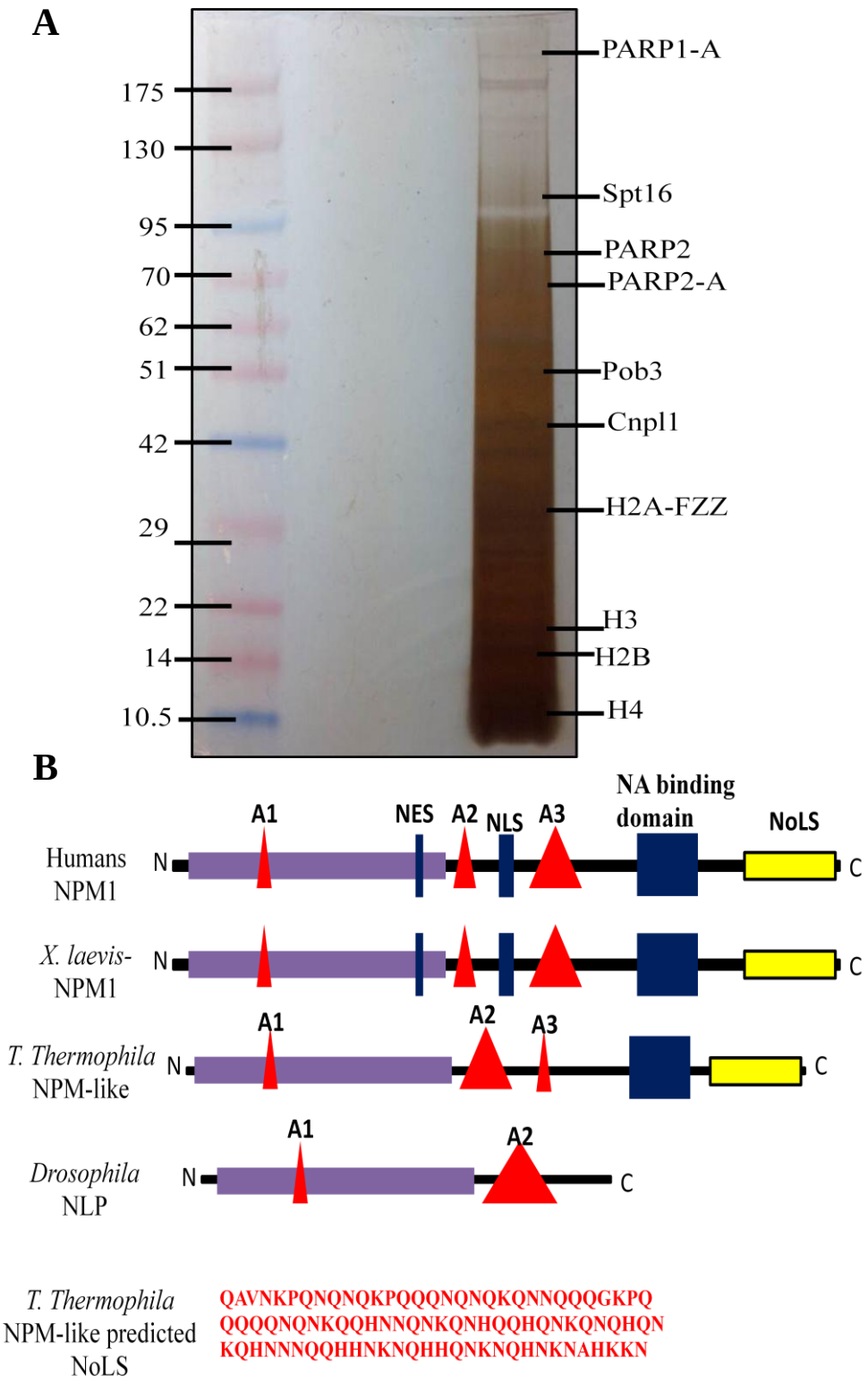

Figure 12: Silver stained SDS-gel of H2A affinity purification and domain architecture of various NPMs across different species. **A-** The bands were labelled based on predicted molecular weights of MS identified proteins. **B-** The image was designed based on SMART domain analysis as well as PFAM analysis. The predicted NoLS sequence of *T. thermophila* putative NPM-like protein is shown in red.

Table 2: AP-MS data from two independent biological replicas filtered using SAINT analysis (**BFDR ≤ 1%******)***

Bait	**Prey**	**Gene ID**	**Spectral Counts Sum**
H2A	-	TTHERM_00790790/ TTHERM_00316500**	493
H2A	Spt16	TTHERM_00283330	379
H2A	POB3	TTHERM_00049080	74
H2A	NPM-like (CNPL1)	TTHERM_00429890	77
H2A	PARP2	TTHERM_00726470	58
H2A	PARP4	TTHERM_00823980	39
H2A	PARP6	TTHERM_00502600	125
H2A	H2B	TTHERM_00283180	403
H2A	H2B	TTHERM_00633360	409
H2A	Hv1	TTHERM_00143660	199
H2A	H4	TTHERM_00189170	619
H2A	H3	TTHERM_00189180	61
H2A	Novel?	TTHERM_00242240	25
H2A	HSP70	TTHERM_00105110	20
H2A	Alpha Kinase family protein	TTHERM_00865100	20
H2A	AT hook	TTHERM_01123890	9
H2A	MutS family protein	TTHERM_00150000	7
H2A	Novel??	TTHERM_00648920	5

* Filtered against 9 vegetative cell control;** Due to high degree of similarity between two H2A proteins gene IDs are written for both.

3.2- Analysis of *T. thermophila* FACT complex

FACT is an abundant and highly conserved protein complex that consists of Spt16 and HMG domain containing protein SSRP1(Bruhn et al. 1992). In fungi, Spt16 forms a complex with a truncated SSRP1 homolog POB3 which lacks an HMG domain (Formosa et al. 2001). The HMG domain lies within another protein called Nhp6 which associates with the FACT complex in a stoichiometric manner (Stillman 2010). The FACT complex has been shown to be involved in several processes ranging from transcription initiation, facilitating RNAPII transcription elongation by acting as a histone chaperone via destabilizing, as well as reassembling the nucleosomes (Belotserkovskaya et al. 2003; Stuwe et al. 2008). The co-purification of the *T. thermophila* putative FACT complex along with H2A/H2B suggests an evolutionarily conserved composition of this complex. To begin functional characterization of the *T. thermophila* putative FACT complex, I investigated the structural and sequence features of the identified FACT subunits, i.e. $Spt16^{Tt}$ and $Pob3^{Tt}$. BLAST searches against the NCBI non-redundant database using $Spt16^{Tt}$ and $Pob3^{Tt}$ protein sequences as queries indicated that both proteins share similarity to human as well as to *S. cerevisiae* FACT subunits (sequence identity to *S. cerevisiae* Spt16 and POB3 across the length of the protein is 36% and 30%, respectively) (score e^{-142} and $2e^{-52}$, respectively). These observations suggest that the putative $Spt16^{Tt}$ and $Pob3^{Tt}$ are bona fide FACT subunits in *T. thermophila*.

To further assess their structural features, I performed SMART domain analysis. As shown in figure 13 both $Spt16^{Tt}$ and $Pob3^{Tt}$ have highly conserved domain architectures. For example, $Pob3^{Tt}$, similar to *S. cerevisiae* and humans, contains a PFAM structure-specific recognition domain (SSrecog; PF03531) as well as an Rtt106 domain. The Rtt106 domain belongs to a family of histone chaperones which function in nucleosome formation and heterochromatin-mediated silencing (Huang et al. 2005). In contrast to humans, $Pob3^{Tt}$ does

not contain any HMG domain. This suggests that structurally Pob3^{T} might be more similar to the budding yeast POB3. *T. thermophila* genome encodes several HMG proteins. BLAST searches using *S. cerevisiae* Nhp6 against *T. thermophila* genome identified TTHERM_00216040 as the closest match (e^{-11}). Thus it is possible that *T. thermophila* FACT complex might contain additional subunit to compensate for the lack of HMG domain in POB3^{Tt}.

Similarly, my analysis suggests that the Spt16^{Tt} domain organisation is highly conserved from yeast to human. Similar to *S. cerevisiae* and human proteins, Spt16^{Tt} contains an N-terminal lobe domain (Nlob), a Pfam Peptidase_M24 (PF00557) domain, a central Spt16 signature domain and a C-terminal Rtt106 domain (see Figure 13). The highly conserved domain architecture of the FACT subunits suggests that purifying selection might have been significantly strong over the course of evolution in order to preserve essential structural features required for the proper functioning of these proteins.

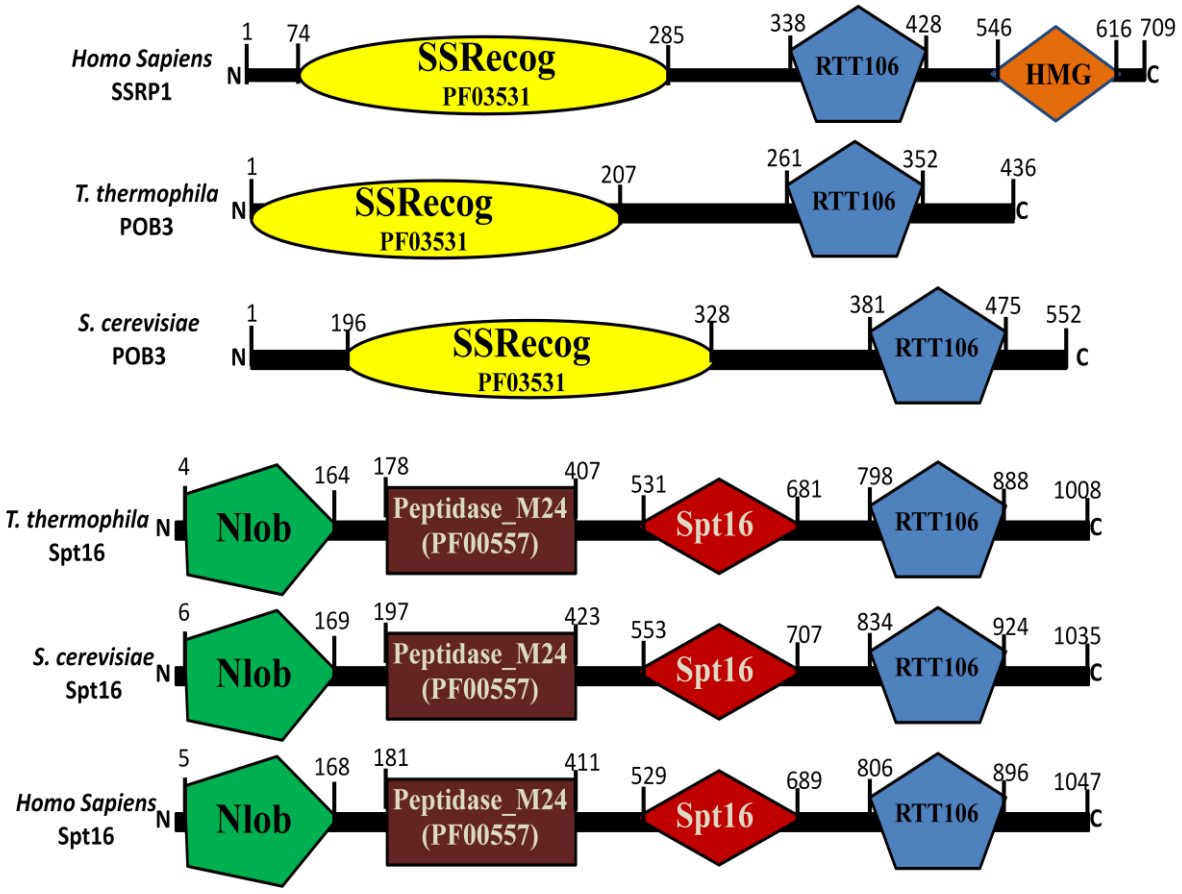

Figure 13: Domain comparison of various POB3 and SPT16 homologs. The image was designed based on SMART domain analysis as well as Pfam analysis. The position of each domain is indicated with respective to amino acid that comprise the domain.

3.2.1- Characterization of Spt16^{Tt}

To begin characterizing the putative FACT complex, I initiated my analysis by engineering a stable *T. thermophila* cell line expressing Spt16^{Tt} with a C-terminal FZZ epitope tag from the MAC locus. I assessed the successful expression of the tagged proteins by Western blots using whole cell extracts generated from both Spt16^{Tt}-FZZ and wild type strains. As shown in figure 14, no signal was detected in the wild type lane when probed with anti-FLAG antibody whereas a signal corresponding to the predicted size of the fusion protein was apparent in the lanes loaded with Spt16^{Tt}-FZZ cell extracts.

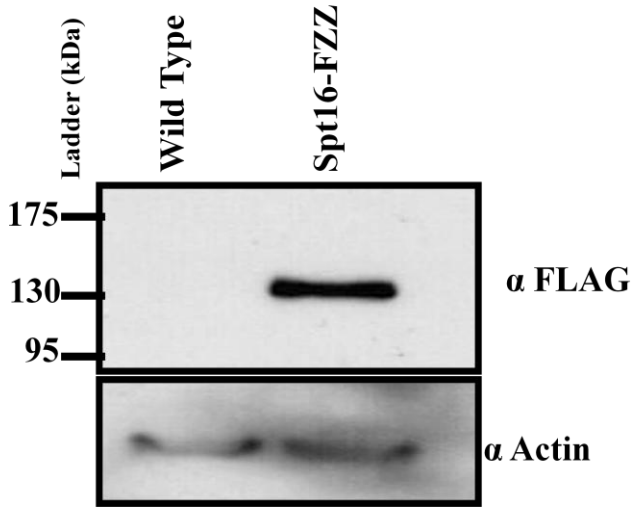

Figure 14: Western blot analysis indicating the successful expression of SPT16-FZZ. The top panel shows the expression of SPT16-FZZ when probed with anti-FLAG antibody. The bottom panel is a loading control probed with anti-actin antibody. Note the SPT16-FZZ signal was observed at ~132kDa which is the expected size of the fusion protein (SPT16 size 116kDa+FZZ size 18kDa).

Subsequently, I performed one-step affinity purification to isolate the native complexes of Spt16^{Tt}-FZZ. It is important to note that one step AP was employed in order to increase the likelihood of capturing weak and/or transient interactions which can be lost due in the more stringent two step purification procedure (Fillingham, Lambert and Pearlman unpublished observations). To assess the recovery of the affinity purified proteins, Western blotting was performed and a strong signal was observed in the Spt16^{Tt}-FZZ lanes when

probed with anti-FLAG antibody. In contrast no signal was detected in the wild type lanes (Figure 15). As apparent from figure 15, the size of Spt16^{Tt}-FZZ in the input lanes is equal to that detected in the affinity purified lanes. This is due to the TEV-cleavage step being eliminated in the one step AP procedure resulting is no reduction of size in the purified fusion proteins.

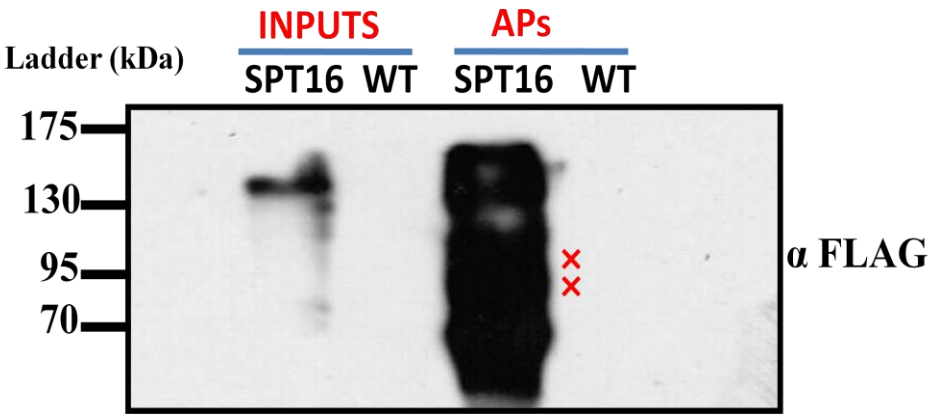

Figure 15: Western blot indicating the recovery of purified Spt16-FZZ. The blot was probed with anti-FLAG antibody and shows the recovery of Spt16-FZZ whereas no signal was detected in the wild type lanes. Note there is no difference of size (132kDa) between input and affinity purified lanes because the TEV cleavage step was omitted in the one step affinity purification procedure. Red crosses indicate proteolysis of the affinity purified protein.

The purified material was then analyzed by gel-free LC-MS/MS to detect any co-purifying proteins. Both histones H2A/H2B were detected in the MS data although they did not pass the SAINT validation. It is important to note that histones are highly abundant proteins and often are detected as contaminating "frequent flyers" in MS analysis (Choi et al. 2012). They are generally considered as common background contaminants in a typical AP-MS pipeline and thus do not pass the SAINT validation threshold (Choi et al. 2012). SAINT analysis revealed that Spt16^{Tt}-FZZ co-purifies with Pob3^{Tt} (see table 3). In addition to reciprocally verifying the H2A-Spt16 interaction, these results indicate that Spt16^{Tt}-Pob3^{Tt} form a stable FACT complex in *T. thermophila* and likely have conserved functions similar to those described in other eukaryotes such as budding yeast (see above). In addition,

consistent with a role in transcription regulation, several subunits of RNA polymerase I, II and III (RNAP) including RPA1, RPA2, RPC5 and RBP81 were identified by SAINT analysis (Note: RNA polymerase subunit nomenclature was adopted from the existing annotations available on ciliate.org). Furthermore, several novel proteins that do not share homology to any known proteins in the NCBI database were also detected. The functional significance of these novel proteins remain unknown and requires further investigation. Curiously, none of HMG proteins co-purified with Spt16^{Tt}. It is possible that *T. thermophila* FACT complex transiently interacts with yet to be identified HMG protein and this interaction might have been lost during purification procedure.

Table 3: AP-MS data from two independent biological replicas filtered using SAINT analysis (**BFDR ≤ 1%******)***

Bait	**Prey**	**Gene ID**	**Spectral counts sum**
SPT16	-	TTHERM_00283330	1109
SPT16	POB3^{Tt}	TTHERM_00049080	587
SPT16	RPA1	TTHERM_00047550	104
SPT16	RPA2	TTHERM_01075780	47
SPT16	RPC5	TTHERM_00094210	31
SPT16	RPB81	TTHERM_00549610	21
SPT16	Novel?	TTHERM_00382370	46
SPT16	Novel?	TTHERM_00249630	21
SPT16	HSP70	TTHERM_01014750	21
SPT16	HSP60	TTHERM_00196370	20
SPT16	PLU-1-like	TTHERM_01046850	18
SPT16	CHC1 Clathrin heavy chain	TTHERM_00275740	19
SPT16	H2A	TTHERM_00316500/	23
SPT16	H2B	TTHERM_00633360	127

* validated against 9 vegetative cell control

3.2.2- Spt16^{Tt} localizes to MAC and MIC

In order to gain further insights into functional aspects of Spt16^{Tt}, I carried out an indirect IF using anti-FLAG primary antibody in vegetatively growing cells (Figure 16). The signal was observed both in the MAC and MIC of vegetatively growing cells. This pattern of localization overlaps with that of H2A-FZZ (Fig. 10) suggesting that histones H2A/H2B and FACT are functionally linked. One key function of the FACT complex is to regulate transcription initiation as well as elongation (Belotserkovskaya et al. 2003; Stuwe et al. 2008). In accordance with previous findings, the localization of Spt16^{Tt} in the transcriptionally active MAC suggests a role for the *T. thermophila* FACT complex in transcription regulation.

The localization in the transcriptionally inert MIC suggests additional roles for Spt16^{Tt} distinct from those of transcription regulation. For example, FACT might be involved in regulating DNA replication or heterochromatin maintenance as shown previously (Lejeune et al. 2007) (see Discussion). Taken together, these results establish an evolutionarily conserved composition of the FACT complex and suggest roles in transcription regulation as well as DNA replication in *T. thermophila*.

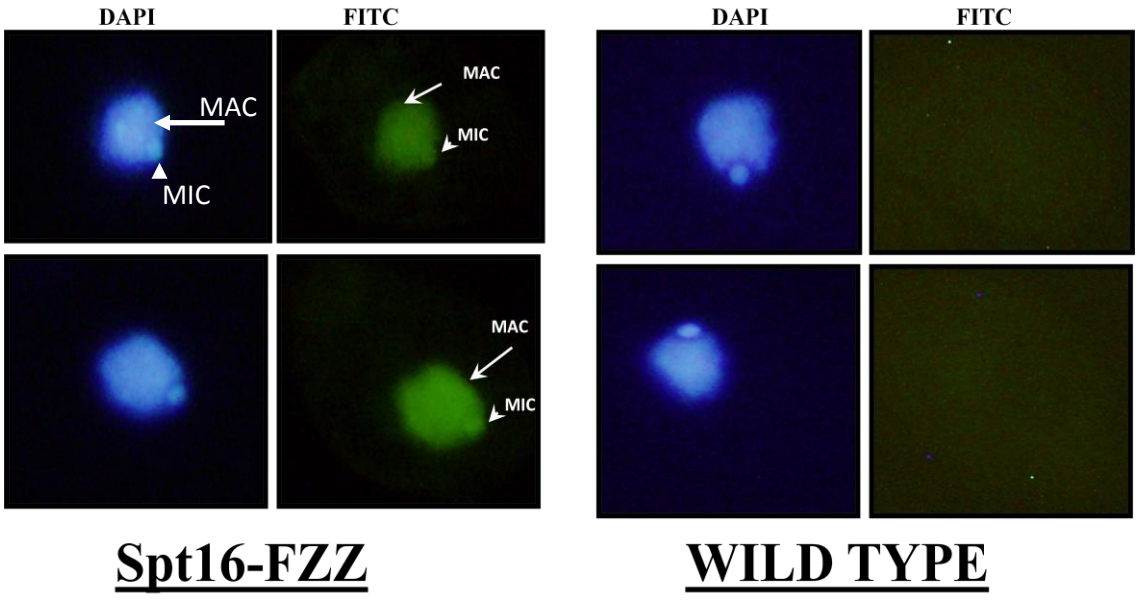

Figure 16: Indirect immunofluorescence analysis of Spt16-FZZ and untagged wild type cells using anti-FLAG antibody. To observe the nuclei positions, cells were stained with the DNA-specific dye DAPI. Spt16 localizes to both the MAC and the MIC whereas no signal was detected in the wild type cells. Arrows represent MAC whereas arrow heads denote MICs

3.3- Characterization of PARP6^{Tt}

The *T. thermophila* genome encodes at least 10 PARP^{Tt} proteins (assessed by BLAST searches as well as available gene annotations at www.ciliate.org; also Citarelli et al. 2010). Among H2A co-purifying proteins, three of the PARP family members including PARP2^{Tt}, PARP4^{Tt} and PARP6^{Tt} (as annotated on TGD www.ciliate.org) were detected. To assess the structural features as well as categorize them into known PARP subfamilies, I performed BLAST searches as well carrying out SMART domain analysis. Among PARP family members, PARP2 and PARP3 are known to have PARP-catalytic domains, a regulatory domain (PARP-reg), as well as a WGR domain whereas PARP4 lacks WGR and contains additional BRCT, VWA and VIT domains (Daugherty et al. 2014). Interestingly, BLAST as well as domain analysis of PARP2^{Tt} and PARP4^{Tt} indicate that PARP4^{Tt} does not share similarity with any known PARP4 proteins and in fact belongs to the PARP2 subfamily as delineated by (Citarelli et al. 2010) (score $2e^{-111}$) (also see Figure17 for domain analysis). To further ascertain the correct assignment of *T. thermophila* PARP sub-family members and exclude the possibility that PARP4^{Tt} might be a PARP3^{Tt}, I assessed the *T. thermophila* genome and observed the presence of a distinct putative PARP3^{Tt} protein (accession TTHERM_00030430). These observations helped to correctly assign TTHERM_00823980 as a PARP2 sub-family member (PARP2-A hereafter) rather than a PARP4 (Figure17).

Similarly, domain analysis of PARP6^{Tt} revealed that this protein contains 25 tandem ankyrin repeats (ANK) as well as two DNA binding AT-hook domains. In addition, PARP6^{Tt} has PARP-catalytic as well as regulatory (PARP-reg) domains. This domain organisation is unique to Amoebozoa (*Dictyostelium*), Opisthokonta (fungi) and Chromalveolates (ciliates) and has been found to belong to the PARP1 sub-family (Citarelli et al. 2010). Interestingly, human PARP5a, b (known as tankyrase 1 and 2, respectively), also contain tandem ANK

repeats as well as a PARP-catalytic domain but lack PARP-reg (Daugherty et al. 2014). Tankyrase 1 and 2 have been shown to be functionally redundant and involved in maintenance of telomeres (Chiang et al. 2008). Thus the presence of tandem ANK repeats as well as WGR, PARP-catalytic and PARP-reg domains suggest that these PARP1 subfamily members might be responsible for diverse functions including genome integrity, telomere maintenance and ribosylation of target molecules. Nevertheless, it is important to note that true Tankyrases are confined to animals (Citarelli et al. 2010). Bases on domain architecture as well as previous evolutionary studies (Citarelli et al. 2010), I assigned PARP6^{Tt} as PARP1A^{Tt} (see Figure17).

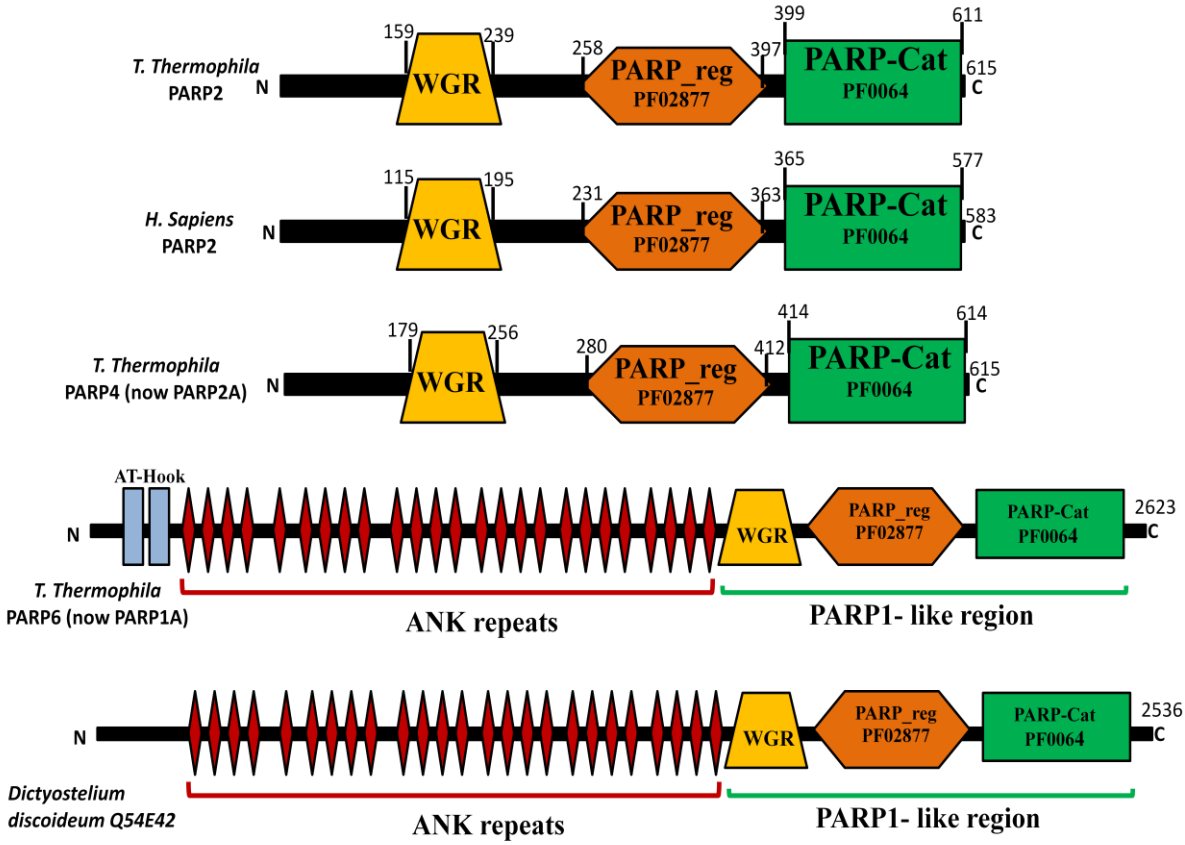

Figure 17: Domain comparison of various PARP proteins across different species. The image was designed based on SMART domain analysis as well as PFAM analysis. The position of each domain in PARP2 proteins is indicated with respect to the amino acids that comprise the domain. Comparison of two PARP1 subfamily members containing tandem ANK repeats is also presented.

3.3.1- Functional analysis of PARP1-A^{Tt} (formerly PARP6^{Tt})

In order to address questions about the functional aspects of PARPs co-purifying with H2A, I initiated my analysis by characterizing PARP1A^{Tt} protein-protein interactions. I generated a stable *T. thermophila* cell line expressing PARP1A^{Tt} with a C-terminal FZZ epitope tag from the MAC locus. The successful expression of the tagged protein was examined by Western blotting using vegetative whole cell extracts of both PARP1A^{Tt}-FZZ and wild type strains (Figure 18). Subsequently, one step AP was performed and recovery of the purified protein was assessed by Western blotting probed with anti-FLAG antibody (Figure 19).

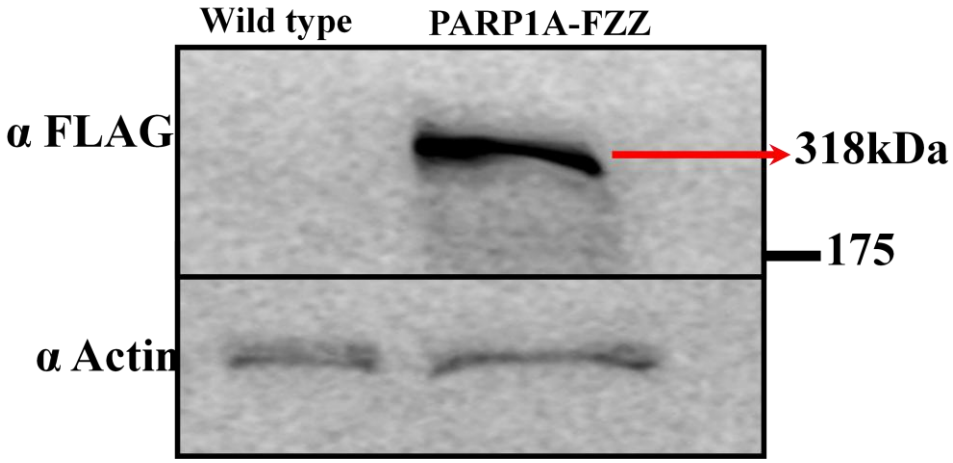

Figure 18: Western blot analysis indicates the successful expression of PARP1A-FZZ. The top panel shows the expression of PARP1A-FZZ when probed with anti-FLAG antibody whereas the bottom panel is loading control probed with anti-actin antibody. Note the PARP1A-FZZ signal was observed at ~318kDa which is the expected size of the fusion protein (PARP1A-FZZ size 300kDa+FZZ size 18kDa).

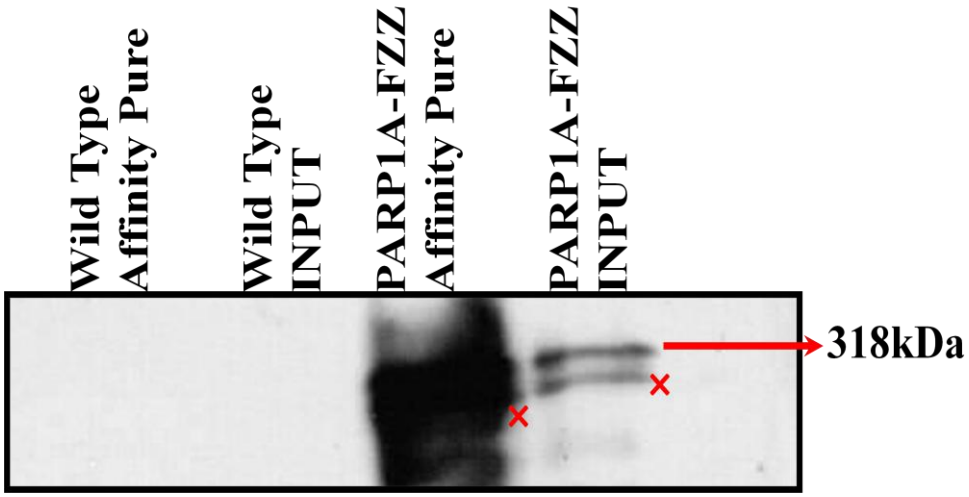

Figure 19:Western blot indicating the recovery of purified PARP1A-FZZ. The blot was probed with anti-FLAG antibody and shows the recovery of PARP1A-FZZ whereas no signal is detected in the wild type lanes. The red crosses indicate the proteolytic products.

SAINT analysis of MS data revealed the recovery of bait PARP1A^{Tt}-FZZ as well as co-purifying histones (Table 4). The total spectral counts for two independent biological replicas were 841 for PARP1A-FZZ which was not detected in any of the control purifications. In addition, for H2A, H2B, H3 and H4 total spectral counts of 34, 22, 3 and 52, respectively, were also detected, although they did not pass the SAINT validation. Consistent with the role of PARP1 as a regulator of transcription (Aguilar-Quesada et al. 2007), SAINT analysis also validated interactions with several subunits of *T. thermophila* RNAP (I, II,III). These results suggest that PARP1A^{Tt} might be involved in various aspects of chromatin dynamics ranging from structural organisation to transcription regulation.

Table 4: AP-MS data from two independent biological replicas filtered using SAINT analysis (BFDR ≤ 1%*)

Bait	Prey	Gene ID	Spectral counts sum
PARP1A	-	TTHERM_00502600	1268
PARP1A	RPA1	TTHERM_00047550	76
PARP1A	RPA2	TTHERM_01075780	55
PARP1A	RBP81	TTHERM_00549610	24
PARP1A	TTN1	TTHERM_00052160	30
PARP1A	Cytochrome b5-like	TTHERM_00066830	22
PARP1A	Novel??	TTHERM_00773780	10
PARP1A	SFR13	TTHERM_00522830	8
PARP1A	PRS1 (Prolyl-tRNA synthetase1)	TTHERM_00487020	6

* validated against 9 vegetative cell control

In order to examine the function of PARP1A^{Tt}, I performed an indirect IF using anti-FLAG primary antibody in vegetatively growing cells (Figure 20). Interestingly, similar to Spt16^{Tt}, PARP1A^{Tt} was also found to localize to both the MAC and MIC consistent with functional linkage with H2A. These localization patterns suggest that consistent with previous studies (D'Amours et al. 1999; Kraus 2008; Ko and Ren 2012), PARP1A^{Tt} might be involved in a broad range of processes including general maintenance of chromatin structure, nucleosome assembly and regulation of gene expression through its enzymatic activities.

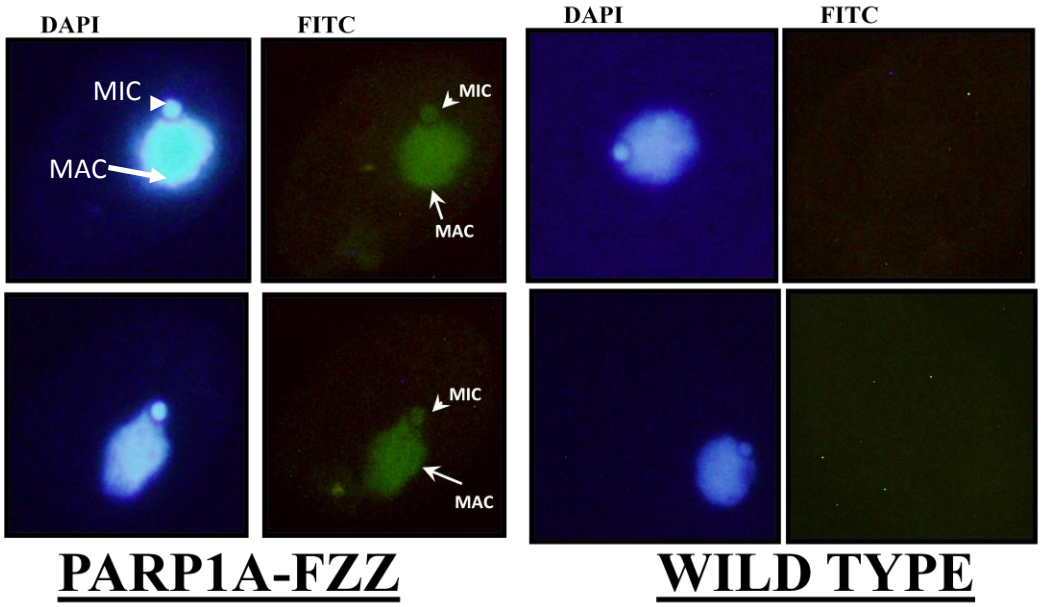

Figure 20: Indirect immunofluorescence analysis of PARP1A-FZZ and untagged wild type cells using anti-FLAG antibody. Nuclei were stained with DNA-specific dye DAPI. Spt16 localizes to both the MAC and MIC whereas no signal was detected in the wild type cells. Arrows represent MAC whereas arrow heads denote MICs

3.4- Proteomic analysis of H2A variant Hv1

Histone H2A variant Hv1 (H2A.Z in mammals) is an essential gene in *T. thermophila* (Liu et al. 1996). Previous studies have also established that Hv1 exclusively localizes to the transcriptionally active MAC during vegetative growth and thus links this histone variant with active chromatin (Stargell et al. 1993). Intriguingly, mechanistic details of how Hv1 is specifically targeted to the MAC remain unknown. To gain insight into Hv1 functions in transcription and possible mechanism of its transport to the MAC, I initiated my analysis by engineering stable *T. thermophila* cell lines expressing C-terminal FZZ epitope tagged Hv1 from its native MAC locus. The successful expression of Hv1-FZZ fusion protein was assessed by Western blots of whole cell extracts. As apparent from figure 21A, a strong signal was detected in the Hv1-FZZ lanes when probed with anti-FLAG antibody whereas no signal was present in the wild type lanes. To examine the correct MAC localization of FZZ epitope tagged Hv1, I carried out an indirect IF analysis using vegetatively growing cells. In accordance with previous studies (Stargell et al. 1993), Hv1-FZZ was found to localize exclusively to the MAC suggesting that the presence of the epitope tag does not alter the protein's localization pattern figure 21-B and is consistent with its proper function.

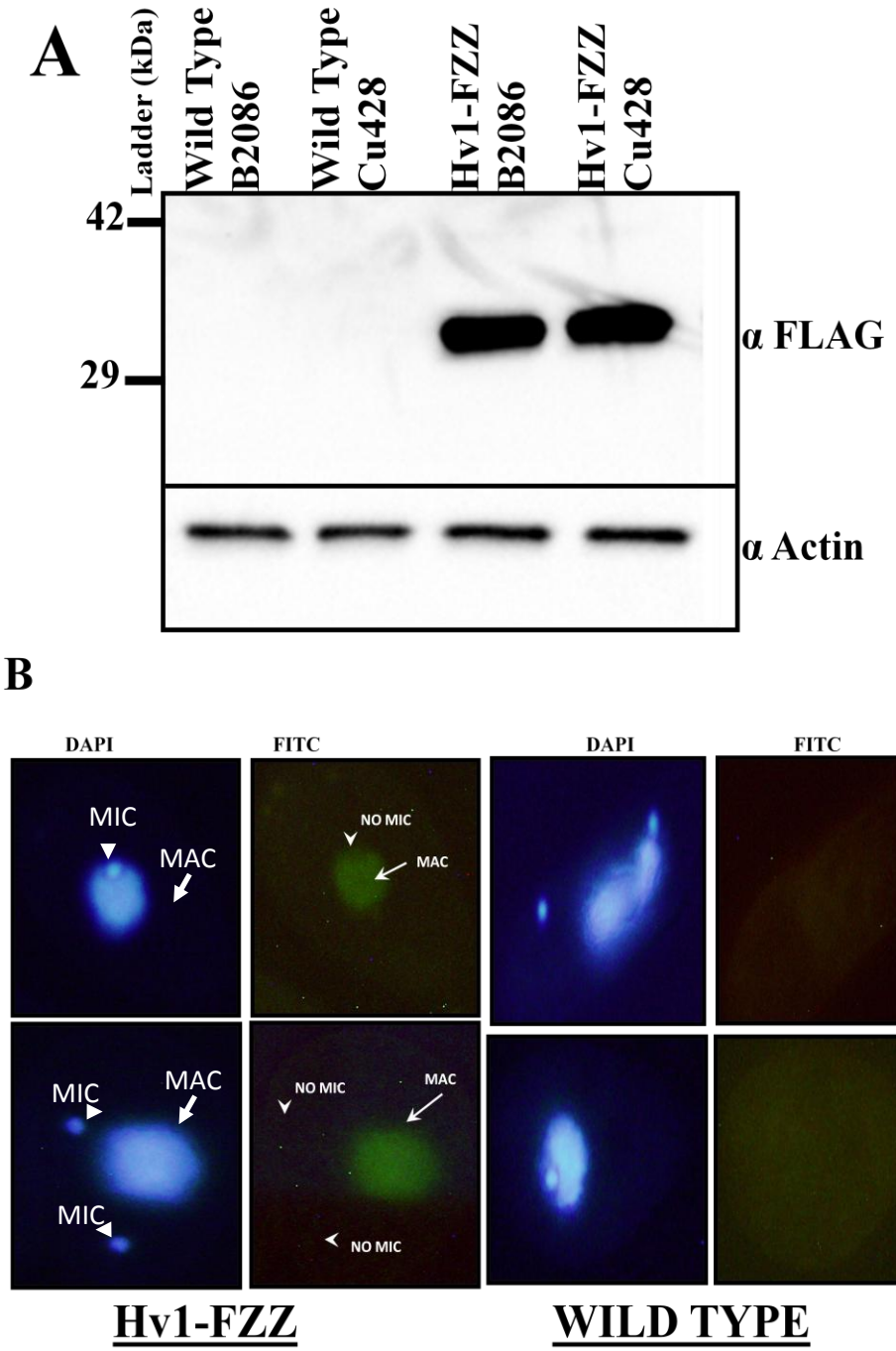

Figure 21: Western blot and IF analysis of Hv1-FZZ. A- The top panel shows the expression of Hv1-FZZ when probed with anti-FLAG antibody whereas the bottom panel is the loading control probed with anti-Actin antibody. Note the Hv1-FZZ signal was observed at ~33kDa which is the expected size of the fusion protein (Hv1 size 15 kDa+FZZ size 18kDa). Cu428 and B2086 are strains of Mating Type II and VII, respectively. **B-** Indirect immunofluorescence analysis of Hv1-FZZ and untagged wild type cells using anti-FLAG antibody. To capture the orientation of nuclei, DNA specific dye DAPI was used. IF indicates that Hv1 localizes exclusively to the MAC whereas no signal was detected in the MIC. In the control cells no signal was observed.

Subsequently, I performed TAP as well as a one step AP procedure using vegetatively growing Hv1-FZZ as well as wild type strains. The recovery of the bait protein Hv1-FZZ, was monitored by Western blotting probed with anti-FLAG antibody (Figure 22). In order to identify any co-purifying proteins, MS analysis was carried out which was followed by SAINT to provide for statistical significance (BFDR$\leq$ *1%*). As expected, SAINT analysis revealed that the bait Hv1 along with H2B were successfully recovered. In addition, SAINT also revealed TTHERM_00550700 as an Hv1 co-purifying partner (Table 5). Previous studies have shown that TTHERM_00550700 belongs to a large family of karyopherin proteins and the *T. thermophila* genome encodes 13 putative importin (imp) α- and 11 imp β-like proteins (Malone et al. 2008). Importantly, TTHERM_00550700 which has been annotated as Impβ3 is one of only two impβ proteins that exclusively localize to the MAC (Malone et al. 2008). The fact that Hv1-Impβ3 physically interact with each other suggests that Impβ3 might be responsible for Hv1 MAC specific targeting. Taken together, these results provide initial evidence for the possible mechanism through which this transcription-related essential histone variant might be targeted to the MAC.

Among other Hv1 co-purifying proteins, BLAST searches indicated that TTHERM_00582070 shares homology to the budding yeast Cse1 protein (Chromosome SEgregation) (33% full length sequence identity). Cse1p has been shown to be involved in the export of imp-alpha from the nucleus (Solsbacher et al. 1998). Thus it is possible that *T. thermophila* putative Cse1-like protein might also be responsible for the re-cycling of importins. Nevertheless, further examination will be required to fully assess this hypothesis. Similar to H2A (see above Table 2), Hv1 also co-purified with PARP1-A and PARP2, further emphasizing the role of PARPs in histone dynamics.

Interestingly, several subunits of *T. thermophila* putative proteosome complex were identified as high confidence hits (BFDR≤1%). The exact role and functional aspects are unclear however it is possible that Hv1 levels might be tightly monitored via proteosome mediated degradation.

Table 5: AP-MS data from two independent biological replicas filtered using SAINT analysis (BFDR ≤ 1%*)

Bait	Prey	Gene ID	Spectral counts sum
Hv1	-	TTHERM_00143660	177
Hv1	BTU1	TTHERM_00348510	557
Hv1	ATU1	TTHERM_00558620	268
Hv1	HSP82	TTHERM_00158520	313
Hv1	HSP90	TTHERM_00444670	42
Hv1	H4	TTHERM_00189170	212
Hv1	H2B	TTHERM_00633360	195
Hv1	VMA1 (Vacuolar Membrane Atpase)	TTHERM_00339640	30
Hv1	Lap2 (Leucyl aminopeptidase)	TTHERM_00579060	19
Hv1	Impβ3	TTHERM_00550700	15
Hv1	Cse1p	TTHERM_00582070	21
Hv1	PARP1-A	TTHERM_00502600	14
Hv1	PARP2	TTHERM_00726470	6
Hv1	NRS1 (asparaginyl-tRNA synthetase 1)	TTHERM_00691890	14
Hv1	TRS1 (Threonyl-tRNA synthetase 1)	TTHERM_00194650	9
Hv1	ARS2 (alanyl-tRNA synthetase 2)	TTHERM_00221140	8
Hv1	PRS1 (Prolyl-tRNA synthetase 1)	TTHERM_00487020	8
Hv1	Novel??	TTHERM_00382330	13
Hv1	CCT8	TTHERM_00037060	11
Hv1	CCT4	TTHERM_00037050	5
Hv1	Novel??	TTHERM_00079270	10

Hv1	RPT5 (26S proteasome regulatory subunit T5)	TTHERM_00136360	9
Hv1	RPT2 (26S proteasome regulatory subunit T2)	TTHERM_01014660	7
Hv1	RPT4 (26S proteasome regulatory subunit T4)	TTHERM_00469100	6
Hv1	RPN8 (26S proteasome regulatory subunit N8)	TTHERM_00267990	7
Hv1	RPN12 (26S proteasome regulatory subunit N12)	TTHERM_00649110	6
Hv1	Cdc48	TTHERM_00365340	8
Hv1	URA7	TTHERM_00459390	9
Hv1	Alcohol dehydrogenase I	TTHERM_00145230	7
Hv1	Glycosyl transferase	TTHERM_00069210	5
Hv1	NOG1	TTHERM_00242500	7
Hv1	Gcn1	TTHERM_00444500	7
Hv1	Sec27	TTHERM_00476510	7
Hv1	Sec61	TTHERM_00035580	6
Hv1	Novel??	TTHERM_00313610	5
Hv1	RVB2 (RuVB-like)	TTHERM_00046920	4

* Validated against 9 vegetative cell control; Note: Standard protein names as available through ciliate.org are listed unless specified in text.

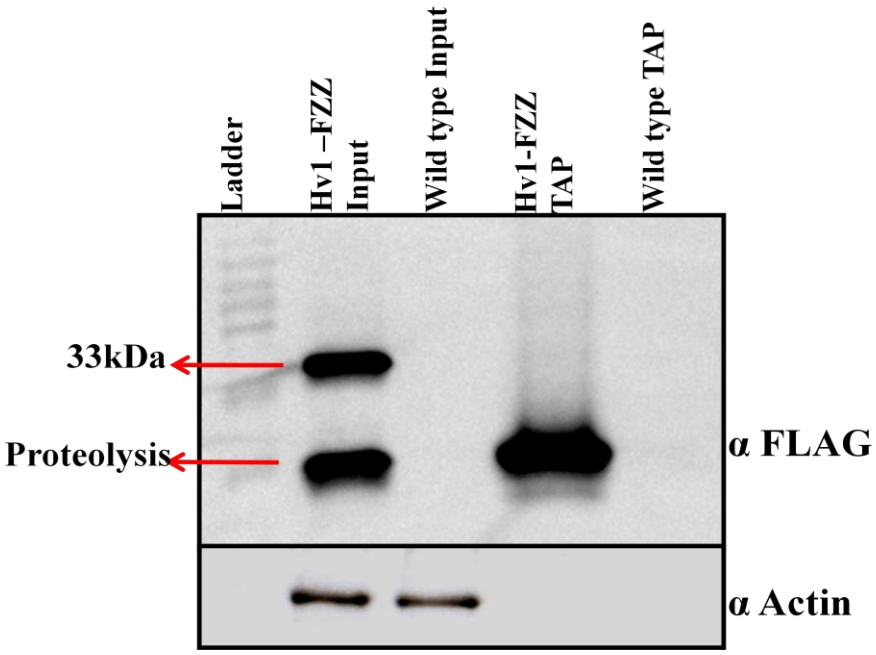

Figure 22: Western blot indicating the recovery of tandem affinity purified Hv1-FZZ. The top panel which was probed with anti-FLAG antibody shows the recovery of Hv1-FZZ. No signal was observed in the wild type lanes. The bottom panel used as loading control was probed with anti-Actin. The size of the major Hv1-FZZ band after TAP is lower than the 33kDa band which was detected in the input lane. This is due to the TEV cleavage of the ZZ peptide.

3.5- Proteomic characterization of H3 variant H3.3

T. thermophila H3.3 has been shown to be non-essential for vegetative growth (Cui et al. 2006). It was found to predominantly localize to the transcriptionally active MAC (Cui et al. 2006), consistent with H3.3 association with an active chromatin state (McKittrick et al. 2004; Hake and Allis 2006). As a replacement histone variant, *T. thermophila* H3.3 is primarily deposited via the replication independent (RI) chromatin assembly pathway (Cui et al. 2006). Interestingly, it was also observed that H3.3 faintly localizes to the MIC via an inefficient entry into the replication dependent (RD) chromatin assembly pathway (Cui et al. 2006). To understand the molecular basis of chromatin assembly pathways and to identify specific protein factors involved in these processes, I generated stable *T. thermophila* cell lines expressing C-terminally FZZ epitope tagged H3.3 from its native MAC locus. After the

completion of phenotypic assortment, the expression of H3.3-FZZ was assessed by Western blots using WCE and probed with an antibody against the ZZ portion of the epitope tag (anti-IgG). As shown in figure 23, a strong band of expected size (~33kDa) was observed in the H3.3-FZZ lanes whereas no signal was detected in the wild type lanes indicating successful expression of the fusion protein. To confirm that the presence of a C-terminal FZZ tag does not interfere in protein localization, I performed IFs on vegetative cell H3.3-FZZ as well as wild type strains using anti-IgG antibody. This specific antibody was used because recent experiments by others in our laboratory have shown that particularly in conjugating cells, it reduces non-specific background (Pearlman et al. un-published observations). Consistent with previous findings (Cui et al. 2006), H3.3-FZZ was found to predominantly localize to the MAC and faintly to the MIC (Figure 24) suggesting that the tagged protein is likely functional as it is found in the expected cellular compartments.

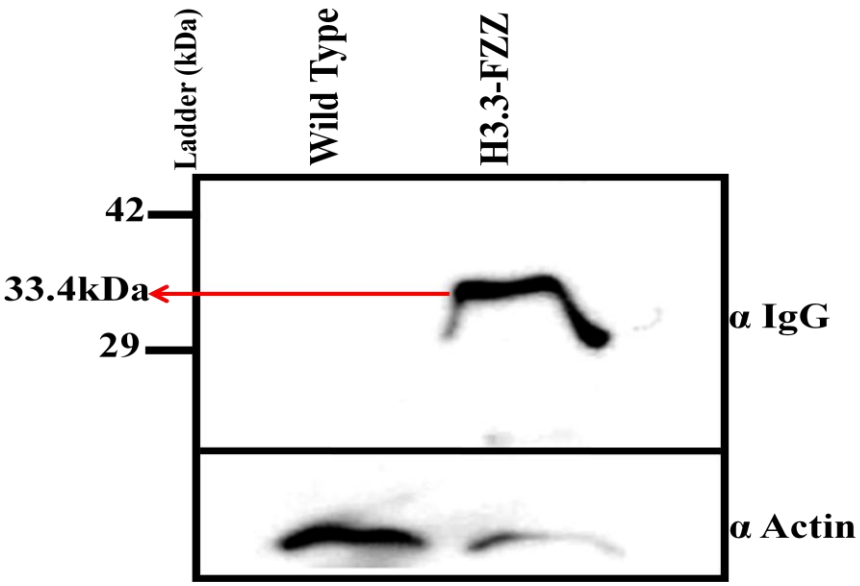

Figure 23: Western blot analysis of H3.3-FZZ. The top panel probed with anti-IgG antibody indicates the successful expression of H3.3-FZZ where no signal was detected in the wild type lanes. The bottom panel is loading control probed with anti-Actin antibody. Note the H3.3-FZZ signal was observed at ~33kDa which is the expected size of the fusion protein (H3.3 size 15.4 kDa+FZZ size 18kDa).

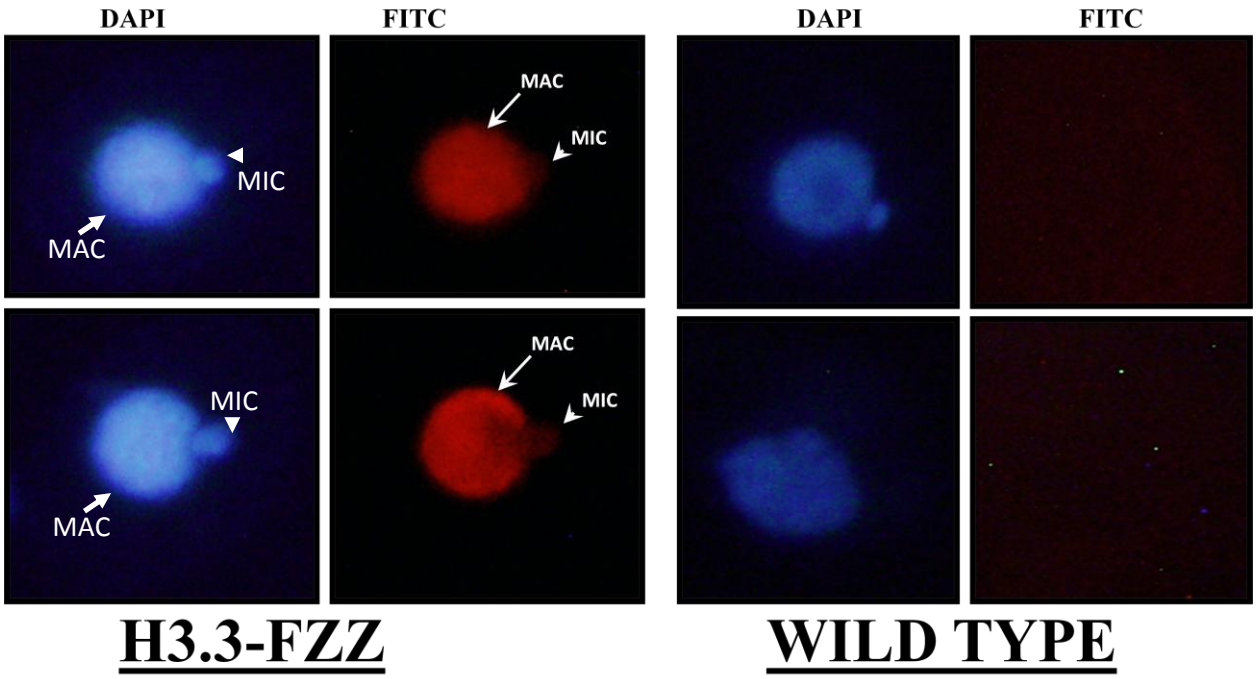

Figure 24: Indirect immunofluorescence analysis of H3.3-FZZ and untagged wild type cells using anti-IgG antibody. Nuclei were stained with DNA-specific dye DAPI. H3.3 predominantly localizes to the MAC and only faintly to the MIC. In contrast no signal was detected in the wild type cells. Arrows represent MAC whereas arrow heads denote MICs

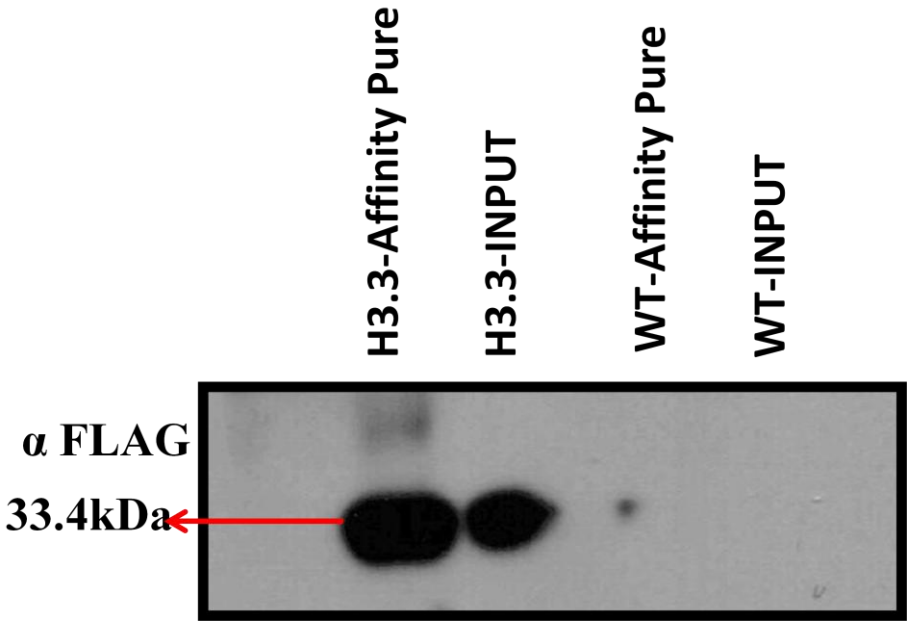

Figure 25: Western blot indicating the recovery of purified H3.3-FZZ. The blot was probed with anti-FLAG antibody which shows signal in H3.3-FZZ lanes. No signal was observed in the wild type lanes.

Subsequently, one step AP was performed on vegetatively growing cells and the recovery of H3.3-FZZ was assessed by Western blotting. As indicated in figure 25, bands were detected only in H3.3-FZZ input as well as AP lanes whereas no signal was present in the wild type lanes when the blot was probed with anti-FLAG antibody. MS analysis revealed the recovery of the bait protein H3.3 along with histone H4 (BFDR $\leq$ 1%) suggesting that both proteins form stable complexes and the presence of the tag does not abolish this interaction. In addition, the SAINT analysis also identified PARP1-A^{Tt}, the NASP homolog in *T. thermophila* Nrp1 (TTHERM_01014770), and a heat shock protein 70 (HSP70) (TTHERM_00105110) as H3.3 co-purifying proteins (Table 6). In addition, Asf1^{Tt} (TTHERM_00442300) was also detected in one of the H3.3-FZZ MS analysis. However it requires biological replicas to be considered for the SAINT analysis and thus further AP-MS experimentation is needed. Previously our laboratory has shown that Nrp1 physically interacts with Asf1^{Tt} and likely functions in the transport of newly synthesized histones H3/H4 (Garg et al. 2013), which is consistent with what has been proposed in humans (Campos et al. 2010). Further characterization of Nrp1 suggests that it also co-purifies with HSP70 and localizes to both the MIC and MAC (Nabeel-Shah and Fillingham un-published). In humans, heat shock proteins have been suggested to assist the proper folding of newly synthesized histones that function upstream of the NASP chaperone in the histone transport chain (Campos et al. 2010). The co-purification of Nrp1, and Asf1^{Tt} with H3.3-FZZ reinforces the previous findings suggesting that Nrp1 and Asf1^{Tt} are bona fide H3/H4 chaperones in *T. thermophila* (Garg et al. 2013).

As noted earlier, PARP1A belongs to a large family of enzymes that function in the ribosylation of target proteins. The co-purification of PARP1A^{Tt} with histones H2A as well

as H3.3 suggests that it is one of the major functional PARPs in *T. thermophila* and likely regulates several aspects of histone metabolism.

Several novel proteins with no known homologs in organisms other than ciliates (as assessed by BLAST) were detected by the SAINT analysis (Table 6). The functional significance of these interactions is currently unclear and begs further investigation. Taken together, I have presented evidence for *T. thermophila* histone H3.3 PPI network which includes evolutionary conserved as well as novel interactions that likely regulate chromatin dynamics in this divergent model organism.

Table 6: AP-MS data from three independent biological replicas filtered using SAINT analysis (BFDR ≤ 1%*)

Bait	Prey	Gene ID	Spectral counts sum
H3.3	-	TTHERM_00016170	49
H3.3	Nrp1	TTHERM_01014770	158
H3.3	PARP1-A	THERM_00502600	263
H3.3	PARP2-A	TTHERM_00823980	11
H3.3	HSP70	TTHERM_00105110	55
H3.3	DnaK	TTHERM_01014750	23
H3.3	H4	TTHERM_00189170	595
H3.3	H2B	TTHERM_00633360	465
H3.3	H2B	TTHERM_00283180	366
H3.3	H2A	TTHERM_00316500	242
H3.3	Hv1	TTHERM_00143660	145
H3.3	RPA1	TTHERM_00047550	192
H3.3	RPA2	TTHERM_01075780	57
H3.3	RPB1	TTHERM_00538940	18
H3.3	RPB	TTHERM_00077230	16
H3.3	RPB5	TTHERM_00941450	11
H3.3	RPC5	TTHERM_00094210	31

H3.3	ATU1	TTHERM_00558620	178
H3.3	Glucosamine-6-phosphate isomerase	TTHERM_00243730	49
H3.3	Cytochrome b5-like	TTHERM_00066830	98
H3.3	CEN1 (CENtrin)	TTHERM_00384910	84
H3.3	TTNB (Tetrin B)	TTHERM_00052160	41
H3.3	NDC80 (Kinetochore-associated Ndc80 complex)***	TTHERM_00249630	37
H3.3	SMC domain protein***	TTHERM_00382370	35
H3.3	Novel??	TTHERM_00266649	31
H3.3	HSP60	TTHERM_00196370	26
H3.3	Novel??	TTHERM_00456860	21
H3.3	Novel??	TTHERM_00487090	12
H3.3	Novel??	TTHERM_00989450	10
H3.3	ADH3	TTHERM_00151670	9
H3.3	Mitochondrial carrier protein	TTHERM_00363210	9
H3.3	SRF13	TTHERM_00522830	9
H3.3	LAP2	TTHERM_00579060	9
H3.3	RVB2 (RuVB-like)	TTHERM_00046920	7
H3.3	Novel??	TTHERM_00969640	7
H3.3	CCT2	TTHERM_00149340	6
H3.3	RPN12	TTHERM_00649110	5
H3.3	Novel??	TTHERM_00426260	4
H3.3	Novel??	TTHERM_00522940	4
H3.3	Novel??	TTHERM_00979780	4
H3.3	Asf1	TTHERM_00442300	13**

* Validated against 9 vegetative cell control; ** Needs experimental replica for SAINT validation, only detected in one purification. **Note**: Standard protein names as available through ciliate.org are listed unless marked by *** in which case BLAST searches were used to detect the homologs.

3.6- Proteomic analysis of MLH1

The *T. thermophila* genome encodes two distinct linker histone proteins which have been shown to have nucleus-specific roles (Allis et al. 1984; Shen et al. 1995). MLH1 is specific to the MIC whereas HHO1 encoded H1 is specific to the transcriptionally active MAC. Neither of these proteins are required for the vegetative growth (Shen et al. 1995). Previous studies have shown that MLH1 is a 71kDa protein which is proteolytically processed into four distinct fragments (Allis et al. 1984; Wu et al. 1994). Initially, through a cleavage of the full length MLH1, two fragments called as alpha (46kDa) and beta (25kDa) are produced such that beta corresponds to the C-terminus of the full length protein. Subsequently, alpha is further processed to give rise to gamma and delta (Wu et al. 1994). These fragments exclusively localize to the MIC and are phosphorylated (Sweet and Allis 1993; Sweet et al. 1997).

In order to examine the PPI of this linker histone, I generated stable cell lines expressing C-terminally FZZ epitope tagged MLH1 from its native chromosomal loci. The expression of the tagged protein was detected on Western blots using whole cell extracts prepared from MLH1-FZZ and wild type cells. The blot was probed with an anti-FLAG antibody. As indicated in Figure 26, a strong signal was detected in the MLH1-FZZ lanes whereas no signal was observed in the wild type suggesting a successful expression of the fusion proteins. Previous studies have indicated that the full length MLH1 is hardly detectable in growing cells because it is immediately processed into alpha and beta fragments (Wu et al. 1994). Therefore the size of MLH1-FZZ on Western blots was expected to be that of the beta fragment fused with the FZZ tag i.e. 43kDa. However, contrary to expectation the band appeared at ~65kDa (Figure 26). As noted earlier, the MLH1 fragments are highly phosphorylated (Sweet and Allis 1993; Sweet et al. 1997), indicating a likely possibility that

phosphorylation of the fusion protein might have retarded its mobility on SDS-PAGE (see discussion).

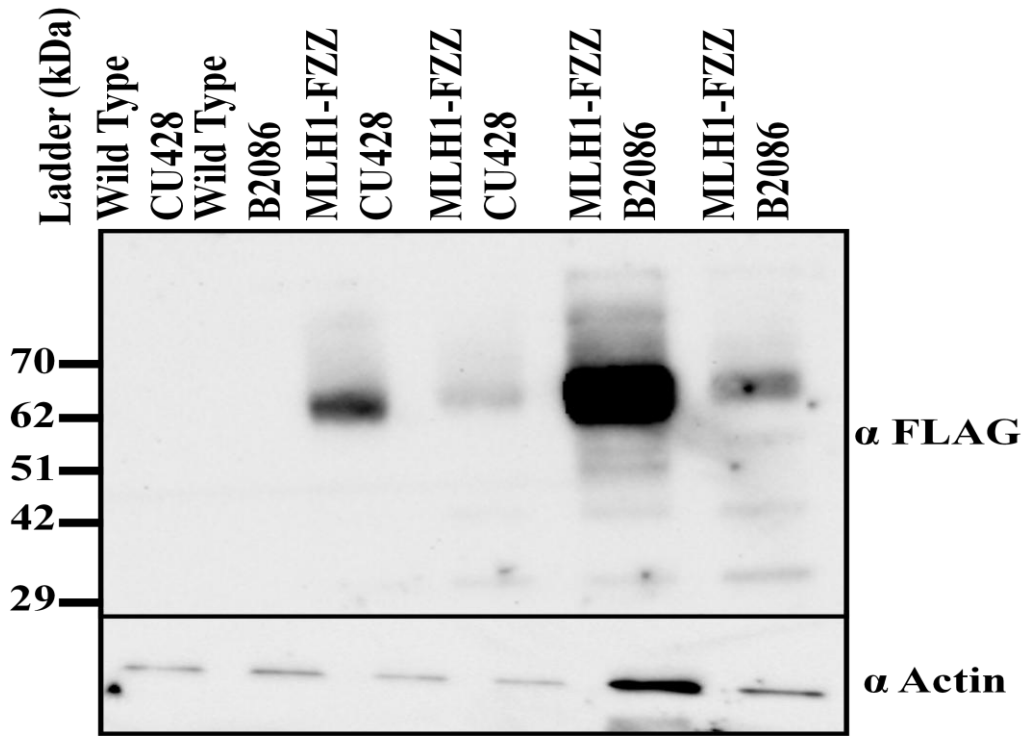

Figure 26: Western blot analysis of MLH1-FZZ. The top panel probed with anti-FLAG antibody indicates the successful expression of MLH1-FZZ. No signal was present in the wild type lanes. Note the discrepancy between expected size of the beta fragment fused to FZZ and the observed location of the major species (see text for details).The bottom panel is a loading control probed with anti-Actin antibody.

To assess the functionality of tagged proteins, I performed IF analysis and observed a signal exclusively in the MIC of growing cells (Figure 27). This result is in agreement with the previous reports (Allis et al. 1984; Wu et al. 1994) and suggests that the tagged protein is likely functional at least for its correct localization. Subsequently, I performed TAP in two biological replicas on vegetatively growing cells. The MS analysis indicated the successful recovery of the bait (Table 7) however no other interacting proteins were detected as assessed by SAINT. To increase the likelihood of capturing transient interactions I took two approaches. First, instead of two step TAP, I performed one step affinity purification, however again no additional interacting partners were detected. Second I used less harsh

conditions during the purification procedure, i.e. 150mM NaCl concentration rather than 300mM NaCl. I was however still unable to recover any additional co-purifying proteins that could be validated by the SAINT analysis. Taken together, these studies suggest that I have successfully generated the MLH1 tagged cell line which most likely expressed the beta-FZZ fragment, and exhibits the correct localization pattern as reported in the literature. Further studies will be required to explore the functional aspects of this protein.

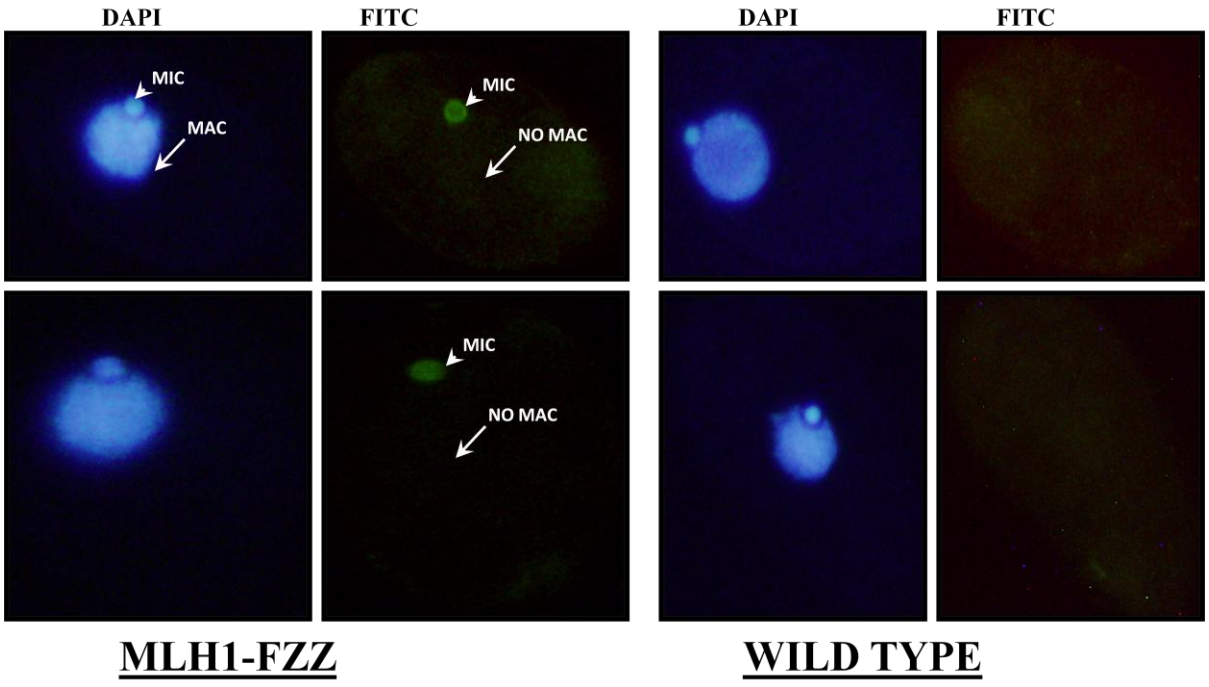

Figure 27: Indirect immunofluorescence analysis of MLH1-FZZ and untagged wild type cells using anti-FLAG antibody. Nuclei were stained with the DNA-specific dye DAPI. MLH1 exclusively localizes to the MIC and no signal was detected in the MAC. Control cells indicated no signal in any of the nuclei. Arrows represent MAC whereas arrow heads denote MICs

Table 7: AP-MS data filtered using SAINT analysis. Various experimental conditions used are also noted.

NAME	**TTHERM #**	**Spectral Counts** (Sum)
MLH1 (Bait) (Using two step TAP @300mM NaCl concentration); 2 Biological replicas	TTHERM_00471820 (Bait) Note: No prey was detected after data validation using SAINT (BFDR $\leq$ 1%)	233 None detected in 9 WT control purifications
One step affinity purification using low salt conditions of 150mM NaCl [ ]		
MLH1 (Bait)	TTHERM_00471820	62 / 0 in WT
One step affinity purification using 300mM NaCl [ ]		
MLH1 (Bait) Two Biological replicas	TTHERM_00471820 Note: No prey was detected after data validation using SAINT(BFDR $\leq$ 1%)	65 for MLH1 None detected in 9 independent WT controls

Chapter 4- Discussion

In eukaryotes the establishment of distinct chromatin states is essential for the proper functioning of various cellular processes including gene expression regulation as well as genome integrity (Avvakumov et al. 2011). Increasingly, links have been discovered between aberrant chromatin states and disease formation in humans (Burgess and Zhang 2013). Chromatin assembly is a highly ordered process which is believed to begin in the cytoplasm where newly synthesized histones are shuttled through a network of several protein factors (reviewed in Gurard-Levin et al. 2014). Numerous studies have revealed the involvement of several histone chaperones as well as histone modifying enzymes in this tightly regulated process (Bannister and Kouzarides 2011; Keck and Pemberton 2012). For example, in humans newly synthesized H3.1/H4 are transported from the cytoplasm to the nucleus via a stepwise process in which NASP and Asf1 histone chaperones as well as HAT1-complex and Impβ4 have been shown to have key roles (Campos et al. 2010; Alvarez et al. 2011). Inside the nucleus histone chaperones such as CAF1 and HIRA mediate the distinct RD and RI chromatin assembly pathways for depositing H3 and H3.3, respectively, onto DNA (Hoek and Stillman 2003; Tang et al. 2006). In budding yeast, histone chaperone Nap1 along with a Kap114 has been shown to function in H2A/H2B transport (Mosammaparast et al. 2001; Keck and Pemberton 2012) whereas SWR1 is the key chromatin remodelling complex responsible for the deposition of H2A.Z (Kobor et al. 2004; Mizuguchi et al. 2004). Despite the identification of these complexes, questions remain with respect to underlying mechanistic details as well as how specific histone variants are targeted to distinct chromatin regions. Clearly, the picture of histone transport as well as their subsequent deposition onto chromatin is far from complete.

T. thermophila features the spatial distinction of two chromatin states in the form of transcriptionally active MAC and silent MIC. This feature provides an excellent opportunity to investigate various chromatin related processes including the histone transport pathway and function of histone chaperones as well as histone modifying enzymes. Here I have presented the proteomic analysis of core as well as variant histones in *T. thermophila* which permitted me to derive useful insights with respect to the functions of various chromatin related proteins and their roles in the assembly pathways.

4.2- Histone H2A and its interacting partners

It has previously been established that the *T. thermophila* genome encodes two major histone H2A proteins, H2A.1 and H2A.2, neither of which are essential for the vegetative growth (Liu et al. 1996). To learn about the protein-protein interactions and gain insight into H2A transport and deposition complexes, I performed AP-MS using cell lines stably expressing FZZ epitope from the native chromosomal locus of histone H2A.1 (H2A hereafter). The IF analysis indicated that consistent with a previous report (Liu et al. 1996), H2A-FZZ localizes to both the MAC and the MIC. While a rigorous analysis is lacking, the expected nuclear localization pattern of H2A-FZZ suggests that the protein is functional for at least its transport to the nuclei and is probably incorporated into chromatin as efficiently as the wild type. Further experiments such as triton extraction of the chromosomes (as previously employed by Cui et al. 2006) followed by assessing the retention of H2A-FZZ within chromatin will be helpful to fully establish that FZZ tagged histones are functional and are incorporated as efficiently as their wild type counterparts. Additionally, Southern blotting can be used to establish a complete replacement of the endogenous H2A locus with H2A-FZZ, which can be followed by ChIP experiments to demonstrate the functionality of the tagged proteins.

SAINT analysis of APMS data revealed that H2A-FZZ co-purifies with *T. thermophila* putative PARP2^{Tt}, PARP2A^{Tt} and PARP1A^{Tt} proteins as well as an NPM-like histone chaperone which I have named Cnpl-1. As noted earlier, vertebrates have three NPM [1-3] proteins that likely arose via gene duplication whereas invertebrates such as fruit flies have only one NPM-like protein (Eirín-López et al. 2006). Domain analysis of Cnpl-1 suggests that it contains a predicted N-terminal NPM-core domain, three acidic regions, a nucleic acid binding domain as well as a putative NoLS. This domain organisation is similar to that of the vertebrate NPM1 consistent with the previous reports indicating a closer phylogenetic relationship between vertebrate NPM1 and invertebrate NPM-like proteins (Eirín-López et al. 2006). NPM1 functions as a histone chaperone (Okuwaki et al. 2001) and has been shown to be involved in a variety of processes including nucleosome assembly (Dutta et al. 2001) , ribosome biogenesis, centrosome duplication, cell proliferation, genomic stability and regulation of tumor suppressors p53/TP53 and ARF (Okuda et al. 2000; Pang et al. 2003; reviewed in Finn et al. 2012) . In *X. laevis* oocytes and eggs, NPM is thought to provide a buffering mechanism for the soluble reservoirs of H2A/H2B that are required for DNA replication after fertilization (Dingwall et al. 1987; Dingwall and Laskey 1990).

The NPM proteins have previously been predominantly studied in eukaryotes such as fruit flies and vertebrates (Frehlick et al. 2007; reviewed in Finn et al. 2012), and their functional significance in unicellular organisms remain unknown. The fact that *T. thermophila* H2A co-purified with a putative Cnpl-1 protein suggests that the evolutionarily conserved function of NPM-like proteins is to chaperone H2A/H2B. Histone chaperones are often negatively charged and contain acidic stretches necessary for their interaction with positively charged histones. For example, the NASP family of histone chaperones contain a large acidic stretch which has been shown to be essential for their interaction with H3/H4

(Dunleavy et al. 2007; Wang et al. 2008). The presence of acidic domains within Cnpl-1 further reinforces the idea that it is a bona fide histone chaperone. Considering the polyploid MAC which requires huge amounts of histones, it is tempting to speculate that Cnpl-l might function as a histone storage buffer. Further studies will be required to elucidate the exact functions of Cnpl-1. It will be useful to study the localization patterns as well as generation of KO strains in order to understand the functional significance of this putative histone chaperone.

Previous studies have shown that H2A/H2B are transported by Nap1 histone chaperone and Kap114 (Mosammaparast et al. 2001; Mosammaparast et al. 2002). The *T. thermophila* genome encodes a putative $Nap1^{Tt}$ (TTHERM_00786930) protein which did not co-purify with H2A-FZZ. It is possible that $Nap1^{Tt}$ transiently interacts with H2A/H2B heterodimer and this interaction was lost due to stringent experimental conditions e.g. high salt concentration (300mM) or due to the presence of an epitope tag. Studying protein-protein interactions as well as KO analysis of $Nap1^{Tt}$ will provide insights into its functional significance. The *T. thermophila* genome encodes 24 karyopherins (Malone et al. 2008), however I did not recover any of those in H2A-FZZ tandem affinity purifications. Currently, more sensitive one-step affinity purifications are underway and it will be interesting to see whether any H2A/H2B specific importins do exist in *T. thermophila.*

It has been shown that ribosylation of histones have several important functions. For example, upon DNA DSB, histones are heavily ribosylated by PARP1 which functions in the repair pathway (Kreimeyer et al. 1984; Boulikas 1989). Furthermore, ribosylation of chromatin functions to loosen it thus making it more accessible for the transcription machinery (Ko and Ren 2012). It has recently been shown that PARP1 can switch its roles from a chromatin architectural protein to a histone chaperone (Muthurajan et al. 2014).

Furthermore, newly synthesized histones H3/H4 are transiently ribosylated in humans, although the functional significance and specific PARP enzyme responsible for this PTM is currently unknown (Alvarez et al. 2011). It has been suggested that the ribosylation of new histones might be required for their proper folding (Alvarez et al. 2011). The *T. thermophila* genome encodes at least 10 putative PARP proteins, out of which three were co-purified with H2A-FZZ. Based on domain architecture and sequence similarity, I have classified the co-purified proteins as PARP2^{Tt}, PARP2A^{Tt} and PARP1A^{Tt}. Previous evolutionary studies as well as biochemical analysis of PARPs in humans have categorized PARP1/2/4/6 as catalytically active and capable of ribosylation of substrate proteins (Citarelli et al. 2010; Vyas et al. 2013). The co-purification of *T. thermophila* putative PARP2^{Tt} and PARP2A^{Tt} with H2A and PARP1A^{Tt} with both H2A and H3.3 suggests that similar to other eukaryotes, histones might be ribosylated in this model organism. While a functional analysis of *T. thermophila* PARP proteins is lacking, initial evidence from the IF studies of PARP1A^{Tt} suggest that similar to H2A it also localizes to both the MAC and MIC, consistent with their functional linkage. A plausible hypothesis would be that PARP1A^{Tt} carries out histone ribosylation which might be important for chromatin assembly process. To assess this hypothesis an *in vitro* ribosylation assay using purified native PARP1A^{Tt} and histones should be carried out. This will experimentally establish the catalytic activity of *T. thermophila* PARP1A. *In vitro* nucleosome assembly assays might also be helpful to gain insights whether PARP1-A^{Tt} is capable of chromatin assembly. Furthermore, a KO analysis may yield insights into *in vivo* functions of PARP1A^{Tt} including any defects in chromatin assembly and/or developmental phenotypes. For example, isolation of the MACs from both the KO and WT strains followed by MNase digestion may yield insights into any global alterations in the bulk chromatin structure. Considering the role of γH2A.X as well as PARP1

in DNA DSBs, it will be interesting to induce the DNA damage (using damaging agents such as methyl methanesulfonate (MMS) in growing *T. thermophila* cells followed by AP-MS to identify any DNA repair related PPIs.

4.2.1- FACT complex is evolutionarily conserved

Proteomic characterization of the putative *T. thermophila* FACT complex indicates that similar to the other eukaryotes (Formosa et al. 2001; Biswas et al. 2005) it consists of two proteins $Spt16^{Tt}$ and $Pob3^{Tt}$. These observations suggest that the composition of the FACT complex is evolutionarily conserved. The conserved domain architecture of each of $Spt16^{Tt}$ and $Pob3^{Tt}$ supports the idea that the *T. thermophila* putative FACT complex is functionally conserved as well. FACT is an abundant protein complex that has been shown to have critical roles in transcription elongation (Orphanides et al. 1998). *In vivo* studies have linked replication and transcription defects with the lack of a functional FACT complex (Biswas et al. 2005). While much of the research has highlighted its roles in transcription regulation (Biswas et al. 2005; Reinberg and Sims 2006), several studies have revealed expanded functions of FACT in various other chromatin related processes. For example, FACT has been shown to be involved in DNA replication as well as in DNA damage repair (Li et al. 2005; Dinant et al. 2008). FACT has been shown to co-purify in a complex with H2A.X, DNA-PK and PARP1 (Heo et al. 2008). The phosphorylation of H2A.X increases the exchange of H2A.X-H2B whereas PARP1-mediated ribosylation of FACT inhibits this exchange during DNA damage repair (Heo et al. 2008). These experiments suggested a possible mechanism through which FACT function might be regulated during DNA repair.

Consistent with the known functions of FACT in transcription regulation (Voth et al. 2014), IF analysis of $Spt16^{Tt}$ showed that it predominantly localizes to the transcriptionally active MAC. In addition to the MAC, $Spt16^{Tt}$ was also found to localize in the MIC during *T.*

thermophila vegetative growth. It is possible that Spt16^{Tt} functions in the overall maintenance of the MIC genome or have roles during MIC mitosis consistent with the demonstrated involvement of the FACT complex during DNA replication and damage repair (Li et al. 2005; Dinant et al. 2008). A recent structural study indicated that a 'U-turn' motif scaffolded onto a Rtt106-like module of *Chaetomium thermophilum* Spt16 is responsible for a direct interaction with H2B (Hondele et al. 2013). As noted above, both the Spt16^{Tt} and Pob3^{Tt} contain Rtt106 like domains which have been shown to function as histone chaperones as well as in heterochromatin-mediated silencing (Huang et al. 2005). FACT has also been shown to be required for centromeric-heterochromatin integrity and accurate chromosome segregation (Lejeune et al. 2007). Thus it is possible that the *T. thermophila* FACT complex might have a role in the maintenance of silent MIC chromatin, although conclusive evidence requires further investigation. It will be interesting to study Pob3^{Tt} function and its localization patterns to further gain insights into function of the FACT complex. A KO analysis of *SPT16^{Tt}* followed by RNA-seq will be instructive to assess the global defects in gene transcription due to the lack of a functional FACT. Furthermore, elucidating any possible developmental roles of FACT during *T. thermophila* conjugation will be of interest.

4.3- Histone variant Hv1 physically interacts with an Impβ3

Histone H2A variant Hv1 (also known as H2A.Z in *S. cerevisiae*) is an evolutionarily conserved variant which has been linked to transcriptionally active chromatin (Jackson and Gorovsky 2000; Krogan et al. 2003; Meneghini et al. 2003; Thakar et al. 2009; Biterge and Schneider 2014). H2A.Z has been found to be enriched at gene promoters in *S. cerevisiae* (Guillemette et al. 2005; Zhang et al. 2005), mammals (Bernstein et al. 2007) and plants (Zilberman et al. 2008) indicating its essential roles in the gene transcription. Evolutionarily

conserved ATP-dependent chromatin remodelling complex SWR-1 has been shown to be important for the incorporation of H2A.Z in *S. cerevisiae* (Krogan et al. 2003; Kobor et al. 2004; Mizuguchi et al. 2004). The SWR-1 complex exchanges H2A-H2B dimmers for free H2A.Z-H2B and selectively targets them to euchromatic regions (Luk et al. 2010). In *T. thermophila* Hv1 has been shown to exclusively localize to the MAC indicating that it is a transcription related histone variant (Stargell et al. 1993). This observation was further supported by the fact that Hv1 is an essential gene in *T. thermophila* and cells lacking this gene are not viable (Liu et al. 1996). This observation indicates that Hv1 has functions distinct from those of the major H2A genes.

H2A. Z also carries PTMs including acetylation, sumoylation and ubiquitination with various functional consequences (Thambirajah et al. 2009). For example, H2A.Z sumoylation in *S. cerevisiae* has been linked with DNA repair (Kalocsay et al. 2009) whereas acetylation of N-terminal lysine residues results in nucleosomal destabilization (Thambirajah et al. 2006). In budding yeast acetylation of lysin 14 has been shown to be enriched at transcriptionally active promoters (Millar et al. 2006). In *T. thermophila* lysine residues have been shown to be essential for viability suggesting that the aceytlation of hv1 has crucial roles (Ren and Gorovsky 2001). Interestingly, H2A.Z has also been found to be present in the heterochromatin where it can function in the formation of pericentric and centric chromatin (Rangasamy et al. 2003; Greaves et al. 2007). Consistent with a role in heterochromatin formation, monoubiquitylation of H2A.Z has been linked with gene silencing (Sarcinella et al. 2007).

As noted earlier *T. thermophila* features two distinct nuclei in the form of the MAC and MIC. This raises an additional challenge of how functionally specialized proteins such as Hv1 are targeted to a particular nucleus. To provide insights into Hv1 transport machinery in

T. thermophila, I began to characterize the PPI network of this essential histone variant. IF analysis indicated that in accordance with previous studies (Stargell et al. 1993), Hv1-FZZ localizes to transcriptionally active MAC indicating that the tagged protein is functional at least for its correct nuclear localization. Proteomic analysis of Hv1-FZZ indicated that it physically interacts with an Impβ3 protein. Impβ3 is one of the 24 karyopherins (13 encoded by imp α-like genes and 11 encoded by imp β-like genes) which have previously been shown to be encoded by the *T. thermophila* genome (Malone et al. 2008). Karyopherins are a large group of evolutionarily conserved nucleo-cytoplasmic transport factors that shuttle NLS-containing cargo via nuclear pore complexes (NPCs) (O'Reilly et al. 2011). The Impβ3 is a homolog of *S. cerevisiae* Kap121 which has previously been shown to function in histone transport pathways (Mosammaparast et al. 2001). Interestingly, Impβ3 is one of the only two Impβ proteins (Impβ4 being the other) which have previously been shown to predominantly localize to the MAC whereas all remaining Impβs have been found to localize to both nuclei (Malone et al. 2008). These observations along with the proteomic analysis presented here suggest a possible mechanism of targeting Hv1 specifically to the MAC. I propose that Hv1 forms a stable complex with Impβ3 in the cytoplasm which ensures the specific targeting of this essential histone variant to the MAC and not to the MIC. It should be noted however that because Hv1 is an essential gene in *T. thermophila*, it is likely that multiple pathways exist to ensure its sufficient supply to the MAC. A KO analysis of Impβ3, providing it is not essential for the cell viability, followed by an analysis of Hv1 localization using anti-hv1 antibody (available from Stargell et al. 1993) will help further elucidating the mechanistic details of the Hv1 transport pathway.

It is also worthwhile to note that in budding yeast Kap114 and Nap1 have been shown to be involved in Htz1 transport from the cytoplasm to the nucleus (Straube et al. 2010). In

addition Kap123 appears to have a redundant role with Kap114 to transport Htz1 (Straube et al. 2010). As noted earlier, Kap114 and Nap1 also form a major pathway for H2A/H2B transport in budding yeast (Mosammaparast et al. 2001) indicating that core histone H2A and its variant Htz1 utilize the same karyopherin. In contrast to the situation in budding yeast, it is unlikely that H2A and Hv1 in *T. thermophila* share the same major pathway. It is because Impβ3 predominantly localizes to the MAC (Malone et al. 2008) whereas core histone H2A is present in both nuclei. Nevertheless, it will be interesting to investigate the potential role of Nap1 in Hv1 transport and metabolism because it has been shown to function as a buffer to maintain soluble pools of H2A.Z in yeast (Straube et al. 2010).

I did not recover any subunits of the putative *T. thermophila* SWR-1 complex. As assessed by genome annotations, *T. thermophila* encodes putative homologs of SWR-1 subunits including Yaf9 (TTHERM_00248210), nucleosome-binding component of the Swr1 complex Vps71 (TTHERM_01298590), Swc4 (TTHERM_00357110) and Swi2/Snf2-related ATPase Swr1 (TTHERM_01546860). One possible reason for this could be the experimental conditions including using 300mM NaCl which was used during Hv1-FZZ purifications (see Materials and Methods). Such high salt concentrations potentially could disrupt any transient interactions. In addition, the possibility of the FZZ tag destabilizing the interaction cannot be excluded. Further studies will be required to establish a more comprehensive view of how Hv1 is deposited onto chromatin in *T. thermophila* and what other protein factors are involved in handing over Hv1 to the Swr-1 complex once it finds its way inside the nucleus.

4.4- Histone H3.3 interacts with Nrp1 and Asf1^{Tt}

Canonical histones H3.1 and H3.2 are exclusively expressed during S-phase of the cell cycle and in humans are deposited onto chromatin in a RD assembly pathway mediated by Caf1 complex (Tagami et al. 2004). In contrast, the replacement histone variant H3.3 is

expressed throughout the cell cycle and is mainly deposited by the RI pathway mediated by the HIRA complex (Wu et al. 1982; Ahmad and Henikoff 2002; Tagami et al. 2004). A notable exception to this general trend is *Drosophila* H3.3 which can be deposited via both the RD and RI pathways (Ahmad and Henikoff 2002). H3.3 containing nucleosomes are thought to be less structured and associated with a more transcriptionally active chromatin state (McKittrick et al. 2004). Consistent with this, H3.3 deposition into nucleosomes has been associated with transcriptional activity and this histone variant has been found to be highly enriched within actively transcribed genes (Mito et al. 2005; Jin et al. 2009). *In T. thermophila*, two RI histone H3 variants namely H3.3 and H3.4 are known to exist (Cui et al. 2006). Previous studies have revealed that cells harbouring both the single or the double KOs of H3.3 and H3.4 are viable, indicating that the expression of the quantitatively minor H3 variants is not required for vegetative growth (Cui et al. 2006). Immunofluorescence studies of GFP tagged H3.3 have indicated that it predominantly localizes to the MAC (Cui et al. 2006), consistent with the known association of this variant with actively transcribed genes (Mito et al. 2005; Jin et al. 2009). A faint signal of the GFP tagged H3.3 was also observed in the transcriptionally silent MIC which persisted throughout vegetative growth and disappeared in starved condition when DNA replication is halted (Cui et al. 2006). Based on these observations, it was suggested that similar to *Drosophila, T. thermophila* H3.3 can also be deposited via both RD and RI pathways (Cui et al. 2006). In accordance with these observations, my IF analysis of H3.3-FZZ indicated that it predominantly localizes to the MAC whereas it is found only faintly in the MIC. Unpublished evidence from our laboratory indicates that the H3.3 putative chaperone $HIRA^{Tt}$ also localizes to the MIC during vegetative growth and its signal vanishes from the MIC during prolonged starvation (Nabeel-Shah, Fillingham, et al. unpublished observations). This observation raises the possibility that

the observed H3.3 signal in the MIC might be due to the function of RI chaperone HIRA and not due to RD histone chaperone Caf1. This hypothesis is supported by several lines of recent evidence. For example, it has recently been shown that the HIRA complex deposits H3.3 in the nuclesomal gaps to maintain genome integrity (Ray-Gallet et al. 2011). It has been proposed that while Caf1 mediates deposition of the major histone H3.1 during DNA replication, the HIRA complex fills the nucleosomal gaps in a post-replication manner resulting in a broad distribution of H3.3 throughout the genome (Ray-Gallet et al. 2011). The selective enrichment of H3.3 at actively transcribed chromatic regions has been explained in terms of HIRA association with RNA Pol II (Ray-Gallet et al. 2011). In the same study (Ray-Gallet et al. 2011), it was also shown that depletion of the Caf1 complex impairs H3.1 deposition and enables H3.3 to be deposited onto replication sites via HIRA. Depletion of HIRA resulted in an impairment of H3.3 deposition but without any significant increase in the distribution of H3.1 (Ray-Gallet et al. 2011). This is consistent with the fact that in *T. thermophila* an over expression of H3.3 can support vegetative growth even in the absence of canonical histone H3s (Cui et al. 2006). In contrast, lack of H3.3 does not increase the expression of the canonical H3s (Cui et al. 2006). Taken together these studies along with the observed HIRA^{Tt} localization patterns suggest that H3.3 presence in the MIC might represent a scenario which is similar to what has been proposed in humans where HIRA mediates a nucleosomal gap-filling H3.3 incorporation in a post-replication manner to ensure overall genomic integrity. Furthermore, similar to humans, HIRA^{Tt} and H3.3 presence in the MIC may also represent an alternative mechanism of chromatin assembly which becomes functional if RD chaperone CAF1 is impaired. Additional support for these hypotheses comes from our laboratory's un-published observations which suggest that *HIRA^{Tt}* is an

essential gene in *T. thermophila* whereas the p60 subunit of the putative *CAF1*^{Tt} is not required for vegetative growth (Jeyapala and Fillingham et al. unpublished observations).

Recent evidence indicates that H3.3 is not exclusively associated with euchromatic regions and can also be found within repressed and poised genes (Delbarre et al. 2010; Goldberg et al. 2010). Consistent with this, H3.3 has also been found to be associated with pericentric and telomeric chromatin regions (Wong et al. 2009; Drané et al. 2010; Lewis et al. 2010). Thus it is formally possible that H3.3 presence in the MIC might be due to its additional roles in overall genome integrity. For example, H3.3 is deposited at centromeres as a place holder for newly assembled centromere-specific histone H3 variant CENP-A (Dunleavy et al. 2011). In *T. thermophila,* only MIC chromosomes have centromeres and CENP-A exclusively localizes to the MIC (Cervantes et al. 2006; Cui and Gorovsky 2006).

To further elucidate the functions of H3.3 and its deposition pathway in *T. thermophila,* I carried out AP-MS analyses and investigated its PPI network. My data indicate that H3.3 co-purifies with two evolutionarily conserved H3/H4 chaperones, Asf1 and Nrp1. Recently, our laboratory has shown that Asf1^{Tt} physically interacts with Nrp1, Impβ6 and histones H3/4 (Garg et al. 2013). It has been proposed that Asf1^{Tt} and Nrp1 along with Impβ6 function in the transport of newly synthesized histones H3/H4 (Garg et al. 2013). Nrp1 belongs to a family of H3(H3.3)/H4 chaperones which we have recently shown to be conserved throughout the major eukaryotic lineages (Nabeel-Shah et al. 2014). Taken together, my data confirm previously reported Nrp1 and Asf1 interaction with histones H3(H3.3)/H4 (Garg et al. 2013) and further establishes them as bonafide histone chaperones in *T. thermophila* I did not co-purify putative HIRA^{Tt} with H3.3. Several possible reasons could account for this possibly unexpected observation. For example, HIRA has been shown to directly bind with DNA (Ray-Gallet et al. 2011) and its interaction with H3.3 might be in

the context of chromatin structure. Because my experimental setup only recovers the soluble pool of PPIs, it is possible that the $HIRA^{Tt}$ -H3.3 interaction was not detected. An additional hypothesis for the absence of $HIRA^{Tt}$-H3.3 interaction could be related to the presence of an epitope tag on H3.3 which could have destabilized the interaction. Further studies will be required to fully understand the H3.3 deposition pathway and to unravel the reasons for not detecting a $HIRA^{Tt}$ interaction. To this end, assessing the localization patterns of H3.3 in a $HIRA^{Tt}$ KO will be informative.

4.5- *T. thermophila* MLH1 exclusively is found in the MIC

The *T. thermophila* genome encodes two linker histones which have been shown to have nucleus-specific localization patterns and neither are essential for vegetative growth (Shen et al. 1995). MIC-specific linker histone Mlh1 is a 71kDa protein which has previously been shown to be processed to produce four distinct polypeptides, namely alpha, beta, and gamma, delta both of which are derived from further cleavage of alpha (Wu et al. 1994). Each of these peptides contain phosphorylation sites for cyclic-AMP dependent protein kinase and have been shown to be highly phosphorylated in mitotically dividing nuclei (Sweet and Allis 1993; Sweet et al. 1997). Furthermore, the phosphorylation of the delta peptide occurs in early conjugation, a period when the MIC becomes transcriptionally active, and has therefore been associated with transcription activation (Sweet et al. 1996). These studies have highlighted the functional significance of Mlh1 however the identity of the protease involved in the processing remains obscure.

In an effort to learn about the PPI and to uncover the potential protease that processes the Mlh1 into four peptides, I generated a C-terminal epitope tagged cell line expressing Mlh1-FZZ from its native chromosomal locus. The IF analysis revealed that in accordance with previous reports (Sweet and Allis 1993; Wu et al. 1994; Sweet et al. 1997), tagged Mlh1

localized exclusively to the MIC. This suggests that the protein is functional and likely is incorporated into chromatin. AP-MS analysis revealed the recovery of the bait. However no enrichment of any co-purifying proteins was detected as assessed by statistical SAINT analysis. Previously it has been shown that the full length Mlh1 (71kDa) can hardly be detected in growing cells and it is immediately processed into alpha and beta fragments of 46 and 25 kDa respectively (Wu et al. 1994). Because I used a C-terminal FZZ epitope tag, it is likely that the full length Mlh1 was excluded from my analysis. The beta fragment comprises the C-terminus of the full length Mlh1 (Wu et al. 1994) and therefore might have been the only fragment recognized in my analysis. The Western blot detected a strong signal at ~65kDa which was higher than the expected size of the beta fusion protein (25kDa + 18kDa FZZ). As noted earlier, all four Mlh1 fragments are highly phosphorylated (Sweet and Allis 1993; Sweet et al. 1997), and phospho proteins have the tendency to move slower on SDS-PAGE (e.g. Wegener and Jones 1984; Delom and Chevet 2006). It is therefore possible that the discrepancy in the expected size of beta-FZZ observed on the Western blot might be due to the hyper-phosphorylation of this fragment. To further resolve these discrepancies, it will be informative to analyse the unique peptides detected in the MS analysis as well as any PTMs present on them.

4.6- Conclusions and future directions

I have characterized the initial PPI network of core histone H2A, its variant Hv1as well as the histone H3 variant H3.3 in *T. thermophila* (See Figure 28). This network will definitely grow as more histone co-purifying proteins will be characterized in future studies. Several important conclusions can be drawn as described below.

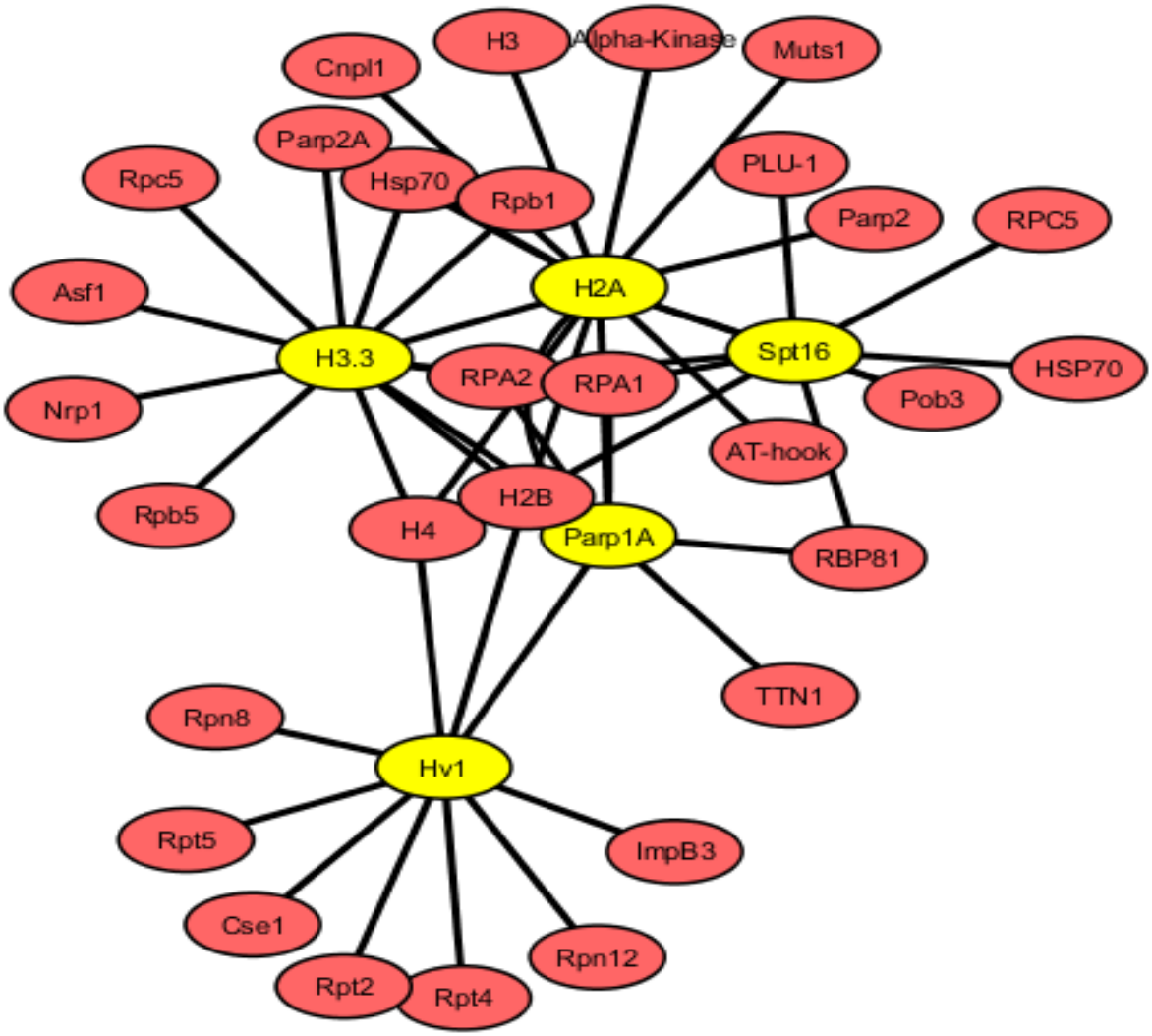

Figure 28: Network representation of PPIs of *T. thermophila* H2A, Hv1, H3.3, Spt16 and Parp1-A based on work presented here. This is an undirected network where nodes denote the proteins and edges indicate the interaction. Baits are indicated in yellow color. Note this subjective network is simplified to include only those SAINT validated PPIs which were recovered in multiple biological replicas. Image was generated using software cytoscape version 3.02 (Shannon et al. 2003)

1- H2A AP-MS data indicate evolutionarily conserved interactions with putative Cnpl-1 and the FACT complex which have previously been studied only in eukaryotes such as humans and frog (Dingwall and Laskey 1990; Orphanides et al. 1998) . My data suggest that in *T. thermophila* the composition of the FACT complex is conserved and is homologous to its budding yeast or human counterparts (Formosa et al. 2001; Biswas et al. 2005). It is comprised of two putative subunits namely Spt16^{Tt} and Pob3-like proteins. The IF analysis of Spt16^{Tt} in turn suggests that it might have roles in determining genome integrity as well as in DNA replication due to its presence in the transcriptionally silent MIC. Furthermore, consistent with the known roles of the FACT complex in transcription regulation (Orphanides et al. 1998), my IF data reveal that Spt16^{Tt} predominantly localizes to the transcriptionally active MAC. This indicates that in addition to the conserved proteomic composition, the FACT complex is functionally conserved as well. To gain further insights into *T. thermophila* FACT complex composition, it will be helpful to study the PPI of Pob3-like^{Tt}. This analysis will help identifying any HMG protein that might be a component of the putative FACT complex. Furthermore, KO analysis of Spt16^{Tt} followed by RNA-seq to assess any global defects in gene transcription will be useful to assess the functional significance of the FACT complex. The co-purification of Cnpl-1 and its conserved domain architecture implicates this protein as a bona fide histone H2A/H2B chaperone in *T. thermophila* that might have functional roles in chromatin assembly or histone transport pathways. Studying PPI as well as localization patterns of Cnpl-1 will be informative to decipher its functional significance. To this end, I have generated an epitope tagged cell line expressing Cnpl1-FZZ from its native chromosomal locus. Currently, cells have finished phenotypic assortment and will be subjected to AP-MS in future.

2- The co-purification of the putative PARP2^{Tt}, PARP2A^{Tt} and PARP1A^{Tt} proteins with H2A and PARP1A^{Tt} with H3.3 suggest that ribosylation of histones might be one of the major histone PTMs in this model organism. While functional analysis is presently lacking, it is tempting to speculate that histone ribosylation might be involved in the chromatin assembly pathway. Preliminary IF analysis of PARP1A^{Tt} indicates that it localizes to both the MAC and MIC suggesting a functional link with histone H2A as well as H3.3 proteins. It will be helpful to assess the PTMs on these histones via MS analysis. Furthermore, *in vitro* ribosylation assay using native PARP1A^{Tt} will help establishing that the protein is catalytically active. Moreover, KO analysis of PARP1A^{Tt} followed by assessing defects in chromatin assembly due to loss of histone ribosylation might be helpful to comprehensively characterize the functional significance of this PTM. Moreover, it will be interesting to study the role of *T. thermophila* PARPs in DNA DSB repair. To this end, inducing DNA damage by MMS followed by AP-MS using PARP1-FZZ (as well as H2A.X) will be helpful to derive initial clues.

3- Proteomic analysis of Hv1 indicates that it physically interacts with an Impβ3 which has previously been shown to localize predominantly to the MAC (Malone et al. 2008). This interaction suggests a possible mechanism of targeting Hv1 specifically to the transcriptionally active MAC and not to the MIC. I propose that Hv1 and Impβ3 form a stable complex in the cytoplasm from where they are shuttled to the MAC (Figure 29). In order to learn more about this transport pathway, it will be helpful to engineer the Impβ3 KO cell lines followed by Hv1 localization analysis using anti-Hv1 antibody. It is important to note however that Hv1 is essential for cell viability, and thus the existence of redundant pathways cannot be excluded. Furthermore, it will be interesting to investigate whether Nap1

has a role in this pathway similar to what has been demonstrated in budding yeast (Straube et al. 2010).

In order to characterize the putative *T. thermophila* SWR-1 complex and its role in Hv1 deposition, it will be important to study the PPI of the SWR-1 complex by generating epitope tagged cell lines of its putative subunits. To this end, in collaboration with a previous laboratory colleague we have engineered the gene targeting constructs of putative Yaf9^{Tt} (Nabeel-Shah and Fillingham et al unpublished).

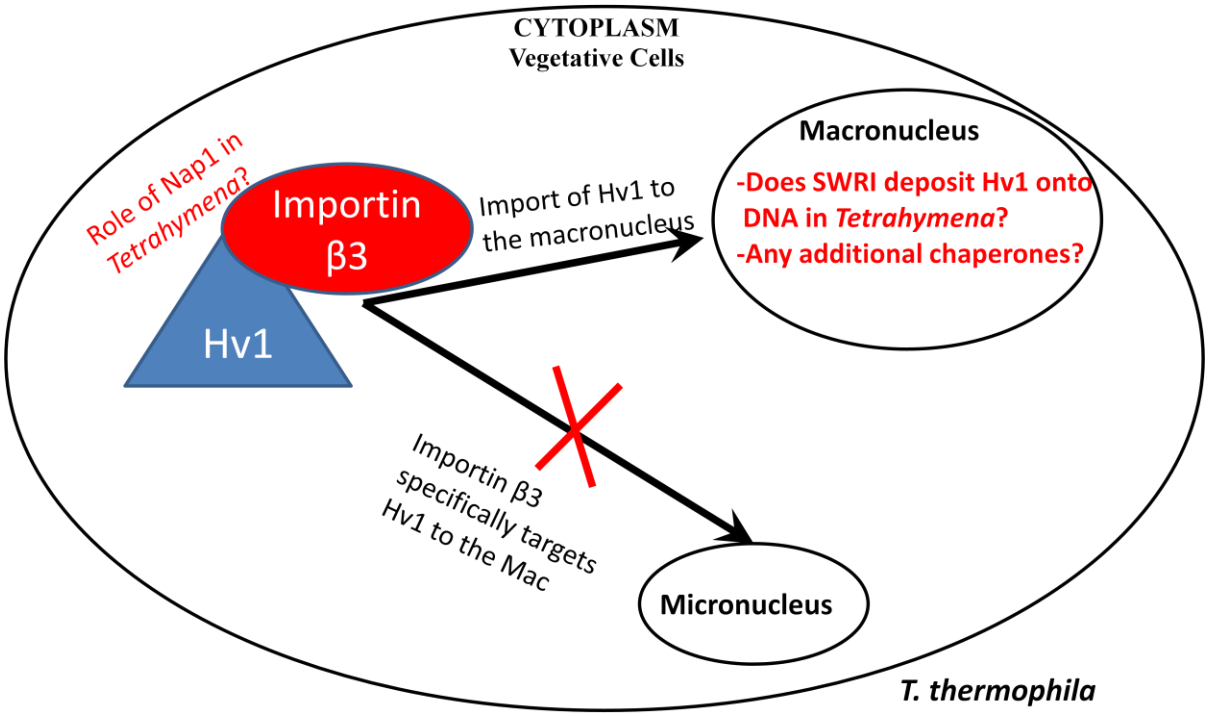

Figure 29: Proposed model for the transport of histone Hv1 in *T. thermophila*. Hv1 forms a physical interaction with Impβ3 which transports it to the MAC.

4- IF analysis of H3.3 confirms its previously reported (Cui et al. 2006) localization patterns where a strong signal was detected in the transcriptionally active MAC and only a faint localization signal was present in the MIC. Along with un-published observations from our laboratory, my data implicate HIRA as the major chaperone that might be responsible for the H3.3 deposition into the MIC. Furthermore, SAINT supported proteomic analysis reveals

that H3.3 co-purifies with highly conserved Nrp1 histone chaperone. These data provide support to a previous report (Garg et al. 2013) which has implicated Asf1^{Tt} and Nrp1 as major histone chaperones involved in the H3/H4 transport pathway. Future studies should focus on analysing the role of HIRA^{Tt} in H3.3 deposition. Furthermore, studying the PPI of core H3 and H4 will be useful to fully delineate the RD as well as RI pathways. To this end, I have engineered the gene targeting vector for H4 whereas H3 is in progress. *T. thermophila* cells carrying H4-FZZ have been subjected to the Western blotting in order to detect the successful expression of the fusion protein. As apparent from the figure 30, strong signals were detected in the H4-FZZ lanes whereas no signal was observed in the wild type lanes when blot was probed with anti-FLAG antibody. In future IF as well as AP-MS analyses should be carried out using H4-FZZ cell lines in order to gain functional insights.

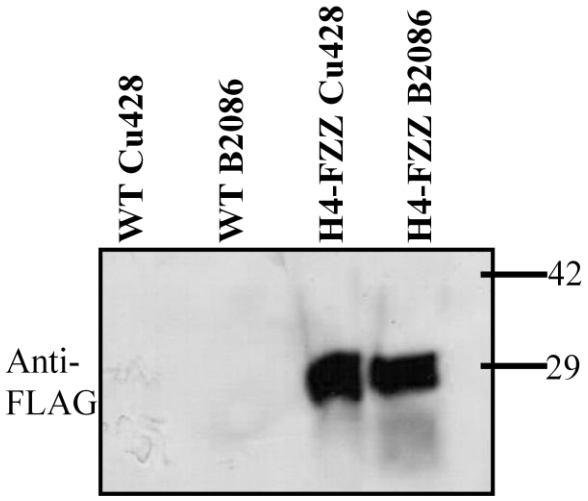

Figure 30: Western blot analysis of H4-FZZ. The blot was probed with anti-FLAG antibody Note the H4-FZZ signal was observed at 29kDa which is the expected size of the fusion protein (H4 size 11 kDa+FZZ size 18kDa)

References

Aalfs JD, Kingston RE. 2000. What does "chromatin remodeling" mean? Trends Biochem. Sci. 25:548–555.

Aguilar-Quesada R, Muñoz-Gámez JA, Martín-Oliva D, Peralta-Leal A, Quiles-Pérez R, Rodríguez-Vargas JM, Ruiz de Almodóvar M, Conde C, Ruiz-Extremera A, Oliver FJ. 2007. Modulation of transcription by PARP-1: consequences in carcinogenesis and inflammation. Curr. Med. Chem. 14:1179–1187.

Ahmad K, Henikoff S. 2002. The Histone Variant H3.3 Marks Active Chromatin by Replication-Independent Nucleosome Assembly. Mol. Cell 9:1191–1200.

Ai X, Parthun MR. 2004. The nuclear Hat1p/Hat2p complex: a molecular link between type B histone acetyltransferases and chromatin assembly. Mol. Cell 14:195–205.

Akematsu T, Endoh H. 2010. Role of apoptosis-inducing factor (AIF) in programmed nuclear death during conjugation in Tetrahymena thermophila. BMC Cell Biol. 11:13.

Alekseev OM, Bencic DC, Richardson RT, Widgren EE, O'Rand MG. 2003. Overexpression of the Linker histone-binding protein tNASP affects progression through the cell cycle. J. Biol. Chem. 278:8846–8852.

Allis CD, Allen RL, Wiggins JC, Chicoine LG, Richman R. 1984. Proteolytic processing of h1-like histones in chromatin: a physiologically and developmentally regulated event in Tetrahymena micronuclei. J. Cell Biol. 99:1669–1677.

Allis CD, Chicoine LG, Richman R, Schulman IG. 1985. Deposition-related histone acetylation in micronuclei of conjugating Tetrahymena. Proc. Natl. Acad. Sci. U. S. A. 82:8048–8052.

Allis CD, Richman R, Gorovsky MA, Ziegler YS, Touchstone B, Bradley WA, Cook RG. 1986. hv1 Is an evolutionarily conserved H2A variant that is preferentially associated with active genes. J. Biol. Chem. 261:1941–1948.

Alva V, Ammelburg M, Söding J, Lupas AN. 2007. On the origin of the histone fold. BMC Struct. Biol. 7:17.

Alvarez F, Muñoz F, Schilcher P, Imhof A, Almouzni G, Loyola A. 2011. Sequential establishment of marks on soluble histones H3 and H4. J. Biol. Chem. 286:17714–17721.

Amé JC, Rolli V, Schreiber V, Niedergang C, Apiou F, Decker P, Muller S, Höger T, Ménissier-de Murcia J, de Murcia G. 1999. PARP-2, A novel mammalian DNA damage-dependent poly(ADP-ribose) polymerase. J. Biol. Chem. 274:17860–17868.

Avvakumov N, Nourani A, Côté J. 2011. Histone chaperones: modulators of chromatin marks. Mol. Cell 41:502–514.

Balaji S, Iyer LM, Aravind L. 2009. HPC2 and ubinuclein define a novel family of histone chaperones conserved throughout eukaryotes. Mol. Biosyst. 5:269–275.

Bannister AJ, Kouzarides T. 2011. Regulation of chromatin by histone modifications. Cell Res. 21:381–395.

Belotserkovskaya R, Oh S, Bondarenko VA, Orphanides G, Studitsky VM, Reinberg D. 2003. FACT facilitates transcription-dependent nucleosome alteration. Science 301:1090–1093.

Bernstein BE, Kamal M, Lindblad-Toh K, Bekiranov S, Bailey DK, Huebert DJ, McMahon S, Karlsson EK, Kulbokas EJ, Gingeras TR, et al. 2005. Genomic maps and comparative analysis of histone modifications in human and mouse. Cell 120:169–181.

Bernstein BE, Mikkelsen TS, Xie X, Kamal M, Huebert DJ, Cuff J, Fry B, Meissner A, Wernig M, Plath K, et al. 2007. High-resolution profiling of histone methylations in the human genome. Cell 129:823–837.

Biswas D, Yu Y, Prall M, Formosa T, Stillman DJ. 2005. The yeast FACT complex has a role in transcriptional initiation. Mol. Cell. Biol. 25:5812–5822.

Biterge B, Schneider R. 2014. Histone variants: key players of chromatin. Cell Tissue Res. 356:457–466.

Bönisch C, Hake SB. 2012. Histone H2A variants in nucleosomes and chromatin: More or less stable? Nucleic Acids Res. 40:10719–10741.

Bönisch C, Schneider K, Pünzeler S, Wiedemann SM, Bielmeier C, Bocola M, Eberl HC, Kuegel W, Neumann J, Kremmer E, et al. 2012. H2A.Z.2.2 is an alternatively spliced histone H2A.Z variant that causes severe nucleosome destabilization. Nucleic Acids Res. 40:5951–5964.

Borer RA, Lehner CF, Eppenberger HM, Nigg EA. 1989. Major nucleolar proteins shuttle between nucleus and cytoplasm. Cell 56:379–390.

Boulikas T. 1989. DNA strand breaks alter histone ADP-ribosylation. Proc. Natl. Acad. Sci. U. S. A. 86:3499–3503.

Bright LJ, Kambesis N, Nelson SB, Jeong B, Turkewitz AP. 2010. Comprehensive analysis reveals dynamic and evolutionary plasticity of Rab GTPases and membrane traffic in Tetrahymena thermophila. PLoS Genet. 6:e1001155.

Bruhn SL, Pil PM, Essigmann JM, Housman DE, Lippard SJ. 1992. Isolation and characterization of human cDNA clones encoding a high mobility group box protein that recognizes structural distortions to DNA caused by binding of the anticancer agent cisplatin. Proc. Natl. Acad. Sci. U. S. A. 89:2307–2311.

Bruns PJ, Cassidy-Hanley D. 2000. Biolistic transformation of macro- and micronuclei. Methods Cell Biol. 62:501–512.

Burgess RJ, Zhang Z. 2013. Histone chaperones in nucleosome assembly and human disease. Nat. Struct. Mol. Biol. 20:14–22.

Burns KH, Viveiros MM, Ren Y, Wang P, DeMayo FJ, Frail DE, Eppig JJ, Matzuk MM. 2003. Roles of NPM2 in chromatin and nucleolar organization in oocytes and embryos. Science 300:633–636.

Burzio LO, Riquelme PT, Koide SS. 1979. ADP ribosylation of rat liver nucleosomal core histones. J. Biol. Chem. 254:3029–3037.

Bush KM, Yuen BT, Barrilleaux BL, Riggs JW, O'Geen H, Cotterman RF, Knoepfler PS. 2013. Endogenous mammalian histone H3.3 exhibits chromatin-related functions during development. Epigenetics Chromatin 6:7.

Campos EI, Fillingham J, Li G, Zheng H, Voigt P, Kuo W-HW, Seepany H, Gao Z, Day L a, Greenblatt JF, et al. 2010. The program for processing newly synthesized histones H3.1 and H4. Nat. Struct. Mol. Biol. 17:1343–1351.

Campos EI, Reinberg D. 2010. New chaps in the histone chaperone arena. Genes Dev. 24:1334–1338.

Cervantes MD, Xi X, Vermaak D, Yao M-C, Malik HS. 2006. The CNA1 histone of the ciliate Tetrahymena thermophila is essential for chromosome segregation in the germline micronucleus. Mol. Biol. Cell 17:485–497.

Chiang YJ, Hsiao SJ, Yver D, Cushman SW, Tessarollo L, Smith S, Hodes RJ. 2008. Tankyrase 1 and tankyrase 2 are essential but redundant for mouse embryonic development. PLoS One 3:e2639.

Choi ES, Shin JA, Kim HS, Jang YK. 2005. Dynamic regulation of replication independent deposition of histone H3 in fission yeast. Nucleic Acids Res. 33:7102–7110.

Choi H, Liu G, Mellacheruvu D, Tyers M, Gingras A-C, Nesvizhskii AI. 2012. Analyzing protein-protein interactions from affinity purification-mass spectrometry data with SAINT. Curr. Protoc. Bioinformatics Chapter 8:Unit8.15.

Citarelli M, Teotia S, Lamb RS. 2010. Evolutionary history of the poly(ADP-ribose) polymerase gene family in eukaryotes. BMC Evol. Biol. 10:308.

Cook AJL, Gurard-Levin ZA, Vassias I, Almouzni G. 2011. A Specific Function for the Histone Chaperone NASP to Fine-Tune a Reservoir of Soluble H3-H4 in the Histone Supply Chain. Mol. Cell 44:918–927.

Costanzi C, Pehrson JR. 1998. Histone macroH2A1 is concentrated in the inactive X chromosome of female mammals. Nature 393:599–601.

Cui B, Gorovsky MA. 2006. Centromeric histone H3 is essential for vegetative cell division and for DNA elimination during conjugation in Tetrahymena thermophila. Mol. Cell. Biol. 26:4499–4510.

Cui B, Liu Y, Gorovsky MA. 2006. Deposition and function of histone H3 variants in Tetrahymena thermophila. Mol. Cell. Biol. 26:7719–7730.

Czaja W, Mao P, Smerdon MJ. 2012. The Emerging Roles of ATP-Dependent Chromatin Remodeling Enzymes in Nucleotide Excision Repair. Int. J. Mol. Sci. 13:11954–11973.

D'Amours D, Desnoyers S, D'Silva I, Poirier GG. 1999. Poly(ADP-ribosyl)ation reactions in the regulation of nuclear functions. Biochem. J. 342 (Pt 2:249–268.

Van Daal A, Elgin SC. 1992. A histone variant, H2AvD, is essential in Drosophila melanogaster. Mol. Biol. Cell 3:593–602.

Das C, Lucia MS, Hansen KC, Tyler JK. 2009. CBP/p300-mediated acetylation of histone H3 on lysine 56. Nature 459:113–117.

Daugherty MD, Young JM, Kerns J a, Malik HS. 2014. Rapid evolution of PARP genes suggests a broad role for ADP-ribosylation in host-virus conflicts. PLoS Genet. 10:e1004403.

Delbarre E, Jacobsen BM, Reiner AH, Sørensen AL, Küntziger T, Collas P. 2010. Chromatin environment of histone variant H3.3 revealed by quantitative imaging and genome-scale chromatin and DNA immunoprecipitation. Mol. Biol. Cell 21:1872–1884.

Delom F, Chevet E. 2006. Phosphoprotein analysis: from proteins to proteomes. Proteome Sci. 4:15.

Dilworth SM, Black SJ, Laskey RA. 1987. Two complexes that contain histones are required for nucleosome assembly in vitro: role of nucleoplasmin and N1 in Xenopus egg extracts. Cell 51:1009–1018.

Dinant C, Houtsmuller AB, Vermeulen W. 2008. Chromatin structure and DNA damage repair. Epigenetics Chromatin 1:9.

Dingwall C, Dilworth SM, Black SJ, Kearsey SE, Cox LS, Laskey RA. 1987. Nucleoplasmin cDNA sequence reveals polyglutamic acid tracts and a cluster of sequences homologous to putative nuclear localization signals. EMBO J. 6:69–74.

Dingwall C, Laskey RA. 1990. Nucleoplasmin: the archetypal molecular chaperone. Semin. Cell Biol. 1:11–17.

Dion MF, Kaplan T, Kim M, Buratowski S, Friedman N, Rando OJ. 2007. Dynamics of replication-independent histone turnover in budding yeast. Science 315:1405–1408.

Van Doninck K, Mandigo ML, Hur JH, Wang P, Guglielmini J, C.Milinkovitch M, Lane WS, Meselson M. 2009. Phylogenomics of unusual histone H2A variants in bdelloid rotifers. PLoS Genet. 5.

Downs JA, Lowndes NF, Jackson SP. 2000. A role for Saccharomyces cerevisiae histone H2A in DNA repair. Nature 408:1001–1004.

Drané P, Ouararhni K, Depaux A, Shuaib M, Hamiche A. 2010. The death-associated protein DAXX is a novel histone chaperone involved in the replication-independent deposition of H3.3. Genes Dev. 24:1253–1265.

Driscoll R, Hudson A, Jackson SP. 2007. Yeast Rtt109 promotes genome stability by acetylating histone H3 on lysine 56. Science 315:649–652.

Drotschmann K, Yang W, Kunkel TA. 2002. Evidence for sequential action of two ATPase active sites in yeast Msh2-Msh6. DNA Repair (Amst). 1:743–753.

Dunleavy EM, Almouzni G, Karpen GH. 2011. H3.3 is deposited at centromeres in S phase as a placeholder for newly assembled CENP-A in G_1 phase. Nucleus 2:146–157.

Dunleavy EM, Pidoux AL, Monet M, Bonilla C, Richardson W, Hamilton GL, Ekwall K, McLaughlin PJ, Allshire RC. 2007. A NASP (N1/N2)-related protein, Sim3, binds CENP-A and is required for its deposition at fission yeast centromeres. Mol. Cell 28:1029–1044.

Dutta S, Akey I V., Dingwall C, Hartman KL, Laue T, Nolte RT, Head JF, Akey CW. 2001. The crystal structure of nucleoplasmin-core: Implications for histone binding and nucleosome assembly. Mol. Cell 8:841–853.

Eirín-López JM, Frehlick LJ, Ausió J. 2006. Long-term evolution and functional diversification in the members of the nucleophosmin/nucleoplasmin family of nuclear chaperones. Genetics 173:1835–1850.

Eirín-López JM, González-Tizón AM, Martínez A, Méndez J. 2004. Birth-and-death evolution with strong purifying selection in the histone H1 multigene family and the origin of orphon H1 genes. Mol. Biol. Evol. 21:1992–2003.

Eirín-López JM, Ishibashi T, Ausió J. 2008. H2A.Bbd: a quickly evolving hypervariable mammalian histone that destabilizes nucleosomes in an acetylation-independent way. FASEB J. 22:316–326.

Eisen JA, Coyne RS, Wu M, Wu D, Thiagarajan M, Wortman JR, Badger JH, Ren Q, Amedeo P, Jones KM, et al. 2006. Macronuclear genome sequence of the ciliate Tetrahymena thermophila, a model eukaryote. PLoS Biol. 4:e286.

Elsaesser SJ, Allis CD. 2010. HIRA and Daxx constitute two independent histone H3.3-containing predeposition complexes. Cold Spring Harb. Symp. Quant. Biol. 75:27–34.

Eustermann S, Videler H, Yang J-C, Cole PT, Gruszka D, Veprintsev D, Neuhaus D. 2011. The DNA-binding domain of human PARP-1 interacts with DNA single-strand breaks as a monomer through its second zinc finger. J. Mol. Biol. 407:149–170.

Evans DR, Brewster NK, Xu Q, Rowley A, Altheim BA, Johnston GC, Singer RA. 1998. The yeast protein complex containing cdc68 and pob3 mediates core-promoter repression through the cdc68 N-terminal domain. Genetics 150:1393–1405.

Faast R, Thonglairoam V, Schulz TC, Beall J, Wells JR, Taylor H, Matthaei K, Rathjen PD, Tremethick DJ, Lyons I. 2001. Histone variant H2A.Z is required for early mammalian development. Curr. Biol. 11:1183–1187.

Fan Q, Yao MC. 2000. A long stringent sequence signal for programmed chromosome breakage in Tetrahymena thermophila. Nucleic Acids Res. 28:895–900.

Fillingham J, Greenblatt JF. 2008. A histone code for chromatin assembly. Cell 134:206–208.

Finn RM, Browne K, Hodgson KC, Ausió J. 2008. sNASP, a histone H1-specific eukaryotic chaperone dimer that facilitates chromatin assembly. Biophys. J. 95:1314–1325.

Finn RM, Ellard K, Eirin Lopez JM, Ausio J. 2012. Vertebrate nucleoplasmin and NASP: egg histone storage proteins with multiple chaperone activities. FASEB J.

Fischle W, Wang Y, Allis CD. 2003. Histone and chromatin cross-talk. Curr. Opin. Cell Biol. 15:172–183.

Formosa T, Eriksson P, Wittmeyer J, Ginn J, Yu Y, Stillman DJ. 2001. Spt16-Pob3 and the HMG protein Nhp6 combine to form the nucleosome-binding factor SPN. EMBO J. 20:3506–3517.

Frehlick LJ, Eirín-López JM, Ausió J. 2007. New insights into the nucleophosmin/nucleoplasmin family of nuclear chaperones. Bioessays 29:49–59.

Gaertig J, Gorovsky MA. 1992. Efficient mass transformation of Tetrahymena thermophila by electroporation of conjugants. Proc. Natl. Acad. Sci. U. S. A. 89:9196–9200.

Gaertig J, Gu L, Hai B, Gorovsky MA. 1994. High frequency vector-mediated transformation and gene replacement in Tetrahymena. Nucleic Acids Res. 22:5391–5398.

Gambus A, Jones RC, Sanchez-Diaz A, Kanemaki M, van Deursen F, Edmondson RD, Labib K. 2006. GINS maintains association of Cdc45 with MCM in replisome progression complexes at eukaryotic DNA replication forks. Nat. Cell Biol. 8:358–366.

Garcia BA, Hake SB, Diaz RL, Kauer M, Morris SA, Recht J, Shabanowitz J, Mishra N, Strahl BD, Allis CD, et al. 2007. Organismal differences in post-translational modifications in histones H3 and H4. J. Biol. Chem. 282:7641–7655.

Garg J, Lambert JP, Karsou A, Marquez S, Nabeel-Shah S, Bertucci V, Retnasothie D V., Radovani E, Pawson T, Gingras AC, et al. 2013. Conserved Asf1-importin ?? physical interaction in growth and sexual development in the ciliate Tetrahymena thermophila. J. Proteomics 94:311–326.

Goldberg AD, Banaszynski LA, Noh K-M, Lewis PW, Elsaesser SJ, Stadler S, Dewell S, Law M, Guo X, Li X, et al. 2010. Distinct factors control histone variant H3.3 localization at specific genomic regions. Cell 140:678–691.

Greaves IK, Rangasamy D, Ridgway P, Tremethick DJ. 2007. H2A.Z contributes to the unique 3D structure of the centromere. Proc. Natl. Acad. Sci. U. S. A. 104:525–530.

Green EM, Antczak AJ, Bailey AO, Franco AA, Wu KJ, Yates JR, Kaufman PD. 2005. Replication-independent histone deposition by the HIR complex and Asf1. Curr. Biol. 15:2044–2049.

Greider CW, Blackburn EH. 1985. Identification of a specific telomere terminal transferase activity in Tetrahymena extracts. Cell 43:405–413.

Grisendi S, Bernardi R, Rossi M, Cheng K, Khandker L, Manova K, Pandolfi PP. 2005. Role of nucleophosmin in embryonic development and tumorigenesis. Nature 437:147–153.

Guillemette B, Bataille AR, Gévry N, Adam M, Blanchette M, Robert F, Gaudreau L. 2005. Variant histone H2A.z is globally localized to the promoters of inactive yeast genes and regulates nucleosome positioning. PLoS Biol. 3:1–11.

Gurard-Levin ZA, Quivy J-P, Almouzni G. 2014. Histone chaperones: assisting histone traffic and nucleosome dynamics. Annu. Rev. Biochem. 83:487–517.

Ha M, Kraushaar DC, Zhao K. 2014. Genome-wide analysis of H3.3 dissociation reveals high nucleosome turnover at distal regulatory regions of embryonic stem cells. Epigenetics Chromatin 7:38.

Hai B, Gaertig J, Gorovsky MA. 2000. Knockout heterokaryons enable facile mutagenic analysis of essential genes in Tetrahymena. Methods Cell Biol. 62:513–531.

Hake SB, Allis CD. 2006. Histone H3 variants and their potential role in indexing mammalian genomes: the “H3 barcode hypothesis”. Proc. Natl. Acad. Sci. U. S. A. 103:6428–6435.

Hake SB, Garcia BA, Duncan EM, Kauer M, Dellaire G, Shabanowitz J, Bazett-Jones DP, Allis CD, Hunt DF. 2006. Expression patterns and post-translational modifications associated with mammalian histone H3 variants. J. Biol. Chem. 281:559–568.

Hamiche A, Shuaib M. 2013. Chaperoning the histone H3 family. Biochim. Biophys. Acta 1819:230–237.

Han J, Li Q, McCullough L, Kettelkamp C, Formosa T, Zhang Z. 2010. Ubiquitylation of FACT by the cullin-E3 ligase Rtt101 connects FACT to DNA replication. Genes Dev. 24:1485–1490.

Han J, Zhou H, Horazdovsky B, Zhang K, Xu R-M, Zhang Z. 2007. Rtt109 acetylates histone H3 lysine 56 and functions in DNA replication. Science 315:653–655.

Harshman SW, Young NL, Parthun MR, Freitas MA. 2013. H1 histones: current perspectives and challenges. Nucleic Acids Res. 41:9593–9609.

Heo K, Kim H, Choi SH, Choi J, Kim K, Gu J, Lieber MR, Yang AS, An W. 2008. FACT-mediated exchange of histone variant H2AX regulated by phosphorylation of H2AX and ADP-ribosylation of Spt16. Mol. Cell 30:86–97.

Hoek M, Stillman B. 2003. Chromatin assembly factor 1 is essential and couples chromatin assembly to DNA replication in vivo. Proc. Natl. Acad. Sci. U. S. A. 100:12183–12188.

Hondele M, Ladurner AG. 2011. The chaperone-histone partnership: for the greater good of histone traffic and chromatin plasticity. Curr. Opin. Struct. Biol. 21:698–708.

Hondele M, Stuwe T, Hassler M, Halbach F, Bowman A, Zhang ET, Nijmeijer B, Kotthoff C, Rybin V, Amlacher S, et al. 2013. Structural basis of histone H2A-H2B recognition by the essential chaperone FACT. Nature 499:111–114.

Hottiger MO. 2011. ADP-ribosylation of histones by ARTD1: an additional module of the histone code? FEBS Lett. 585:1595–1599.

Huang S, Zhou H, Katzmann D, Hochstrasser M, Atanasova E, Zhang Z. 2005. Rtt106p is a histone chaperone involved in heterochromatin-mediated silencing. Proc. Natl. Acad. Sci. U. S. A. 102:13410–13415.

Iouzalen N, Moreau J, Méchali M. 1996. H2A.ZI, a new variant histone expressed during Xenopus early development exhibits several distinct features from the core histone H2A. Nucleic Acids Res. 24:3947–3952.

Ivanauskiene K, Delbarre E, McGhie JD, Küntziger T, Wong LH, Collas P. 2014. The PML-associated protein DEK regulates the balance of H3.3 loading on chromatin and is important for telomere integrity. Genome Res. 24:1584–1594.

Jackson JD, Gorovsky MA. 2000. Histone H2A.Z has a conserved function that is distinct from that of the major H2A sequence variants. Nucleic Acids Res. 28:3811–3816.

Jackson V, Shires A, Tanphaichitr N, Chalkley R. 1976. Modifications to histones immediately after synthesis. J. Mol. Biol. 104:471–483.

Jagtap P, Szabó C. 2005. Poly(ADP-ribose) polymerase and the therapeutic effects of its inhibitors. Nat. Rev. Drug Discov. 4:421–440.

Jamai A, Imoberdorf RM, Strubin M. 2007. Continuous histone H2B and transcription-dependent histone H3 exchange in yeast cells outside of replication. Mol. Cell 25:345–355.

Jiang C, Pugh BF. 2009. Nucleosome positioning and gene regulation: advances through genomics. Nat. Rev. Genet. 10:161–172.

Jimeno-González S, Gómez-Herreros F, Alepuz PM, Chávez S. 2006. A gene-specific requirement for FACT during transcription is related to the chromatin organization of the transcribed region. Mol. Cell. Biol. 26:8710–8721.

Jin C, Felsenfeld G. 2007. Nucleosome stability mediated by histone variants H3.3 and H2A.Z. Genes Dev. 21:1519–1529.

Jin C, Zang C, Wei G, Cui K, Peng W, Zhao K, Felsenfeld G. 2009. H3.3/H2A.Z double variant-containing nucleosomes mark "nucleosome-free regions" of active promoters and other regulatory regions. Nat. Genet. 41:941–945.

Kalocsay M, Hiller NJ, Jentsch S. 2009. Chromosome-wide Rad51 spreading and SUMO-H2A.Z-dependent chromosome fixation in response to a persistent DNA double-strand break. Mol. Cell 33:335–343.

Kamakaka RT, Biggins S. 2005. Histone variants: deviants? Genes Dev. 19:295–310.

Karaczyn AA, Cheng RYS, Buzard GS, Hartley J, Esposito D, Kasprzak KS. 2009. Truncation of histone H2A's C-terminal tail, as is typical for Ni(II)-assisted specific peptide bond hydrolysis, has gene expression altering effects. Ann. Clin. Lab. Sci. 39:251–262.

Keck KM, Pemberton LF. 2012. Histone chaperones link histone nuclear import and chromatin assembly. Biochim. Biophys. Acta 1819:277–289.

Keogh M-C, Mennella TA, Sawa C, Berthelet S, Krogan NJ, Wolek A, Podolny V, Carpenter LR, Greenblatt JF, Baetz K, et al. 2006. The Saccharomyces cerevisiae histone H2A variant Htz1 is acetylated by NuA4. Genes Dev. 20:660–665.

Kepper N, Foethke D, Stehr R, Wedemann G, Rippe K. 2008. Nucleosome geometry and internucleosomal interactions control the chromatin fiber conformation. Biophys. J. 95:3692–3705.

Kleine H, Poreba E, Lesniewicz K, Hassa PO, Hottiger MO, Litchfield DW, Shilton BH, Lüscher B. 2008. Substrate-assisted catalysis by PARP10 limits its activity to mono-ADP-ribosylation. Mol. Cell 32:57–69.

Kleinschmidt JA, Fortkamp E, Krohne G, Zentgraf H, Franke WW. 1985. Co-existence of two different types of soluble histone complexes in nuclei of Xenopus laevis oocytes. J. Biol. Chem. 260:1166–1176.

Knapp AR, Wang H, Parthun MR. 2014. The yeast histone chaperone Hif1p functions with RNA in nucleosome assembly. PLoS One 9.

Ko HL, Ren EC. 2012. Functional Aspects of PARP1 in DNA Repair and Transcription. Biomolecules 2:524–548.

Kobor MS, Venkatasubrahmanyam S, Meneghini MD, Gin JW, Jennings JL, Link AJ, Madhani HD, Rine J. 2004. A protein complex containing the conserved Swi2/Snf2-related ATPase Swr1p deposits histone variant H2A.Z into euchromatin. PLoS Biol. 2:E131.

De Koning L, Corpet A, Haber JE, Almouzni G. 2007. Histone chaperones: an escort network regulating histone traffic. Nat. Struct. Mol. Biol. 14:997–1007.

Kraus WL, Lis JT. 2003. PARP goes transcription. Cell 113:677–683.

Kraus WL. 2008. Transcriptional control by PARP-1: chromatin modulation, enhancer-binding, coregulation, and insulation. Curr. Opin. Cell Biol. 20:294–302.

Kraushaar DC, Jin W, Maunakea A, Abraham B, Ha M, Zhao K. 2013. Genome-wide incorporation dynamics reveal distinct categories of turnover for the histone variant H3.3. Genome Biol. 14:R121.

Kreimeyer A, Wielckens K, Adamietz P, Hilz H. 1984. DNA repair-associated ADP-ribosylation in vivo. Modification of histone H1 differs from that of the principal acceptor proteins. J. Biol. Chem. 259:890–896.

Krogan NJ, Keogh M-C, Datta N, Sawa C, Ryan OW, Ding H, Haw RA, Pootoolal J, Tong A, Canadien V, et al. 2003. A Snf2 family ATPase complex required for recruitment of the histone H2A variant Htz1. Mol. Cell 12:1565–1576.

Kruger K, Grabowski PJ, Zaug AJ, Sands J, Gottschling DE, Cech TR. 1982. Self-splicing RNA: autoexcision and autocyclization of the ribosomal RNA intervening sequence of Tetrahymena. Cell 31:147–157.

Langelier M-F, Planck JL, Roy S, Pascal JM. 2011. Crystal structures of poly(ADP-ribose) polymerase-1 (PARP-1) zinc fingers bound to DNA: structural and functional insights into DNA-dependent PARP-1 activity. J. Biol. Chem. 286:10690–10701.

Langelier M-F, Planck JL, Roy S, Pascal JM. 2012. Structural basis for DNA damage-dependent poly(ADP-ribosyl)ation by human PARP-1. Science 336:728–732.

Lejeune E, Bortfeld M, White SA, Pidoux AL, Ekwall K, Allshire RC, Ladurner AG. 2007. The chromatin-remodeling factor FACT contributes to centromeric heterochromatin independently of RNAi. Curr. Biol. 17:1219–1224.

Lewis PW, Elsaesser SJ, Noh K-M, Stadler SC, Allis CD. 2010. Daxx is an H3.3-specific histone chaperone and cooperates with ATRX in replication-independent chromatin assembly at telomeres. Proc. Natl. Acad. Sci. U. S. A. 107:14075–14080.

Li Q, Burgess R, Zhang Z. 2012. All roads lead to chromatin: Multiple pathways for histone deposition. Biochim. Biophys. Acta 1819:238–246.

Li Y, Keller DM, Scott JD, Lu H. 2005. CK2 phosphorylates SSRP1 and inhibits its DNA-binding activity. J. Biol. Chem. 280:11869–11875.

Liu X, Li B, GorovskyMA. 1996. Essential and nonessential histone H2A variants in Tetrahymena thermophila. Mol. Cell. Biol. 16:4305–4311.

Lodish H. 2008. Molecular Cell Biology. W. H. Freeman

Loeffler PA, Cuneo MJ, Mueller GA, DeRose EF, Gabel SA, London RE. 2011. Structural studies of the PARP-1 BRCT domain. BMC Struct. Biol. 11:37.

Lorain S, Demczuk S, Lamour V, Toth S, Aurias A, Roe BA, Lipinski M. 1996. Structural Organization of the WD repeat protein-encoding gene HIRA in the DiGeorge syndrome critical region of human chromosome 22. Genome Res. 6:43–50.

Loyola A, Bonaldi T, Roche D, Imhof A, Almouzni G. 2006. PTMs on H3 variants before chromatin assembly potentiate their final epigenetic state. Mol. Cell 24:309–316.

Luger K, Mäder AW, Richmond RK, Sargent DF, Richmond TJ. 1997. Crystal structure of the nucleosome core particle at 2.8 A resolution. Nature 389:251–260.

Luk E, Ranjan A, FitzGerald PC, Mizuguchi G, Huang Y, Wei D, Wu C. 2010. Stepwise histone replacement by SWR1 requires dual activation with histone H2A.Z and canonical nucleosome. Cell 143:725–736.

Luk E, Vu N-D, Patteson K, Mizuguchi G, Wu W-H, Ranjan A, Backus J, Sen S, Lewis M, Bai Y, et al. 2007. Chz1, a nuclear chaperone for histone H2AZ. Mol. Cell 25:357–368.

Lynn DH, Doerder FP. 2012. The life and times of Tetrahymena. Methods Cell Biol. 109:9–27.

Malone CD, Falkowska KA, Li AY, Galanti SE, Kanuru RC, LaMont EG, Mazzarella KC, Micev AJ, Osman MM, Piotrowski NK, et al. 2008. Nucleus-specific importin alpha proteins and nucleoporins regulate protein import and nuclear division in the binucleate Tetrahymena thermophila. Eukaryot. Cell 7:1487–1499.

Mariño-Ramírez L, Kann MG, Shoemaker BA, Landsman D. 2005. Histone structure and nucleosome stability. Expert Rev. Proteomics 2:719–729.

Marques M, Laflamme L, Gervais AL, Gaudreau L. 2010. Reconciling the positive and negative roles of histone H2A.Z in gene transcription. Epigenetics 5:267–272.

Martindale DW, Allis CD, Bruns PJ. 1982. Conjugation in Tetrahymena thermophila. A temporal analysis of cytological stages. Exp. Cell Res. 140:227–236.

Marzluff WF, Duronio RJ. 2002. Histone mRNA expression: multiple levels of cell cycle regulation and important developmental consequences. Curr. Opin. Cell Biol. 14:692–699.

Marzluff WF, Wagner EJ, Duronio RJ. 2008. Metabolism and regulation of canonical histone mRNAs: life without a poly(A) tail. Nat. Rev. Genet. 9:843–854.

Mason PB, Struhl K. 2003. The FACT complex travels with elongating RNA polymerase II and is important for the fidelity of transcriptional initiation in vivo. Mol. Cell. Biol. 23:8323–8333.

Masumoto H, Hawke D, Kobayashi R, Verreault A. 2005. A role for cell-cycle-regulated histone H3 lysine 56 acetylation in the DNA damage response. Nature 436:294–298.

McKittrick E, Gafken PR, Ahmad K, Henikoff S. 2004. Histone H3.3 is enriched in covalent modifications associated with active chromatin. Proc. Natl. Acad. Sci. U. S. A. 101:1525–1530.

McLay DW, Clarke HJ. 2003. Remodelling the paternal chromatin at fertilization in mammals. Reproduction 125:625–633.

Meneghini MD, Wu M, Madhani HD. 2003. Conserved histone variant H2A.Z protects euchromatin from the ectopic spread of silent heterochromatin. Cell 112:725–736.

Messner S, Altmeyer M, Zhao H, Pozivil A, Roschitzki B, Gehrig P, Rutishauser D, Huang D, Caflisch A, Hottiger MO. 2010. PARP1 ADP-ribosylates lysine residues of the core histone tails. Nucleic Acids Res. 38:6350–6362.

Messner S, Hottiger MO. 2011. Histone ADP-ribosylation in DNA repair, replication and transcription. Trends Cell Biol. 21:534–542.

Miao W, Xiong J, Bowen J, Wang W, Liu Y, Braguinets O, Grigull J, Pearlman RE, Orias E, Gorovsky MA. 2009. Microarray analyses of gene expression during the Tetrahymena thermophila life cycle. PLoS One 4:e4429.

Millar CB, Xu F, Zhang K, Grunstein M. 2006. Acetylation of H2AZ Lys 14 is associated with genome-wide gene activity in yeast. Genes Dev. 20:711–722.

Mito Y, Henikoff JG, Henikoff S. 2005. Genome-scale profiling of histone H3.3 replacement patterns. Nat. Genet. 37:1090–1097.

Mizuguchi G, Shen X, Landry J, Wu W-H, Sen S, Wu C. 2004. ATP-driven exchange of histone H2AZ variant catalyzed by SWR1 chromatin remodeling complex. Science 303:343–348.

Mochizuki K, Fine NA, Fujisawa T, Gorovsky MA. 2002. Analysis of a piwi-related gene implicates small RNAs in genome rearrangement in tetrahymena. Cell 110:689–699.

Morillo-Huesca M, Maya D, Muñoz-Centeno MC, Singh RK, Oreal V, Reddy GU, Liang D, Géli V, Gunjan A, Chávez S. 2010. FACT prevents the accumulation of free histones evicted from transcribed chromatin and a subsequent cell cycle delay in G1. PLoS Genet. 6:17.

Mosammaparast N, Ewart CS, Pemberton LF. 2002. A role for nucleosome assembly protein 1 in the nuclear transport of histones H2A and H2B. EMBO J. 21:6527–6538.

Mosammaparast N, Jackson KR, Guo Y, Brame CJ, Shabanowitz J, Hunt DF, Pemberton LF. 2001. Nuclear import of histone H2A and H2B is mediated by a network of karyopherins. J. Cell Biol. 153:251–262.

Muthurajan UM, Hepler MRD, Hieb AR, Clark NJ, Kramer M, Yao T, Luger K. 2014. Automodification switches PARP-1 function from chromatin architectural protein to histone chaperone. Proc. Natl. Acad. Sci. U. S. A. 111:12752–12757.

Nabeel-Shah S, Ashraf K, Pearlman RE, Fillingham J. 2014. Molecular evolution of NASP and conserved histone H3/H4 transport pathway. BMC Evol. Biol. 14:139.

Ng RK, Gurdon JB. 2008. Epigenetic memory of an active gene state depends on histone H3.3 incorporation into chromatin in the absence of transcription. Nat. Cell Biol. 10:102–109.

Nguyen VQ, Ranjan A, Stengel F, Wei D, Aebersold R, Wu C, Leschziner AE. 2013. Molecular architecture of the ATP-dependent chromatin-remodeling complex SWR1. Cell 154:1220–1231.

O'Reilly AJ, Dacks JB, Field MC. 2011. Evolution of the karyopherin-β family of nucleocytoplasmic transport factors; ancient origins and continued specialization. PLoS One 6:e19308.

Okuda M, Horn HF, Tarapore P, Tokuyama Y, Smulian AG, Chan PK, Knudsen ES, Hofmann IA, Snyder JD, Bove KE, et al. 2000. Nucleophosmin/B23 is a target of CDK2/cyclin E in centrosome duplication. Cell 103:127–140.

Okuhara K, Ohta K, Seo H, Shioda M, Yamada T, Tanaka Y, Dohmae N, Seyama Y, Shibata T, Murofushi H. 1999. A DNA unwinding factor involved in DNA replication in cell-free extracts of Xenopus eggs. Curr. Biol. 9:341–350.

Okuwaki M, Matsumoto K, Tsujimoto M, Nagata K. 2001. Function of nucleophosmin/B23, a nucleolar acidic protein, as a histone chaperone. FEBS Lett. 506:272–276.

Old RW, Woodland HR. 1984. Histone genes: Not so simple after all. Cell 38:624–626.

Orias E, Cervantes MD, Hamilton EP. 2011. Tetrahymena thermophila, a unicellular eukaryote with separate germline and somatic genomes. Res. Microbiol. 162:578–586.

Orphanides G, LeRoy G, Chang CH, Luse DS, Reinberg D. 1998. FACT, a factor that facilitates transcript elongation through nucleosomes. Cell 92:105–116.

Orphanides G, Wu WH, Lane WS, Hampsey M, Reinberg D. 1999. The chromatin-specific transcription elongation factor FACT comprises human SPT16 and SSRP1 proteins. Nature 400:284–288.

Orsi GA, Algazeery A, Meyer RE, Capri M, Sapey-Triomphe LM, Horard B, Gruffat H, Couble P, Aït-Ahmed O, Loppin B. 2013. Drosophila Yemanuclein and HIRA cooperate for de novo assembly of H3.3-containing nucleosomes in the male pronucleus. PLoS Genet. 9:e1003285.

Osley MA. 1991. The regulation of histone synthesis in the cell cycle. Annu. Rev. Biochem. 60:827–861.

Pang Q, Christianson TA, Koretsky T, Carlson H, David L, Keeble W, Faulkner GR, Speckhart A, Bagby GC. 2003. Nucleophosmin interacts with and inhibits the catalytic function of eukaryotic initiation factor 2 kinase PKR. J. Biol. Chem. 278:41709–41717.

Park Y-J, Dyer PN, Tremethick DJ, Luger K. 2004. A new fluorescence resonance energy transfer approach demonstrates that the histone variant H2AZ stabilizes the histone octamer within the nucleosome. J. Biol. Chem. 279:24274–24282.

Parthun MR. 2007. Hat1: the emerging cellular roles of a type B histone acetyltransferase. Oncogene 26:5319–5328.

Parthun MR. 2012. Histone acetyltransferase 1: More than just an enzyme? Biochim. Biophys. Acta 1819:256–263.

Piontkivska H, Rooney AP, Nei M. 2002. Purifying selection and birth-and-death evolution in the histone H4 gene family. Mol. Biol. Evol. 19:689–697.

Prieto C, Saperas N, Arnan C, Hills MH, Wang X, Chiva M, Aligué R, Subirana JA, Ausió J. 2002. Nucleoplasmin interaction with protamines. Involvement of the polyglutamic tract. Biochemistry 41:7802–7810.

Puig O, Caspary F, Rigaut G, Rutz B, Bouveret E, Bragado-Nilsson E, Wilm M, Séraphin B. 2001. The tandem affinity purification (TAP) method: a general procedure of protein complex purification. Methods 24:218–229.

Raisner RM, Hartley PD, Meneghini MD, Bao MZ, Liu CL, Schreiber SL, Rando OJ, Madhani HD. 2005. Histone variant H2A.Z Marks the 5??? ends of both active and inactive genes in euchromatin. Cell 123:233–248.

Rangasamy D, Berven L, Ridgway P, Tremethick DJ. 2003. Pericentric heterochromatin becomes enriched with H2A.Z during early mammalian development. EMBO J. 22:1599–1607.

Ray-Gallet D, Woolfe A, Vassias I, Pellentz C, Lacoste N, Puri A, Schultz DC, Pchelintsev NA, Adams PD, Jansen LET, et al. 2011. Dynamics of histone H3 deposition in vivo reveal a nucleosome gap-filling mechanism for H3.3 to maintain chromatin integrity. Mol. Cell 44:928–941.

Recht J, Tsubota T, Tanny JC, Diaz RL, Berger JM, Zhang X, Garcia BA, Shabanowitz J, Burlingame AL, Hunt DF, et al. 2006. Histone chaperone Asf1 is required for histone H3 lysine 56 acetylation, a modification associated with S phase in mitosis and meiosis. Proc. Natl. Acad. Sci. U. S. A. 103:6988–6993.

Redon C, Pilch D, Rogakou E, Sedelnikova O, Newrock K, Bonner W. 2002. Histone H2A variants H2AX and H2AZ. Curr. Opin. Genet. Dev. 12:162–169.

Reinberg D, Sims RJ. 2006. De FACTo nucleosome dynamics. J. Biol. Chem. 281:23297–23301.

Ren Q, Gorovsky MA. 2001. Histone H2A.Z acetylation modulates an essential charge patch. Mol. Cell 7:1329–1335.

Ren Q, Gorovsky MA. 2003. The nonessential H2A N-terminal tail can function as an essential charge patch on the H2A.Z variant N-terminal tail. Mol. Cell. Biol. 23:2778–2789.

Richardson RT, Alekseev OM, Grossman G, Widgren EE, Thresher R, Wagner EJ, Sullivan KD, Marzluff WF, O'Rand MG. 2006. Nuclear autoantigenic sperm protein (NASP), a linker histone chaperone that is required for cell proliferation. J. Biol. Chem. 281:21526–21534.

Richardson RT, Batova IN, Widgren EE, Zheng LX, Whitfield M, Marzluff WF, O'Rand MG. 2000. Characterization of the histone H1-binding protein, NASP, as a cell cycle-regulated somatic protein. J. Biol. Chem. 275:30378–30386.

Rivera C, Gurard-Levin ZA, Almouzni G, Loyola A. 2014. Histone lysine methylation and chromatin replication. Biochim. Biophys. Acta.

Rogakou EP, Pilch DR, Orr AH, Ivanova VS, Bonner WM. 1998. DNA Double-stranded Breaks Induce Histone H2AX Phosphorylation on Serine 139. J. Biol. Chem. 273:5858–5868.

Ronan JL, Wu W, Crabtree GR. 2013. From neural development to cognition: unexpected roles for chromatin. Nat. Rev. Genet. 14:347–359.

Roth SY, Allis CD. 1996. Histone acetylation and chromatin assembly: a single escort, multiple dances? Cell 87:5–8.

Rowley A, Singer RA, Johnston GC. 1991. CDC68, a yeast gene that affects regulation of cell proliferation and transription, encodes a protein with a highly acidic carboxyl terminus. Mol. Cell. Biol. 11:5718–5726.

Rulten SL, Fisher AEO, Robert I, Zuma MC, Rouleau M, Ju L, Poirier G, Reina-San-Martin B, Caldecott KW. 2011. PARP-3 and APLF function together to accelerate nonhomologous end-joining. Mol. Cell 41:33–45.

Sakai A, Schwartz BE, Goldstein S, Ahmad K. 2009. Transcriptional and developmental functions of the H3.3 histone variant in Drosophila. Curr. Biol. 19:1816–1820.

Sarcinella E, Zuzarte PC, Lau PNI, Draker R, Cheung P. 2007. Monoubiquitylation of H2A.Z distinguishes its association with euchromatin or facultative heterochromatin. Mol. Cell. Biol. 27:6457–6468.

Saunders A, Werner J, Andrulis ED, Nakayama T, Hirose S, Reinberg D, Lis JT. 2003. Tracking FACT and the RNA polymerase II elongation complex through chromatin in vivo. Science 301:1094–1096.

Sawatsubashi S, Murata T, Lim J, Fujiki R, Ito S, Suzuki E, Tanabe M, Zhao Y, Kimura S, Fujiyama S, et al. 2010. A histone chaperone, DEK, transcriptionally coactivates a nuclear receptor. Genes Dev. 24:159–170.

Schlesinger MB, Formosa T. 2000. POB3 is required for both transcription and replication in the yeast Saccharomyces cerevisiae. Genetics 155:1593–1606.

Schreiber V, Dantzer F, Ame J-C, de Murcia G. 2006. Poly(ADP-ribose): novel functions for an old molecule. Nat. Rev. Mol. Cell Biol. 7:517–528.

Shackleford GM, Ganguly A, Macarthur CA. 2001. chaperones. BMC Genomics 21.

Shall S, de Murcia G. 2000. Poly(ADP-ribose) polymerase-1: what have we learned from the deficient mouse model? Mutat. Res. 460:1–15.

Shannon P, Markiel A, Ozier O, Baliga NS, Wang JT, Ramage D, Amin N, Schwikowski B, Ideker T. 2003. Cytoscape: a software environment for integrated models of biomolecular interaction networks. Genome Res. 13:2498–2504.

Shen X, Yu L, Weir JW, Gorovsky MA. 1995. Linker histones are not essential and affect chromatin condensation in vivo. Cell 82:47–56.

Sherwood PW, Tsang S V, Osley MA. 1993. Characterization of HIR1 and HIR2, two genes required for regulation of histone gene transcription in Saccharomyces cerevisiae. Mol. Cell. Biol. 13:28–38.

Simpson RT. 1978. Structure of the chromatosome, a chromatin particle containing 160 base pairs of DNA and all the histones. Biochemistry 17:5524–5531.

Smith S, Stillman B. 1991. Immunological characterization of chromatin assembly factor I, a human cell factor required for chromatin assembly during DNA replication in vitro. J. Biol. Chem. 266:12041–12047.

Sobel RE, Cook RG, Perry CA, Annunziato AT, Allis CD. 1995. Conservation of deposition-related acetylation sites in newly synthesized histones H3 and H4. Proc. Natl. Acad. Sci. U. S. A. 92:1237–1241.

Solsbacher J, Maurer P, Bischoff FR, Schlenstedt G. 1998. Cse1p is involved in export of yeast importin alpha from the nucleus. Mol. Cell. Biol. 18:6805–6815.

Song X, Gjoneska E, Ren Q, Taverna SD, Allis CD, Gorovsky MA. 2007. Phosphorylation of the SQ H2A.X motif is required for proper meiosis and mitosis in Tetrahymena thermophila. Mol. Cell. Biol. 27:2648–2660.

Stargell LA, Bowen J, Dadd CA, Dedon PC, Davis M, Cook RG, Allis CD, Gorovsky MA. 1993. Temporal and spatial association of histone H2A variant hv1 with transcriptionally competent chromatin during nuclear development in Tetrahymena thermophila. Genes Dev. 7:2641–2651.

Stellfox ME, Bailey AO, Foltz DR. 2013. Putting CENP-A in its place. Cell. Mol. Life Sci. 70:387–406.

Stillman DJ. 2010. Nhp6: a small but powerful effector of chromatin structure in Saccharomyces cerevisiae. Biochim. Biophys. Acta 1799:175–180.

Stone PR, Lorimer WS, Kidwell WR. 1977. Properties of the complex between histone H1 and poly(ADP-ribose synthesised in HeLa cell nuclei. Eur. J. Biochem. 81:9–18.

Straube K, Blackwell JS, Pemberton LF. 2010. Nap1 and Chz1 have separate Htz1 nuclear import and assembly functions. Traffic 11:185–197.

Stuwe T, Hothorn M, Lejeune E, Rybin V, Bortfeld M, Scheffzek K, Ladurner AG. 2008. The FACT Spt16 “peptidase” domain is a histone H3-H4 binding module. Proc. Natl. Acad. Sci. U. S. A. 105:8884–8889.

Suto RK, Clarkson MJ, Tremethick DJ, Luger K. 2000. Crystal structure of a nucleosome core particle containing the variant histone H2A.Z. Nat. Struct. Biol. 7:1121–1124.

Swaminathan V, Kishore AH, Febitha KK, Kundu TK. 2005. Human histone chaperone nucleophosmin enhances acetylation-dependent chromatin transcription. Mol. Cell. Biol. 25:7534–7545.

Sweet MT, Allis CD. 1993. Phosphorylation of linker histones by cAMP-dependent protein kinase in mitotic micronuclei of Tetrahymena. Chromosoma 102:637–647.

Sweet MT, Carlson G, Cook RG, Nelson D, Allis CD. 1997. Phosphorylation of linker histones by a protein kinase A-like activity in mitotic nuclei. J. Biol. Chem. 272:916–923.

Sweet MT, Jones K, Allis CD. 1996. Phosphorylation of linker histone is associated with transcriptional activation in a normally silent nucleus. J. Cell Biol. 135:1219–1228.

Szenker E, Ray-Gallet D, Almouzni G. 2011. The double face of the histone variant H3.3. Cell Res. 21:421–434.

Tagami H, Ray-Gallet D, Almouzni G, Nakatani Y. 2004. Histone H3.1 and H3.3 complexes mediate nucleosome assembly pathways dependent or independent of DNA synthesis. Cell 116:51–61.

Takemura M, Sato K, Nishio M, Akiyama T, Umekawa H, Yoshida S. 1999. Nucleolar protein B23.1 binds to retinoblastoma protein and synergistically stimulates DNA polymerase alpha activity. J. Biochem. 125:904–909.

Talbert PB, Ahmad K, Almouzni G, Ausió J, Berger F, Bhalla PL, Bonner WM, Cande WZ, Chadwick BP, Chan SWL, et al. 2012. A unified phylogeny-based nomenclature for histone variants. Epigenetics Chromatin 5:7.

Tan BC-M, Chien C-T, Hirose S, Lee S-C. 2006. Functional cooperation between FACT and MCM helicase facilitates initiation of chromatin DNA replication. EMBO J. 25:3975–3985.

Tang Y, Poustovoitov M V, Zhao K, Garfinkel M, Canutescu A, Dunbrack R, Adams PD, Marmorstein R. 2006. Structure of a human ASF1a-HIRA complex and insights into specificity of histone chaperone complex assembly. Nat. Struct. Mol. Biol. 13:921–929.

Teo G, Liu G, Zhang J, Nesvizhskii AI, Gingras A-C, Choi H. 2014. SAINTexpress: improvements and additional features in Significance Analysis of INTeractome software. J. Proteomics 100:37–43.

Thakar A, Gupta P, Ishibashi T, Finn R, Silva-Moreno B, Uchiyama S, Fukui K, Tomschik M, Ausio J, Zlatanova J. 2009. H2A.Z and H3.3 histone variants affect nucleosome structure: biochemical and biophysical studies. Biochemistry 48:10852–10857.

Thambirajah AA, Dryhurst D, Ishibashi T, Li A, Maffey AH, Ausió J. 2006. H2A.Z stabilizes chromatin in a way that is dependent on core histone acetylation. J. Biol. Chem. 281:20036–20044.

Thambirajah AA, Li A, Ishibashi T, Ausió J. 2009. New developments in post-translational modifications and functions of histone H2A variants. Biochem. Cell Biol. 87:7–17.

Thatcher TH, Gorovsky MA. 1994. Phylogenetic analysis of the core histones H2A, H2B, H3, and H4. Nucleic Acids Res. 22:174–179.

Timmermann S, Lehrmann H, Polesskaya A, Harel-Bellan A. 2001. Histone acetylation and disease. Cell. Mol. Life Sci. 58:728–736.

Tjeertes J V, Miller KM, Jackson SP. 2009. Screen for DNA-damage-responsive histone modifications identifies H3K9Ac and H3K56Ac in human cells. EMBO J. 28:1878–1889.

Tolstorukov MY, Goldman JA, Gilbert C, Ogryzko V, Kingston RE, Park PJ. 2012. Histone variant H2A.Bbd is associated with active transcription and mRNA processing in human cells. Mol. Cell 47:596–607.

Turkewitz AP, Orias E, Kapler G. 2002. Functional genomics: the coming of age for Tetrahymena thermophila. Trends Genet. 18:35–40.

VanDemark AP, Blanksma M, Ferris E, Heroux A, Hill CP, Formosa T. 2006. The structure of the yFACT Pob3-M domain, its interaction with the DNA replication factor RPA, and a potential role in nucleosome deposition. Mol. Cell 22:363–374.

Vignali M, Hassan AH, Neely KE, Workman JL. 2000. ATP-dependent chromatin-remodeling complexes. Mol. Cell. Biol. 20:1899–1910.

Vissers JH, Nicassio F, van Lohuizen M, Di Fiore PP, Citterio E. 2008. The many faces of ubiquitinated histone H2A: insights from the DUBs. Cell Div. 3:8.

De Vos M, Schreiber V, Dantzer F. 2012. The diverse roles and clinical relevance of PARPs in DNA damage repair: current state of the art. Biochem. Pharmacol. 84:137–146.

Voth WP, Takahata S, Nishikawa JL, Metcalfe BM, Näär AM, Stillman DJ. 2014. A role for FACT in repopulation of nucleosomes at inducible genes. PLoS One 9:e84092.

Vyas S, Chesarone-Cataldo M, Todorova T, Huang Y-H, Chang P. 2013. A systematic analysis of the PARP protein family identifies new functions critical for cell physiology. Nat. Commun. 4:2240.

Wang D, Baumann A, Szebeni A, Olson MOJ. 1994. The nucleic acid binding activity of nucleolar protein B23.1 resides in its carboxyl-terminal end. J. Biol. Chem. 269:30994–30998.

Wang H, Ge Z, Walsh STR, Parthun MR. 2012. The human histone chaperone sNASP interacts with linker and core histones through distinct mechanisms. Nucleic Acids Res. 40:660–669.

Wang H, Walsh STR, Parthun MR. 2008. Expanded binding specificity of the human histone chaperone NASP. Nucleic Acids Res. 36:5763–5772.

Weber CM, Henikoff S. 2014. Histone variants: dynamic punctuation in transcription. Genes Dev. 28:672–682.

Wegener AD, Jones LR. 1984. Phosphorylation-induced mobility shift in phospholamban in sodium dodecyl sulfate-polyacrylamide gels. Evidence for a protein structure consisting of multiple identical phosphorylatable subunits. J. Biol. Chem. 259:1834–1841.

Welch JE, Zimmerman LJ, Joseph DR, O'Rand MG. 1990. Characterization of a sperm-specific nuclear autoantigenic protein. I. Complete sequence and homology with the Xenopus protein, N1/N2. Biol. Reprod. 43:559–568.

Wielckens K, Bredehorst R, Adamietz P, Hilz H. 1981. Protein-bound polymeric and monomeric ADP-ribose residues in hepatic tissues. Comparative analyses using a new procedure for the quantification of poly(ADP-ribose). Eur. J. Biochem. 117:69–74.

Winkler DD, Luger K. 2011. The histone chaperone FACT: structural insights and mechanisms for nucleosome reorganization. J. Biol. Chem. 286:18369–18374.

Wittmeyer J, Formosa T. 1997. The Saccharomyces cerevisiae DNA polymerase alpha catalytic subunit interacts with Cdc68/Spt16 and with Pob3, a protein similar to an HMG1-like protein. Mol. Cell. Biol. 17:4178–4190.

Wong LH, Ren H, Williams E, McGhie J, Ahn S, Sim M, Tam A, Earle E, Anderson MA, Mann J, et al. 2009. Histone H3.3 incorporation provides a unique and functionally essential telomeric chromatin in embryonic stem cells. Genome Res. 19:404–414.

Wratting D, Thistlethwaite A, Harris M, Zeef LAH, Millar CB. 2012. A conserved function for the H2A.Z C terminus. J. Biol. Chem. 287:19148–19157.

Wu M, Allis CD, Sweet MT, Cook RG, Thatcher TH, Gorovsky MA. 1994. Four distinct and unusual linker proteins in a mitotically dividing nucleus are derived from a 71-kilodalton polyprotein, lack p34cdc2 sites, and contain protein kinase A sites. Mol. Cell. Biol. 14:10–20.

Wu RS, Tsai S, Bonner WM. 1982. Patterns of histone variant synthesis can distinguish G0 from G1 cells. Cell 31:367–374.

Xiong J, Lu X, Zhou Z, Chang Y, Yuan D, Tian M, Zhou Z, Wang L, Fu C, Orias E, et al. 2012. Transcriptome analysis of the model protozoan, Tetrahymena thermophila, using Deep RNA sequencing. PLoS One 7:e30630.

Xu Y, Ayrapetov MK, Xu C, Gursoy-Yuzugullu O, Hu Y, Price BD. 2012. Histone H2A.Z Controls a Critical Chromatin Remodeling Step Required for DNA Double-Strand Break Repair. Mol. Cell 48:723–733.

Yao MC, Yao CH, Monks B. 1990. The controlling sequence for site-specific chromosome breakage in Tetrahymena. Cell 63:763–772.

Yao M-CC, Choi J, Yokoyama S, Austerberry CF, Yao C-HH. 1984. DNA elimination in Tetrahymena: a developmental process involving extensive breakage and rejoining of DNA at defined sites. Cell 36:433–440.

Yu M, Schreek S, Cerni C, Schamberger C, Lesniewicz K, Poreba E, Vervoorts J, Walsemann G, Grötzinger J, Kremmer E, et al. 2005. PARP-10, a novel Myc-interacting protein with poly(ADP-ribose) polymerase activity, inhibits transformation. Oncogene 24:1982–1993.

Zhang H, Roberts DN, Cairns BR. 2005. Genome-wide dynamics of Htz1, a histone H2A variant that poises repressed/basal promoters for activation through histone loss. Cell 123:219–231.

Zhang K, Schrag M, Crofton A, Trivedi R, Vinters H, Kirsch W. 2012. Targeted proteomics for quantification of histone acetylation in Alzheimer's disease. Proteomics 12:1261–1268.

Zilberman D, Coleman-Derr D, Ballinger T, Henikoff S. 2008. Histone H2A.Z and DNA methylation are mutually antagonistic chromatin marks. Nature 456:125–129.

Zlatanova J, Thakar A. 2008. H2A.Z: view from the top. Structure 16:166–179.

Appendices

Appendix 1- Buffer recipes

Item	Composition
1% Agarose Gel (w/v) (50ml)	0.5g agarose 50ml 1xTBE 5µl ethidium bromide (EtBr) (10mg/ml)
0.5M Ammonium Hydroxide (NH_4OH)	1ml 14.5M NH_4OH 28ml ddH_2O
10% APS (Ammonium persulfate) (w/v)	0.1g ammonium persulfate 1ml ddH_2O
AP Lysis Buffer	10ml AP wash buffer 1 tube complete protease inhibitor (Roche) 50µl phenylmethylsulfonyl fluoride (PMSF)
AP Wash Buffer	0.5ml 1M Tris pH 8.0 1.5ml 5M NaCl 0.5ml 10% NP40 47.5ml ddH_2O
1M $CaCl_2$ (1L)	Any of the following hydrated forms is available: CaCl2 = 110.99g/mol CaCl2. 2H2O (Dihydrate) = 147.02g/mol CaCl2.4H2O (Tetrahydrate) = 183.04g/mol CaCl2.6H2O (Hexahydrate) = 219.08g/mol To 1 mole of CaCl2 add ddH20 to 1L
2mM $CaCl_2$/20mM Tris	100µl 1M $CaCl_2$ 1ml 1M Tris pH 8.0 48.9ml ddH_2O
0.5M EDTA, Iron (III) Sodium Salt pH 8.0 (500ml)	91.78g Na_2EDTA (367.1g/mol) ddH_2O to 500ml, pH to 8.0 with NaOH (1N)
2x Lysis Buffer (50ml)	2ml 1M Tris pH 8.0 50µl 1M $MgCl_2$ 42ml ddH_2O; 6ml 5M NaCl
1M $MgCl_2$ (M.W.=203.3g/mol) (100ml)	20.33g $MgCl_2$; ddH_2O to 100ml
1% Milk Solution (50ml)	10ml 5% milk solution 40ml 1x PBS
5% Milk Solution (BLOTTO) (w/v) (100ml)	5g skim milk powder 100ml PBS
100mM NaCl Wash Buffer (IPP100)	500µl 1M Tris pH 8.0 1ml 5M NaCl

	500µl 10% NP-40 48ml ddH_2O
300mM NaCl Wash Buffer (IPP300)	500µl 1M Tris pH 8.0 3ml 5M NaCl 500µl 10% NP-40 46ml ddH_2O
5M NaCl (500ml)	146.1g NaCl ddH20 to 500ml
10% NP-40 (v/v)	2.5ml NP-40 22.5ml ddH_2O
10x PBS pH 7.3 (1L)	82g NaCl 2.64g NaH_2PO_4 16g Na_2HPO_4 ddH20 to 1L, pH 7.3
1x PBST (500ml)	500ml 1x PBS 250µl Tween 20
100mM PMSF (10ml)	0.1742g PMSF 10ml isopropanol
Ponceau (0.1% w/v) (1L)	1g Ponceau S 50ml acetic acid ddH20 to 1L
2x SDS Laemmli Sample Buffer	3g SDS 5ml beta-mercaptoethanol 10ml 100% glycerol 6ml 2M Tris-HCL pH 6.8 50mg bromophenol blue ddH20 to 100ml
SPP (1L)	60mg sequestrin (Sigma) 2g bacto yeast extract 20g proteose peptone 4g glucose ddH20 to 1L
5% Stacking Gel (5ml)	3.5ml ddH_2O 0.625ml 1M Tris pH 6.8 0.95ml acrylamide 29:1 0.05ml 10% SDS 3.75µl TEMED 31.25µl 10% APS
Tetrahymena Lysis Solution (500ml)	210g urea 35ml 5M NaCl 5ml 1M Tris pH 7.4 10ml 0.5M EDTA 50ml 10% SDS ddH_2O to 500ml
1x TEV Cleavage Buffer	500µl 1M Tris pH 8.0 1ml 5M NaCl 500µl 10% NP-40 50µl 0.5M EDTA

	48ml ddH_2O
10mM Tris pH 7.4 (1L)	1.21g Tris ddH_2O to 1L, pH to 7.4
YT Media (1L)	10g bacto-tryptone 5g yeast extract 5g NaCl 15g agar for plates 1L ddH_20

Appendix 2- ClustalX color legends

Residue at position	Applied Colour	{ Threshhold, Residue group }
A,I,L,M,F,W,V	BLUE	{+60%, WLVIMAFCHP}
R,K	RED	{+60%,KR},{+80%, K,R,Q}
N	GREEN	{+50%, N}, {+85%, N,Y}
C	BLUE	{+60%, WLVIMAFCHP}
C	PINK	{100%, C}
Q	GREEN	{+60%,KR},{+50%,QE},{+85%,Q,E,K,R}
E	MAGENTA	{+60%,KR},{+50%,QE},{+85%,E,Q,D}
D	MAGENTA	{+60%,KR}, {+85%, K,R,Q}, {+50%,ED}
G	ORANGE	{+0%, G}
H,Y	CYAN	{+60%, WLVIMAFCHP}, {+85%, W,Y,A,C,P,Q,F,H,I,L,M,V}
P	YELLOW	{+0%, P}
S,T	GREEN	{+60%, WLVIMAFCHP}, {+50%, TS}, {+85%,S,T}

Appendix 3- Primers

3.1- Sequencing primer Sequence

M13R 5'-CAGGAAACAGCTATGAC-3'

HN111 5'-TATCATCATCATCTTTGTAATCAATATC-3'

M13F 5'-TGTAAAACGACGGCCAGT-3'

3.2 – PCR primers to amplify gene sequences for molecular cloning (restriction sites underlines)

SPT16
DOWNSTREAM SPT16 FORWARD
5’ CCCCGCGGCCGCAAAATAATATATAATTATTAAACTCTAG 3’
DOWNSTREAM SPT16 REVERSE
5’CCCGAGCTCTTCAATTAAATATTCTCCTCAGTAAAATAG 3'
UPSTREAM FORWARD:
5’ CCCGGTACCGAAGAAGAGGTCATGACTACGATGAAATAG 3'

PARP1
FORWARD UP:
CCCGGTACCAGTTTA TTA GAA ATG TTT TCGCTGTTGAGA
REVERSE UP:
CCCCTCGAGATCTCTTATTTCAATTAAATATCTTATTCT
DOWNSTREAM PRIMERS:
FORWARD DOWN:
CCCCGCGGCCGCAATAAT TTA ATA AAT TTT TAT AGA TTG TAT
REVERSE DOWN:
CCC GAG CTC CAT TAG AAG GTT TCA ACC GTT CAT GAA TAT

H2A CORE
FORWARD
5’CCC GGT ACC TTA AAT CAT CAT GGT GTG TTT TTA ATT AAT 3’
REVERSE
5’ CCC CTCGAG AAG GTC TTG AGA AGC TTG ACC TCT AGA TTC 3’
DOWNSTREAM FORWARD
: 5’ CCCGCGGCCGC GGA ATT AAA AAT CCA AAA TCT ATC TATTCT3’
DOWNSTREAM REVERSE
5’CCCGAGCTC TTG GAA TTT GTG GCG CCA TTC AGA AAA TTC3’

Hv1
FORWARD UP;
5’ CCC GGTA CC ATT AAA TAG ATA GAT AGT TAG TTA GTT ATG 3’
REVERSE UP:
5’ CCC CTC GAG ACG AGG TTC AGC AGT CTT AGC ACT AGA TCT 3’

DOWNSTREAM FORWARD:
5’CCCGCGGCCGCGTAGTAATGTACATGATTTAAAAAAAAATT3’
DOWNSTREAM REVERSE:
5’CCCGAGCTCCCGCCTGCTTGCTATCGTTCACGCACAATC3’

H3 CORE:
FORWARD UP:
5’ CCC GGT ACC TAG CAG TGA CGG TCT TTC TTC TGG CGT GTT 3’
REVERSE UP:
5’ CCC CTC GAG GAA TCT TTCACC TCT AAT TCT TCT AGC GAG 3’
DOWNSTREAM FORWARD:
CCC GCG GCC GC GCA TAA TAT AAC AAC TAG TCT CTA AAT AAT
DOWNSTREAM REVERSE
CCCGAGCTC ACA AGT TTA AAA CAA TGA TAA AGA TAT TAG

H3.3
FORWARD UP:
5’ CCC GGTACC GAT ATG GTG GGG GTG GGG AGA AAC AAA TAT 3’
REVERSE UP:
5’ CCC CTC GAG GAA TCT TTC TCC TCT AAT TCT TCT AGC AAG 3’
DOWNSTREAM FORWARD:
CCC GCG GCC GC GAG CTC TCT CTA ATA ATT AAC TTA ATA TAT
DOWNSTREAM REVERSE
CCCGAGCTC AGG TTG AGA TTG AGA TGC AGG AGA GCT AAT

MLH1
UPSTREAM FORWARD:
CCC GGTACCAGC TTC ATC TTC TAA GAA CAG AAA ATC ATC
UPSTREAM REVERSE:
CCC CTCGAG TTA TTT TTT ATT TGC CTT CTT GCC ATA AGC
DOWNSTREAM FORWARD:
CCC GCGGCCGC GTT TGA AAT GTT AAG TAT CAA CTT TAA ACC
DOWNSTREAM REVERSE
CCCGAGCTC GGA ATT TCT GAA AAT ATA ATT TAA GCA GTT

HISTONE H4
UPSTREAM FORWARD:
5’ CCCCGGTACC GTG TAT TAT GAT TTA GAT ATA TTT AAT AAA 3’
UPSTREAM REVERSE:
5’ CCCCTCGAG ACC ACC GAA ACC ATA GAG AGT TCT GCC TTG 3’
DOWNSTREAM FORWARD:
5’ CCCC GCGGCCGC ACA AAA TAT TTA TCT TAA AAA ATT AAA AAG 3’
DOWNSTREAM REVERSE:
5’ CCCCGAGCTC GGG AAT ATC ATC TCC TTT TAT GCA TCT AAG 3

Appendix 4- Protein ladder

PiNK plus prestained protein ladder scale (Frogga Bio)

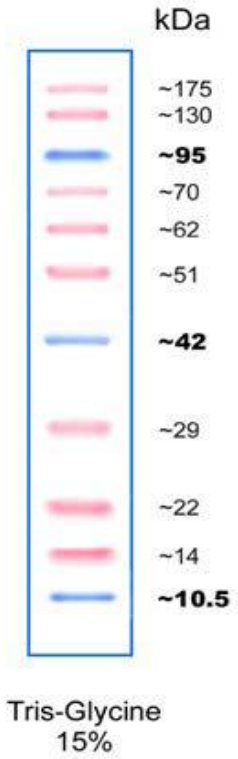

Appendix 5-

Appendix 5A: Restriction maps of Hv1, H2A, H3 and H3.3 genes

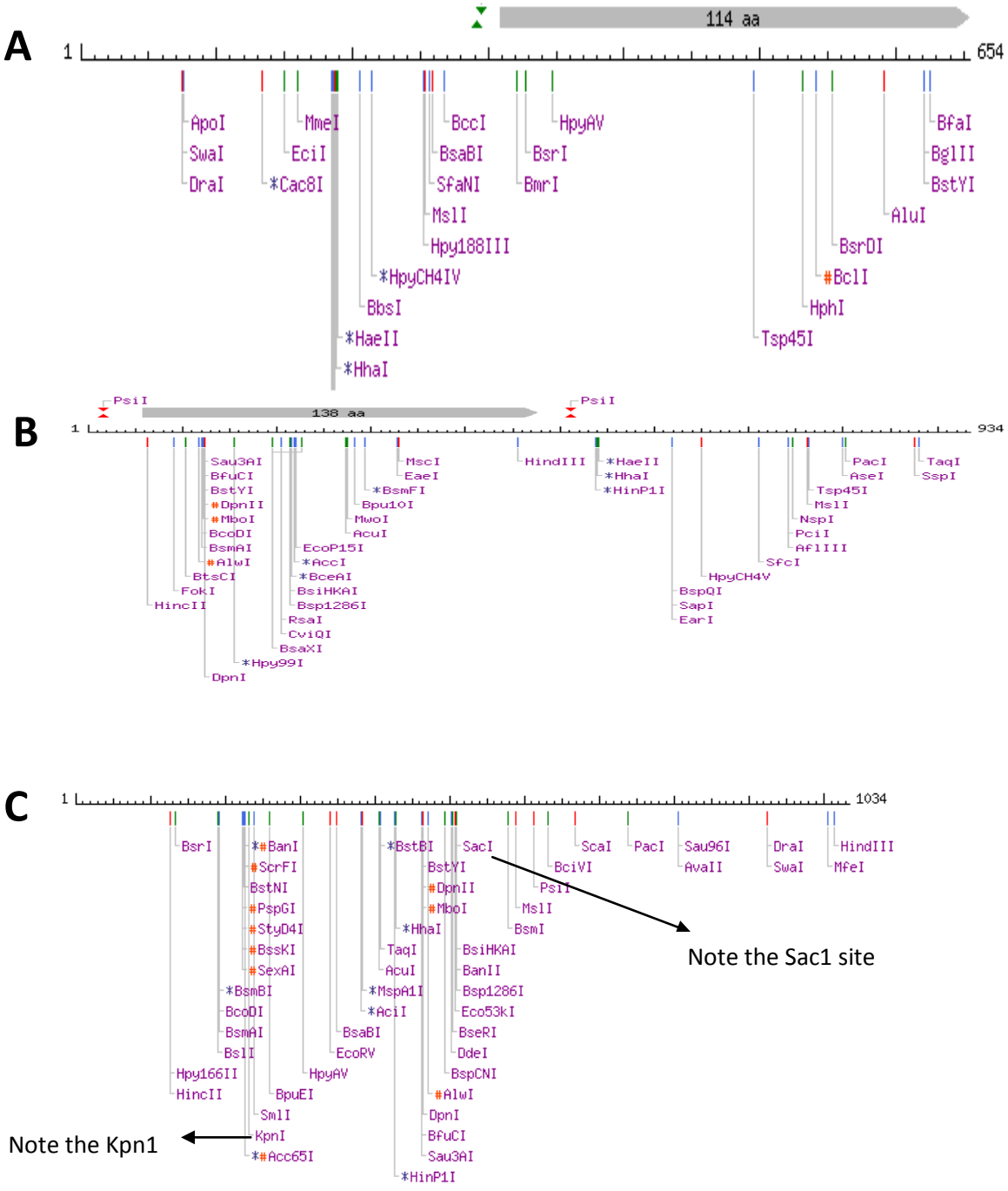

D

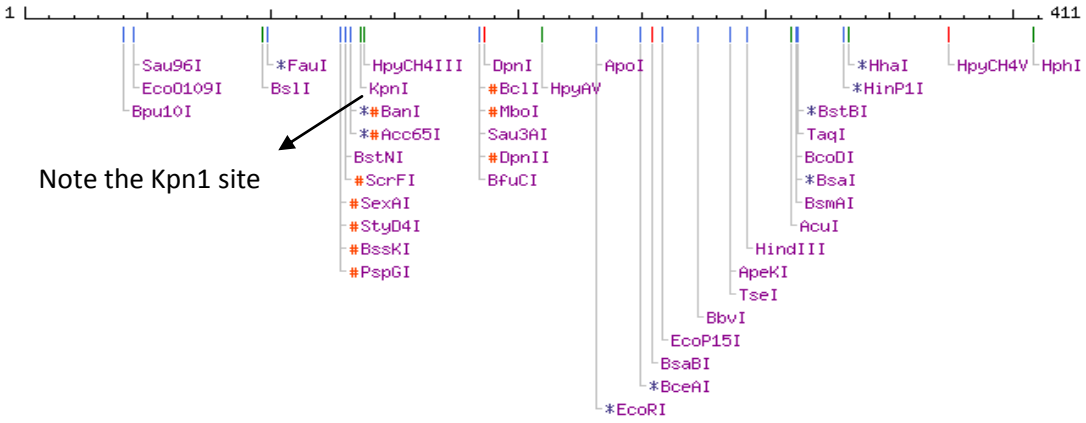

Appendix 5B: Cloning plasmid and PCR products

A

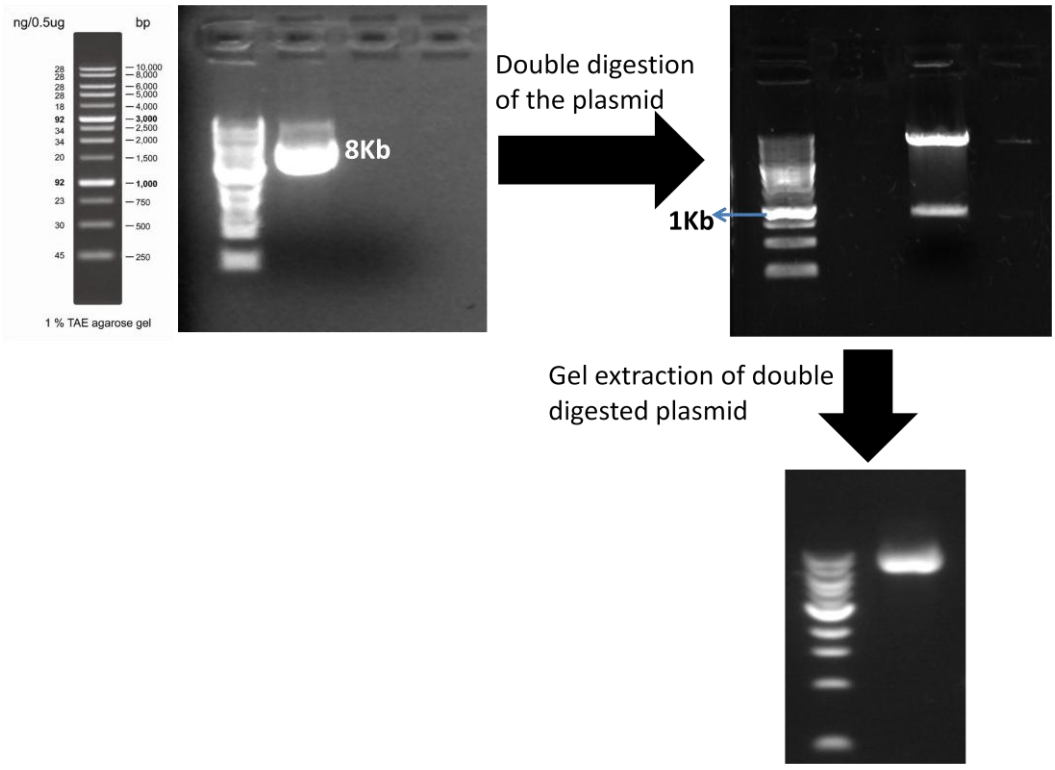

B

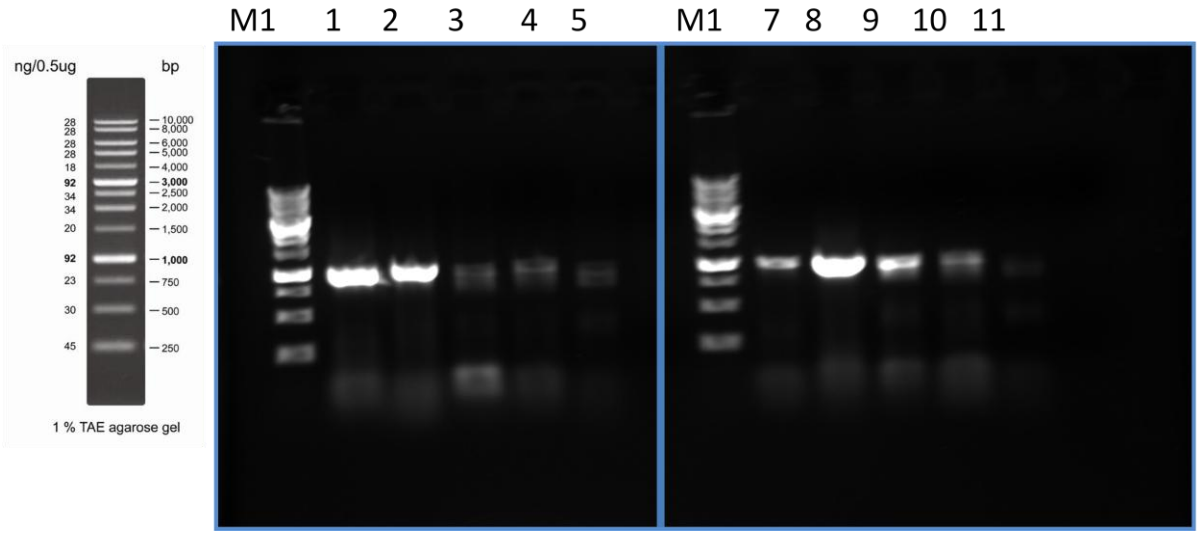

A: Cloning plasmid preparation**.** The plasmid was double digested with appropriate restriction enzymes and was gel purified. **B:** 0.8% Agarose gel. Lanes 1-5 & lane 7-11 represent double digested upstream and downstream PCR products for Hv1, H2A and H3 and H3.3, H4 respectively. Note the products were digested with appropriate restriction enzymes as detailed in the main text. M1 represent 1kb DNA ladder.

Appendix 5C: Confirmation PCR schematic

A

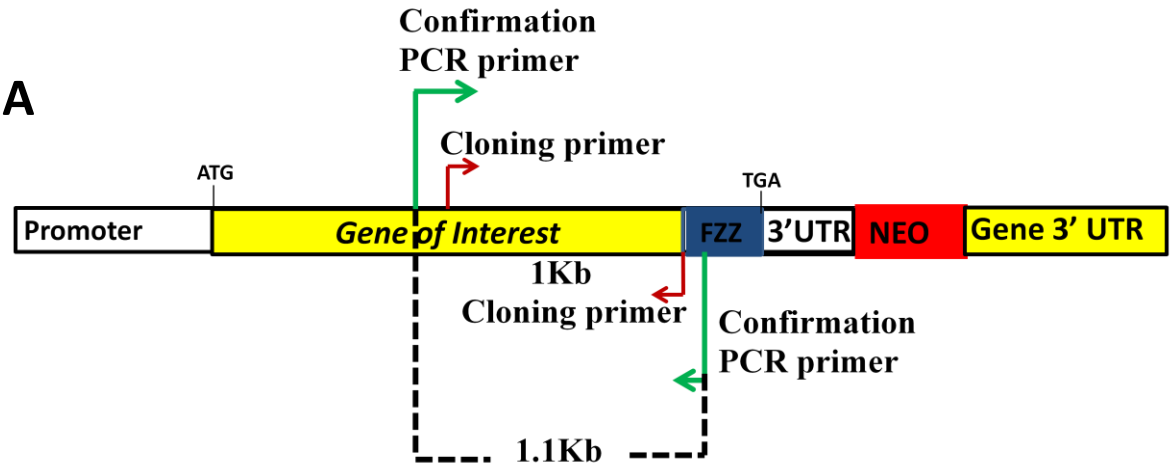

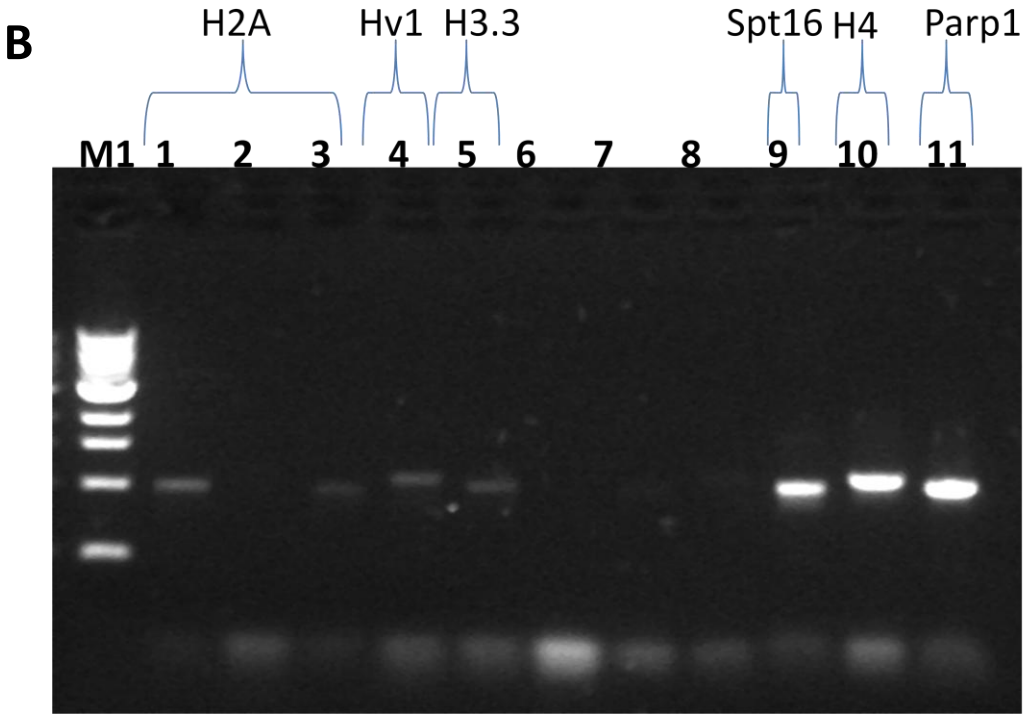

A: Confirmation PCR strategy. The position of cloning primers for upstream fragment and primer position of confirmation PCR is shown. **B:** 0.8% Agarose gel. Lanes 1-11 represent conformation PCR products for various genes studied here. Note the size of each product is approximately 1Kb in accordance with the distance between forward and reverse primers. M1 denotes 1Kb DNA ladder.

Author's Declaration

I hereby declare that I am the sole author of this thesis or dissertation.
I authorize York University to lend this thesis or dissertation to other institutions or individuals for the purpose of scholarly research.

Kanwal Ashraf

I further authorize York University to reproduce this thesis or dissertation by photocopying or by other means, in total or in part, at the request of other institutions or individuals for the purpose of scholarly research.

Kanwal Ashraf